2017-05-01

Desorption Electrospray Ionization (DESI) Mass Spectrometric Imaging of Spatially Regulated *In Vivo* Metabolic Rates

Charlotte Reininger Lewis
Brigham Young University

Desorption Electrospray Ionization (DESI) Mass Spectrometric Imaging

of Spatially Regulated *In Vivo* Metabolic Rates

Charlotte Reininger Lewis

A thesis submitted to the faculty of
Brigham Young University
in partial fulfillment of the requirements for the degree of

Master of Science

Paul B. Farnsworth, Chair
David V. Dearden
John C. Price

Department of Chemistry and Biochemistry

Brigham Young University

ABSTRACT

Desorption Electrospray Ionization (DESI) Mass Spectrometric Imaging
of Spatially Regulated *In Vivo* Metabolic Rates

Charlotte Reininger Lewis
Department of Chemistry and Biochemistry, BYU
Master of Science

Desorption electrospray ionization (DESI) is an ambient ionization technique used for mass spectrometric imaging of biological samples. When coupled with isotopic ratio measurements of deuterium-labeled tissues, DESI provides a means of measuring metabolic rates on a spatially resolved basis. *In vivo* metabolic rates are desired to better understand diseases such as Alzheimer's, Parkinson's, Huntington's, and various forms of cancer that negatively impact metabolic rates within different organs of the human body. Although DESI has been used to image lipids and metabolites of a variety of tissues and other imaging techniques, such as NIMS, have been used to study kinetic turnover rates, DESI has not yet been used to study *in vivo* metabolic rates using deuterium labeled tissue.

This thesis describes how we optimized our DESI source for imaging of biological tissue, how we developed a MATLAB graphical user interface (GUI) to process and interpret the large mass spectral data files, how we conducted our initial mouse brain study for proof-of-concept, and how we plan to implement our DESI imaging in a study with mouse models of Alzheimer's disease. Our initial mouse brain study involved labeling mice with deuterium enriched water, preparing tissue slices for DESI analysis, imaging the tissue slices using DESI coupled with a Bruker mass spectrometer, analyzing the mass spectral data using our custom-designed image_inspector program, confirming identification of lipids using MS/MS, and creating incorporation curves to measure *in vivo* metabolic rates.

ACKNOWLEDGEMENTS

These past few years have had a tremendous impact on my growth as a student, peer, coworker, scientist, and individual. My wonderful parents sacrificed their time and efforts to raise me as their daughter and provided me the opportunity to study at Brigham Young University. Thank you, Dad, for introducing the periodic table of elements to me as a toddler when I was eating my cereal each morning before school and for teaching me to love learning just as much as you always have. Thank you, Mom, for teaching me to work hard, to earn my pay, and to not only set goals but to accomplish them. Thank you both for working so hard in your careers and teaching me the importance of a good education.

Dr. Paul B. Farnsworth, you have been the best advisor, mentor, and friend that I could have ever asked for. I remember the Christmas break of my sophomore year of my undergraduate degree at BYU wanting to join a research group, but I had not heard from the lab groups I had expressed interest in. Then one afternoon, I got an email from you saying you were "looking for a capable and committed undergraduate researcher to take over a critical project" in your lab and I was highly recommended by Dr. Goates based on my performance in Chem 227. From that point on, you taught me to have confidence in my research abilities, trust in the scientific process, and faith in finding the answers in science as well as life. You saw potential in me during the times that I could not see it in myself. Thank you for having patience through all my questions and for relying on me to tackle research problems in the lab. I greatly appreciate all the time you have taken to help me grow personally and professionally. You taught me the importance of a good lab notebook, a tidy research area, and a thorough investigation of a problem. Thank you for always listening to me and helping me become the person I am today.

I would like to thank my other committee members, Dr. John C. Price and Dr. David V. Dearden for their advisement and support through my graduate research.

I would like to thank all my Farnsworth labmates for making the day-to-day life in the lab enjoyable and bearable, especially on days when "science wasn't working." Jessica Ramsey Larsen, thank you for the encouragement and advice in research as well as life. I greatly appreciate your friendship and loved every conversation we had in the office and the research lab. Thank you for helping me become a better friend, researcher, and overall person. Anna Zagieboylo, thank you for teaching me all you knew about DESI and making the project switch such an easy transition. Mercede Erikson, thank you for taking over the DESI imaging project when I left and being so diligent at learning and helping me through my last semesters at BYU. Wade Ellis, thank you for answering all my questions and helping me learn to be self-sufficient in the lab by encouraging me to "google it." Jonathan Wright, thank you for teaching me by example how to work hard and be productive every day in lab. I looked up to your ambitious research goals and admired your hard work ethic. Alisa Edmund, thank you for welcoming me into the lab when I was initially a brand new undergraduate and teaching me to endure through the days when "science wasn't working." Richard Carson, thank you for taking care of all the mice brains and helping so much with the DESI imaging progress.

Thank you, Lillian, for being the best baby ever and taking long naps so I could write my thesis. I cannot wait to share my thesis with you when you are older and I hope I can share my love of science with you throughout your life. I hope you too can follow your dreams and accomplish your goals in life.

I would like to express my appreciation to Sue Mortensen and Janet Fonoimoana for helping me with any questions I had about the department or about the degree requirements.

TABLE OF CONTENTS

LIST OF FIGURES

LIST OF TABLES

1   INTRODUCTION

1.1   Discovery of Desorption Electrospray Ionization (DESI)

In 2004, R. Graham Cooks' research group introduced desorption electrospray ionization (DESI) as a new ambient ionization method for mass spectrometry to simplify the sample introduction process.[1] Sample introduction systems for mass spectrometry have in the past been quite complex. For example, secondary ion mass spectrometry (SIMS)[2] requires that the sample be held under high vacuum. Matrix-assisted laser desorption/ionization (MALDI) requires careful sample pretreatment and is also usually conducted in an evacuated chamber.[3] The novelty of DESI includes the ability to ionize compounds with little sample preparation and without a vacuum system. DESI involves spraying electrically charged solvent droplets onto a sample surface, accompanied by a high-velocity gas jet. The generally-accepted model for DESI analyte ionization involves analyte dissolving in a thin layer of the DESI solvent before being ejected in secondary droplets by impact from the primary spray.[4] The charged secondary droplets evolve into gas-phase ions similar to the theorized electrospray mechanism due to electrostatic and pneumatic forces.[1] The desorbed gas-phase ions are then sucked into a mass spectrometer for detection through a custom built electrically-charged metal inlet. With a soft-ionization mechanism, DESI can be used to see molecular ions of larger biological molecules as well as multiply-charged ions sampled directly from intact biological tissue.[5] The mass spectrum resembles that of electrospray ionization (ESI) because singly and multiply charged species are

detected with little fragmentation. Cooks et al. demonstrated that DESI could be used to ionize both polar and nonpolar molecules including alkaloids, small drugs, peptides, and proteins that were present on varied surfaces that included metals, polymers, and minerals.[1]
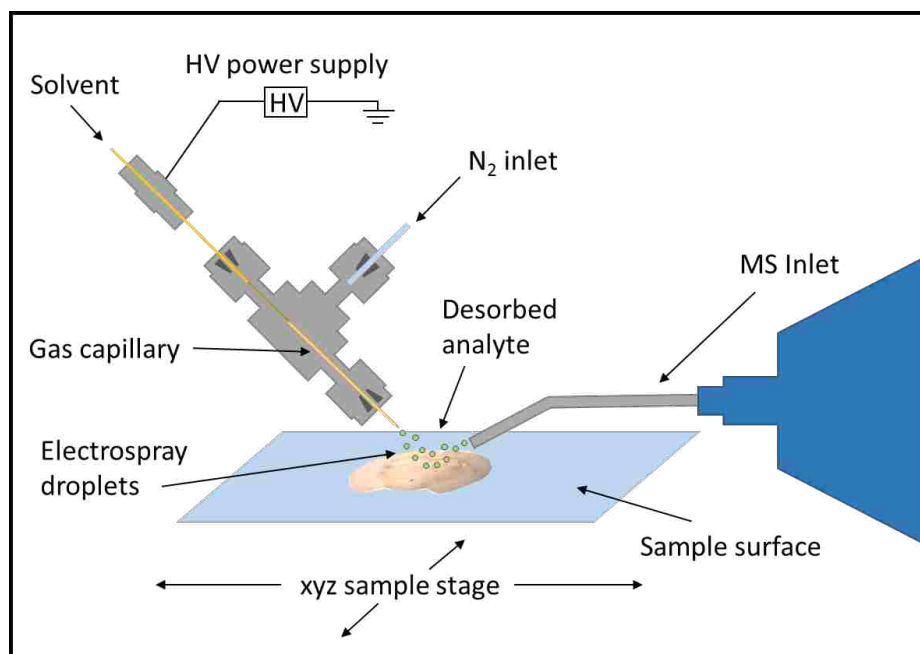
Figure 1.1: Schematic of Desorption Electrospray
Ionization Mass Spectrometry (DESI-MS)

After the initial invention of DESI in 2004, the instrumentation, mechanisms and applications in forensics, chemistry, and biology were described by Cooks et al. in 2005.[6] Instrumentation includes a sprayer assembly, a surface assembly, and a mass spectrometer with an inlet adaptor. The sprayer assembly includes a solvent pump that pumps at a rate of 1-3 µL/min, a high voltage power supply to electrically charge the solvent, and a sprayer tip made of two coaxial glass capillaries for solvent and nitrogen gas. The surface assembly includes

a slide holder on a motorized stage to position the analyte of interest under the sprayer tip. A commercial source has now become available for purchase by Prosolia, Inc. in Indiana, but custom built DESI sources are still widely used.[7] The ionization mechanism is hypothesized to include aspects of both the heterogeneous charge-transfer mechanism as well as the droplet pick-up mechanism.[6] DESI can be used for qualitative as well as quantitative applications. Takats et al. published a linear graph comparing peptide signal intensity to deposited amount on a glass surface, which ranged from 1 pg to 100,000 pg.[6] Analytical performance was demonstrated for many more compounds including insulin, TNT, and glucose. With such a wide range of detectable analytes, applications were predicted to be endless in the fields of forensics, chemistry, and biology.

1.2   Applications of DESI

Areas of current application for DESI include high-throughput sample analysis, clinical studies, food analysis, environmental studies, 2-D and 3-D tissue imaging, as well as forensic investigations.[6] The two applications most relevant to this thesis are 2-D imaging for regiospecific detection of lipids and fatty acids in tissue and DESI imaging of human tissue for clinical applications.

1.2.1   Detection of Lipids and Fatty Acids in Tissue

DESI was first used as an ionization source for biological tissue samples in 2005 by Wiseman et al..[5] Without the need of a high vacuum region, DESI could be used to profile intact biological tissues under ambient conditions by desorbing and ionizing the lipids and fatty acids on the surface. To demonstrate the range of tissues that DESI could profile, Wiseman sampled mouse pancreas, rat brain, and metastatic human-liver adenocarcinoma.[5] Results showed that

DESI was a sensitive ionization source for sampling analytes from intact biological tissues in ambient conditions with a future capacity for chemical imaging (spot size less than 1 mm).

Then in 2006, Wiseman et al. published another paper with improvements to DESI imaging of biological tissue at atmospheric pressure.[8] This was the first time DESI-MS was used for two-dimensional molecular-ion imaging. Spatial resolution was improved to 500 μm while imaging a rat brain. In the low m/z region (m/z < 400) in negative ion mode, fatty acid compounds including palmitate, oleate, stearate, arachidonate, and docosahexaenoate were detected. In the high m/z region (m/z > 600), various sulfatides, phosphatidylserines, and phosphatidylinositols were detected. MS/MS was used to confirm identification of these lipids and fatty acids. A useful table was published in the supplemental information that many other research groups have used to aid in their compound identification process.[8]

More recent DESI imaging advancements are described in publications by Lanekoff et al.[9] and Eberlin et al..[10] Lanekoff et al.[9] describes the evolution of DESI to nanospray desorption electrospray ionization (nano-DESI) in being able to perform three-dimensional imaging of lipids in mouse uterine decidual cells and embryos that are implanted in the uterine walls during pregnancy. Nano-DESI is not the same as DESI because it does not involve spraying solvent onto the sample surface, but rather involves dragging a continuously flowing drop of solvent that then sprays into the inlet of the mass spectrometer through a secondary capillary. The demonstration of the ability to map ionizable lipids in relatively small tissue samples was proof-of-principle for future applications. This study showed that certain lipids, such as acetylcholine, were concentrated in certain sites of the tissue that paralleled their roles as signaling molecules in decidualization.

In the review article by Eberlin et al.,[10] DESI is described as an ionization source for 2D and 3D imaging of lipids. The strengths and weaknesses of DESI-MS are also described along with present and future applications. Biological tissue samples imaged so far have included rat brain, porcine brain extract, rabbit adrenal gland, mouse brain, mouse pancreas, mouse lung extract, rat spinal cord, chicken heart, canine bladder, human liver, human brain, human atherosclerotic plaque, human bladder, human kidney, human testis, human prostate, and human lens.[10] Some of the strengths of DESI include the ability to add reagents to the solvent to undergo reactions with the analyte in reactive-DESI, to analyze small molecules with no interference with the matrix ions (referring to MALDI), to run samples with little sample preparation, and to image under atmospheric pressure. One of the weaknesses of DESI imaging is that matrix effects cause some lipids to suppress ionization of other lipids in the same region. Therefore, DESI is not a quantitative technique yet, since ionization efficiency is matrix dependent. DESI also has problems with isomeric and isobaric compounds causing difficulty with accurate lipid assignment. Future applications of DESI include fast screening of pathological tissue samples, analysis of drug effects on animal models, disease diagnosis, and *in vivo* determination of tumor margins during surgery.

Mass spectrometric imaging of biological tissue using DESI has been thoroughly researched by many research laboratories, but the Fernandez research group has been the most informative for instructing how to image tissues because of their published video article in 2013.[11] Details are provided for how to section tissue, including flash freezing whole tissue, slicing the tissue using a cryomicrotome, thaw mounting the tissue slices to glass slides, and refreezing the slices in a -80°C freezer. Details are provided for DESI optimization as well. Key optimization parameters include the nitrogen gas pressure, solvent flow rate, type of solvent,

angle of the DESI probe, collection angle of the mass spectrometer capillary inlet, height of the mass spectrometer capillary inlet relative to the tissue sample, height of the DESI probe relative to the tissue sample, distance between the DESI probe and the mass spectrometer capillary inlet, and value of the high voltage applied to the solvent. With ambient conditions constantly changing and with inconsistencies in tissue types and slices, careful optimization of each of these parameters is required for acceptable signal intensity and image resolution.

1.2.2   DESI Imaging of Human Tissue for Clinical Applications:

Many papers have been published in the last three years demonstrating the possibility of DESI imaging and DESI lipid profiling for human cancer and tumor applications. Research has been done to understand the repeatability and reproducibility of DESI imaging analysis of human cancer tissue.[12] Other research studies have focused on breast cancer margin analysis[13] and molecular typing of meningiomas for surgical decision-making.[14]

A recent paper published in 2015 in Analytical Methods by Abbassi-Ghadi et al. has demonstrated that DESI-MS has acceptable levels of repeatability and reproducibility for future clinical studies and diagnostics.[12] Oesophageal human cancer tissue was used for the experiment. DESI parameters were first optimized and then kept constant for the remainder of the study. Since ion intensity varies from run to run due to variations in spray conditions, tissue thickness, and slide conductivity, normalization was done using median fold change. Fold change is a term used to describe how much a variable or quantity changes from an initial to a final value. Median fold change in this study describes the median of fold changes for peak intensities for each individual pixel compared to the median profile of all the pixels.[12] Repeatability and reproducibility were measured (mean ± standard deviation) to be 22 ± 7% and 18 ± 8%,

respectively, for lipid intensities in human cancer tissue sections, which are good enough for lipidomic profiling purposes for clinical applications.[12]

In 2014, Calligaris et al. demonstrated a way to improve breast cancer margin analysis to help conserve breast tissue during surgery.[13] DESI imaging was used for differentiating tumor from normal breast tissue with the future possibility of using DESI during surgical procedures by monitoring several fatty acids, including oleic acid, which are more abundant in cancerous regions. Improvements to breast cancer related surgical procedures and reductions in the number of necessary operations are greatly desired because breast cancer is an extremely common carcinoma in women in the United States. A year later, Calligaris et al. published in the International Journal of Mass Spectrometry about the ability to molecular type meningiomas for surgical decision-making.[14] Meningiomas are found in the cranium and are usually slow-growing and difficult to remove. A total of twelve samples including stereotactically resected surgical samples and autopsy samples were analyzed by mass spectrometric DESI imaging. Results revealed that DESI can provide almost real time information about the molecular content of surgical tissue samples and DESI can be used to distinguish between fibroblastic and meningothelial tissue, which are two subtypes of meningioma. Applications of DESI imaging for surgical decision-making seem very promising with more advancements in the current research studies.

The most recent research for DESI imaging this past year of 2016 have included studies of human brain tumors,[15] gliomas,[16] and neurotransmitters.[17] Jarmusch et al. performed a study using 58 patients that proved that DESI mass spectra provided enough information to successfully differentiate between gray matter, white matter, gliomas, meningiomas, and pituitary tumors.[15] Multivariate statistics was used to distinguish these tumors based on

phospholipid-derived signals. An overall sensitivity of 99.4% and a specificity of 99.7% were found using a tumor specific discriminant model. Using DESI-MS in the operating room has the hurdle that tissue needs to be frozen then sectioned before analysis, but this research study has shown that smeared biopsy tissue also works well for providing the same chemical information as frozen tissue slices. Therefore, DESI-MS imaging has a strong possibility for implementation in the operating room using tissue smears. Jarmusch et al. also showed that positive and negative ion modes could both be used to more thoroughly differentiate and analyze brain tumors since some lipids ionize better in positive ion mode and other phospholipids ionize better in negative ion mode.[16] Therefore, positive and negative ion mode lipid profiles were combined in principal component analysis to increase sensitivity and specificity beyond 90% for all grey matter, white matter, and glioma tumors. Shariatgorji et al. demonstrated that DESI imaging could be used to image brain tissue sections to directly analyze multiple neurotransmitters, metabolites, and neuroactive drugs all at once.[17] Metabolites that were monitored in this study included dopamine, dihydroxyphenylacetic acid, 3-methoxytyramine, serotonin, glutamate, glutamine, aspar-tate, γ-aminobutyric acid, and adenosine. The neuroactive drugs in this study were amphetamine, sibutramine, and fluvoxamine. Positive and negative ion modes were once again used to increase the number of molecular targets. Quantitative analysis of drug concentrations in different parts of the brain was also achieved with the use of an external calibration curve. Overall, this study demonstrated the ability of DESI imaging to be used for studying the effects of neuroactive drugs in the brain. Applications in the future will be in the fields of neuroscience, pharmacology, and even pathology.

1.3 Incorporation of D_2O in Tissue for Isotope Labeling

Although many studies had been done to understand deuterium enrichment in the lipids of rats,[18,19] the first study to determine the maximum incorporation number (N) of deuteriums in the synthesis of stearate, palmitate, and cholesterol was Lee et al..[20] D_2O enriched water coupled with mass isotopomer analysis was used to measure the N value to be 22, 24, and 30 for palmitate, stearate, and cholesterol, respectively. This study showed that mass isotopomer analysis after feeding rats deuterium-enriched water could be used to understand the replacement rate of lipids found in various organs in the body to help elucidate the synthetic pathways of specific lipids of interest.

Stable isotope metabolic labeling was demonstrated as a successful method for studying protein turnover in mammalian tissue by combining isotope labeling experiments with compartment modeling.[21] *In vivo* studies of protein turnover rates affected by calorie restriction were also studied using deuterium labeling of mammals.[19]

The most recent and most applicable study for our current research is the demonstration of mass spectrometry imaging to measure *in vivo* kinetic turnover rates of lipids in tumor regions.[18] Typically mass spectrometry imaging is used to see only snapshots of spatial molecular composition within tissues, but when combined with kinetic labeling, the snapshots can be merged to tell a story of how biological processes take place. The kinetic mass spectrometry imaging (kMSI) technique used in this study was nanostructure-initiator mass spectrometry (NIMS), which uses a UV laser to propel tissue into the gas phase to generate a unique mass spectrum for each pixel across an entire tissue slice. Results from this study showed that synthesis of saturated and monounsaturated fatty acids was unique to tumor regions and that kMSI provided information to identify and distinguish these tumor regions from healthy tissue

regions due to their metabolically distinct compositions. Future research studies using kMSI promise to influence the understanding of physiology with a specific focus on disease.

1.4   Objectives and Significance of this Research Study

Desorption electrospray ionization (DESI) is an ambient ionization technique used for mass spectrometric imaging of biological samples.[8] When coupled with isotopic ratio measurements of deuterium-labeled tissues, DESI provides a means of measuring metabolic rates on a spatially resolved basis.[20] *In vivo* metabolic rates are desired to better understand diseases such as Alzheimer's, Parkinson's, Huntington's, and various forms of cancer that negatively impact metabolic rates within different organs of the human body. Although DESI has been used to image lipids and metabolites of a variety of tissues[8] and other imaging techniques such as NIMS have been used to study kinetic turnover rates,[18] DESI has not yet been used to study *in vivo* metabolic rates using deuterium labeled tissue.

2   DESORPTION ELECTROSPRAY IONIZATION (DESI)

2.1   Detailed Description of our DESI Source

The desorption electrospray ionization mass spectrometry (DESI-MS) source, used to acquire mass spectrometric images of mouse brains contained within this thesis, consisted of a DESI emitter, a solvent syringe and pump system, a high voltage power supply, a cylinder of compressed nitrogen, a motorized, programmable translational stage, a glass slide mount, a microscope eyepiece, a light source, and a mass spectrometer with a customized sniffer inlet. The DESI emitter was custom built from a 1/16 inch Swagelok T. The emitter tip consisted of a 4-cm-long spray capillary emitter purchased from Prosolia Scientific (0.05 in ID and 0.15 in OD, Indianapolis, IN, U.S.A.) that was superglued (Loctite 404) into PEEK tubing (us.vwr.com). The PEEK tubing was used to connect the Prosolia capillary emitter to the high voltage connector and then to the solvent syringe (Hamilton 500 µL, Model 1750 CX SYR, 1/4-28 Threads). The syringe was pumped with a Harvard pump (Harvard Apparatus PHD 2000, Holliston, MA, U.S.A.) at a solvent flow rate of 1-3 µL/min. Plastic tubing delivered the compressed nitrogen (Airgas, Salt Lake City, UT, U.S.A.) to the Swagelok T at 160 psi. The gas exited the Swagelok T through an approximately 2-cm-long fused silica capillary (182 µm ID and 354 µm OD, Molex, Polymicro Technologies, Phoenix, AZ, U.S.A.) that coaxially surrounded the Prosolia spray capillary emitter. The Prosolia capillary emitter extended out past the gas capillary approximately 0.5 mm. The emitter tip to sample surface distance was approximately 1 mm, but

was optimized for each tissue scan. The emitter tip to mass spectrometer inlet distance was approximately 4-5 mm. The DESI emitter angle was 55 degrees relative to the tissue surface. High voltage (Stanford Research Systems, Inc. Model PS350, Sunnyvale, CA, U.S.A.) of -5kV was applied to the high voltage no-dead-volume connector to electrically charge the methanol solvent. A microscope eyepiece (Nikon, Melville, NY, U.S.A.) was used to view the DESI emitter tip and the DESI solvent spray spot on the tissue. Our light source (Cole-Palmer Illuminator, Model 41722, Vernon Hills, IL, U.S.A.) was simply used to illuminate the tissue samples on the glass slides to better see contrast with the microscope eyepiece. A custom machined glass slide mount was used to hold the tissue samples on the motorized, programmable translational stage (Prior Scientific, Rockland, MA, U.S.A.), which communicated with the MicrOTOF II mass spectrometer (Bruker Daltonics, Billerica, MA, U.S.A.) to raster the tissue samples and obtain mass spectral data, one pixel (75 µm × 150 µm) at a time. Ions entered the mass spectrometer through a custom-adapted stainless steel sniffer that had a collection angle of 18 degrees (the angle β in Figure 2.2). The mass spectrometer was run in negative ion mode with an inlet voltage of 500 V, which was applied to the glass transfer capillary. The mass range was approximately 200-900 m/z. All these instrumental parameters are summarized in Table 2.1 and Table 2.2. Figure 2.1 contains two photographs with most of the DESI-MS elements labeled.

Table 2.1: DESI Imaging Parameters

Parameter	Setting
N_2 Gas Pressure	160 psi
Solvent Type	100% methanol
Solvent Flow Rate	1-3 µL/min
Applied Solvent Voltage	-5 kV
Mass Range	200 to 900 m/z
Ion Polarity	Negative
MS Inlet Voltage	500 V
Mass Spectra Rolling Average	2
Mass Spectra Rate	1 Hz
Pixel Size	75 µm × 150 µm
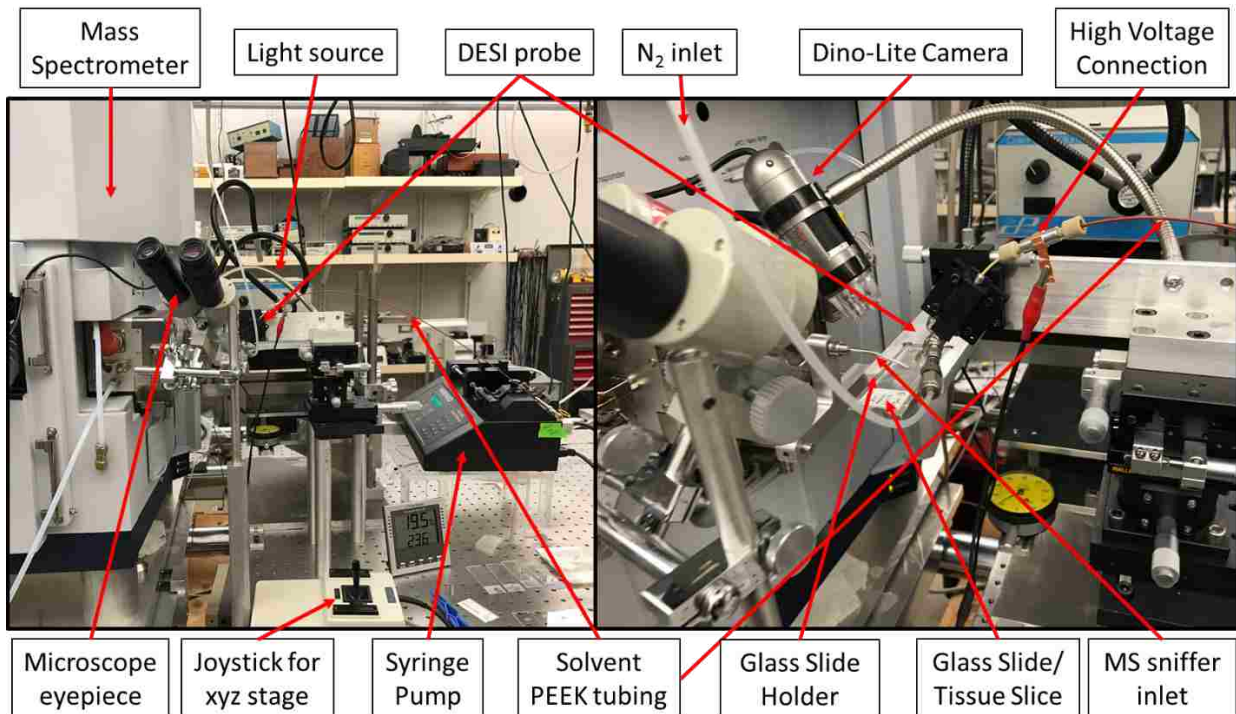
Figure 2.1: Photographs of the DESI-MS setup with Labels

2.2 Geometry Parameters

The detailed description of our DESI source is summarized above, but each of these parameters was significant to the overall performance of DESI for acquiring good quality tissue images. Each parameter is addressed below and significant research articles that have studied or described these parameters are also included. All geometric parameters are diagrammed in Figure 2.2 and included in Table 2.2. A photograph of the DESI probe and mass spectrometer (MS) sniffer inlet is shown in Figure 2.3.

α = DESI probe angle
β = sniffer inlet angle
d_1 = capillary tip extension
d_2 = capillary tip to surface distance
d_3 = capillary tip to sniffer inlet distance
d_4 = sniffer inlet to surface distance

DESI probe

MS sniffer inlet

d_3

d_1

β

d_4

d_2

α

sample surface
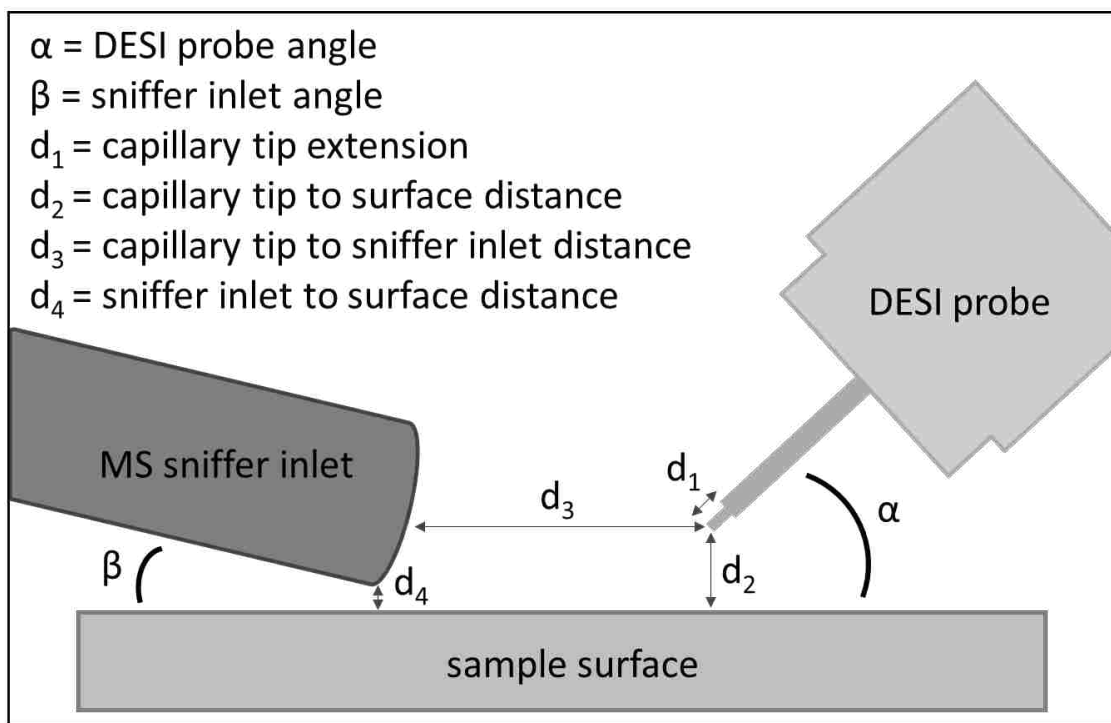
Figure 2.2: Diagram of DESI Geometry Parameters

14

Table 2.2: DESI Geometry Parameters

Parameter	Description	Value
α	DESI probe angle	55°
β	sniffer inlet angle	18°
d_1	capillary tip extension	0.5 mm
d_2	capillary tip to surface distance	1-2 mm
d_3	capillary tip to sniffer inlet distance	4-5 mm
d_4	sniffer inlet to surface distance	< 1 mm
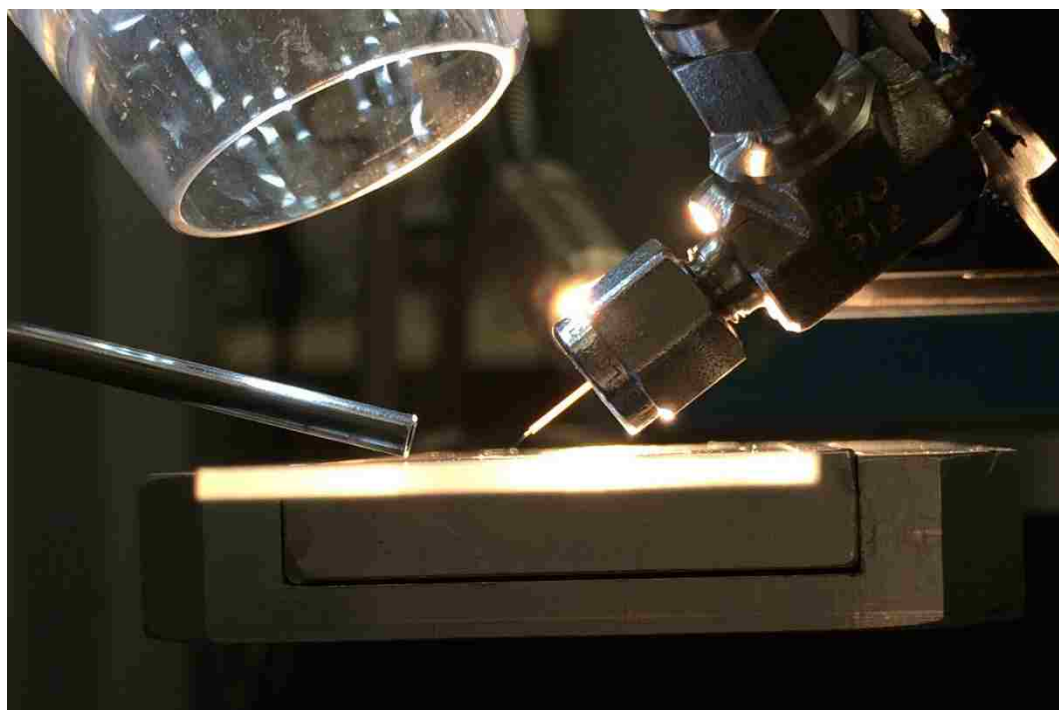
Figure 2.3: DESI Probe and MS Sniffer Inlet Photograph

2.2.1 Angle of the DESI Probe

The angle of the nebulization capillary also known as the DESI probe directly affected the distance the ions needed to travel to reach the mass spectrometer sniffer inlet and directly influenced the solvent spray area and shape. Angles in the literature ranged from 50° to 70° but most were 52° to 55°.[8,11,22] When the angle was closer to 90°, the solvent spot was more circular in shape but the ion trajectory was not directed into the sniffer inlet. When the angle was less than 50°, the solvent spot shape was more elliptical and the ions or secondary droplets lost their ideal trajectory towards the mass spectrometer inlet. Bodzon-Kulakowska et al.[22] claimed that a 4° change in the capillary angle, referring to the DESI probe, caused a near complete loss in signal. After researching the optimized capillary angle chosen in other research studies, we changed our DESI probe from 37° to 55° and noticed a six-fold signal intensity increase.

2.2.2 Angle and Extension of the Solvent Capillary Relative to the Gas Capillary

The importance of the DESI probe sprayer geometry alone was highlighted recently in an article published in 2016 in Analytical Chemistry.[7] A comparative study was performed using the commercialized DESI source from Prosolia Inc. and a custom lab-built DESI source. The repeatability of absolute mass spectral intensity, spectral composition, and the accuracy of compound classification for biological tissues were all items considered in this research study. The shape of the electrospray and solvent spot were highly affected by the solvent type, solvent flow rate, gas pressure, solvent capillary protrusion distance, as well as the position of the solvent capillary in relation to the gas capillary. Extreme variability was seen between the custom lab-built DESI source and the commercial DESI source. Therefore, studies of rhodamine films were used to examine the extreme variability. The results, however, could not be used to directly understand the optimal parameters for optimizing signal for tissue imaging because dyes

16

and tissues are two very different sample types. That is why the repeatability ranged from 1 to 224% for the individual sprayers.[7] However, Tillner et al. still claimed that a sprayer setup with a fixed solvent capillary geometry needed to be developed so that this parameter could be more carefully controlled.

In the Farnsworth laboratory, we found that the best solvent spot and signal intensity was seen when the solvent capillary was positioned downward in relation to the gas capillary as seen in Figure 2.4.
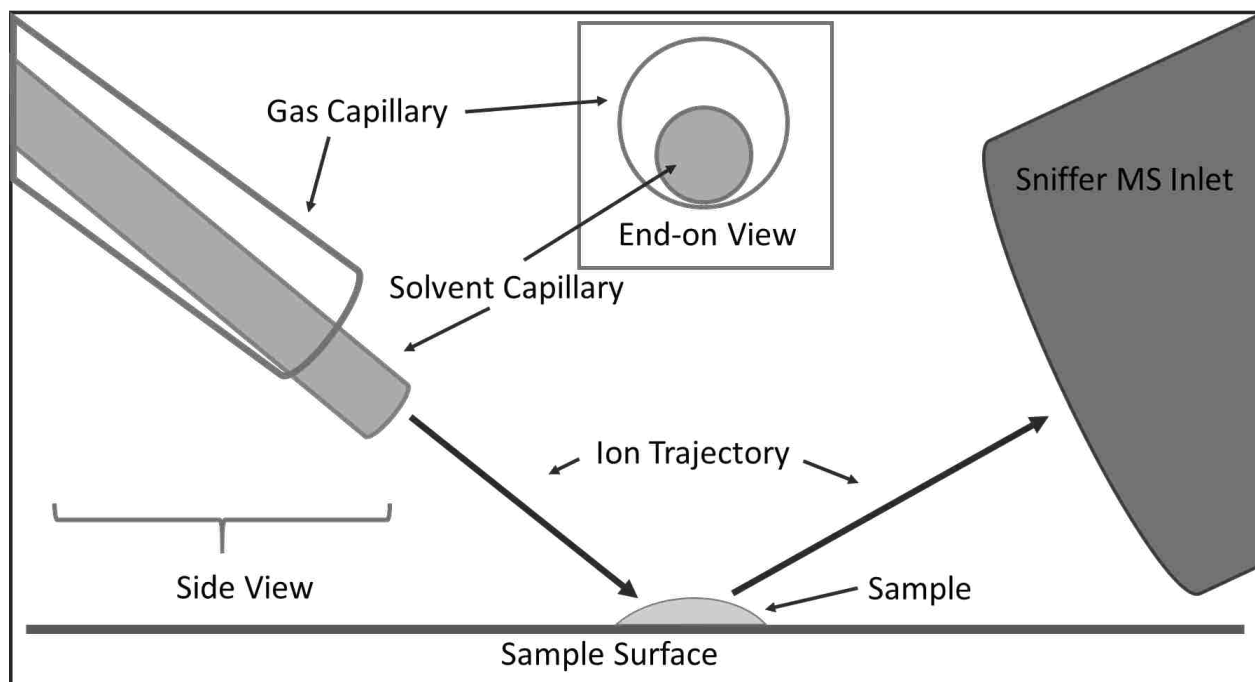
Figure 2.4: Solvent Capillary Orientation

The protrusion of the solvent capillary in relation to the gas capillary was studied more definitively. This parameter was responsible for proper Taylor cone formation and stable signal intensity. In one study, the optimum setting was sample dependent, showing that a protrusion of

1 mm was better for rhodamine dye on a glass slide and 0.5 mm was better for tissue imaging.[22] Most studies found that a 0.5 to 1 mm protrusion was necessary for proper solvent spray and spot shape, which directly affected stable signal intensity.[11] For tissue imaging, an extension of less than 0.5 mm caused the gas flow to curl around the tip of the solvent capillary, preventing proper Taylor cone formation. Extensions greater than 1 mm also prevented formation of the Taylor cone. Proper Taylor cone formation was necessary for a controlled solvent spray for analyte ionization.

2.2.3 Sniffer Inlet Distance from Sample Surface

The distance between the sample surface and the mass spectrometer sniffer inlet needed to be less than 1 mm. All references agreed that minimizing this distance increased the ion intensity.[11,22] However, in our experience, when the sniffer was too close to the tissue surface, the sniffer tip scratched the surface or became misaligned due to contact with the surface. A clamp was later designed as discussed in section 2.6.3 to prevent misalignment of the sniffer in relation to the DESI probe due to uneven tissue slicing or tissue surface roughness.

2.2.4 DESI Probe Height above the Sample Surface

The height of the DESI probe emitter tip above the sample surface ranged from 1 to 4 mm.[22] A study of adrenal glands[23] used a height of 3 mm above the sample surface and a study of rat brains[11] used 1.5 mm above the tissue slices for imaging. Closer proximity caused tissue damage and a larger distance caused a decrease in spatial resolution. A height of 1 to 2 mm was used for all DESI imaging described in this thesis to provide adequate signal intensity and spatial resolution without damaging the tissue surface.

2.2.5 Distance Between the DESI Probe and Sniffer Inlet

The main research article that studied the DESI geometry parameters for tissue imaging concluded that the distance between the nebulization capillary and the mass spectrometer inlet for best signal intensity should be between 5 and 6 mm.[22] Too short of a distance caused arcing between the charged solvent and the charged mass spectrometer inlet and too long of a distance caused the ion intensity to suffer. Bennett et al. published a distance of 5 mm as well for optimum signal intensity, but optimization for each tissue scan was still necessary.[11] Wiseman et al. published a distance of 4 mm for this DESI parameter.[8]

A distance of 4 to 5 mm was found optimum for tissue imaging in the Farnsworth research lab using a 55° angle for the DESI probe relative to the sample surface.

2.3 Gas Parameters

Removing the polyimide coating from the gas capillary, polishing and scoring the gas capillary tip, and choosing the gas type and pressure were the three gas-related parameters studied for adequate DESI imaging.

2.3.1 Removing the Polyimide Coating from the Gas Capillary

The Polymicro capillary that is used for the gas capillary surrounding the solvent capillary has a polyimide coating to protect the fragile thin-walled glass capillary within. However, the polyimide coating causes difficulty for obtaining a clean polished tip, which is crucial for a good DESI solvent spot. A few gas capillaries have been successfully scored and snapped using a ceramic edge but those are rare to acquire. Therefore, a thermal technique was used to remove the polyimide coating to allow the glass capillary within to be polished with fine grit sandpapers.

Heated sulfuric acid was chosen to thermally and chemically remove the polyimide coating. A 50 mL beaker was filled with approximately 20 mL of concentrated sulfuric acid. The beaker was placed on a hot plate in a fume hood with a thermometer to monitor the temperature. The acid was slowly swirled every 5-10 minutes until a temperature of 120°C was reached. The tip of a 3 inch segment of gas capillary was carefully dipped into the hot acid for 30-40 seconds, submerging only 2 mm of the end. After removal from the acid, a pair of tweezers was used to grasp the lose polyimide coating and gently pull it off. The other end of the gas capillary segment was dipped as well to remove a 2 mm portion of the polyimide coating. The capillary piece was placed in deionized water to remove any remaining acid and then wiped off.

2.3.2   Polishing/Scoring Gas Capillary

A polishing station for fiber optics was used to polish the tip of the gas capillary. After an approximately 2 mm segment of the polyimide coating was removed from the gas capillary, the gas capillary was scored and snapped using a ceramic edge to a length of approximately 24 mm. The end with the exposed glass and polyimide coating removed was carefully held vertical in a stabilizing custom-designed holder. A glass polishing disk was blown with compressed air to remove lint and dust. Then a successive series of polishing films was used to polish the tip. Sheets of 5 μm (brown), 3 μm (pink), 1 μm (green), and 0.3 μm (white) polishing films were used. The tip was checked under a microscope after each change in polishing film. When polishing was complete, the gas capillary was tested in the DESI probe.

2.3.3   Gas Type and Pressure

The gas type was chosen to be nitrogen due to its high natural abundance, relatively low cost, and chemical inertness. The gas pressure was held constant at 160 psi which was the same gas pressure published in other research articles using DESI for tissue imaging.[11,22]

2.4   Solvent Parameters

The critical solvent parameters for DESI tissue imaging were solvent choice, solvent flow rate, solvent flow consistency, and solvent tip condition. Solvent flow consistency refers to the elimination of bubbles within the solvent capillary. The solvent tip condition refers to needing a professionally polished or precision cleaved tip for uniform solvent spray.

2.4.1   Solvent Choice

Finding the ideal solvent for our imaging experiments was challenging. The solvent system in DESI imaging affected which analyte molecules were ionized from the sample surface, how intense the analyte signal was, and how reusable the tissue was after an imaging scan. With the choice to focus on negative ion mode DESI tissue imaging, 100% methanol was found to be the best solvent for highest signal intensity and minimal tissue degradation.

Wiseman et al. first demonstrated DESI tissue imaging using methanol:water in a 1:1 v/v ratio as well as 100% methanol.[8] Tillner et al. used methanol:water in a 90:10 v/v ratio.[7] Bennett et al. initially described the use of acetonitrile with 1% acetic acid for DESI imaging.[11] However, she later stated in her PhD dissertation that 100% methanol was used as the solvent for both negative and positive ion modes for all later imaging because the methanol:acetonitrile (1:1 v/v) solvent system she had tried caused chemical background to suppress all lipid signal in negative

ion mode.[24] Overall, a higher percentage of methanol in the solvent system choice seemed to provide better tissue imaging.

The methanol:water solvent system in a 1:1 v/v ratio caused tissue disintegration immediately upon contact with the tissue surface and also produced lower intensity lipid signal. Tissue disintegration could also have been caused by the solvent flow rate, gas flow rate, or from the proximity of the DESI tip to the tissue surface, but no tissue disintegration was noted using pure methanol using the same geometry parameters and same solvent flow rate. The methanol:water solvent system in a 9:1 v/v ratio caused a reduction in lipid signal with no apparent advantages, so 100% methanol was the solvent of choice for all tissue imaging in this thesis.

2.4.2   Solvent Flow Rate

The solvent flow rate depended on the solvent type, solvent capillary inner diameter, sample surface, analyte of interest, desired signal intensity, desired image resolution, as well as the other geometric parameters, such as the DESI emitter height above the tissue surface. Other research groups reported solvent flow rates in the range of 1-5 µL/min, and many mentioned the need to optimize the flow rate for each tissue scan.[11,22] When testing the DESI source on rhodamine dye on a glass slide, the solvent flow rate only needed to be 1 µL/min because rhodamine was highly ionizable and a small solvent spot was desired. When imaging mouse brains, the flow rate was 2-3 µL/min, depending on the tissue scan. The gas pressure was constant at 160 psi. The chosen solvent was 100% methanol for the mouse brain scans in this thesis, so these gas pressure and solvent composition did not affect the choice of solvent flow rate. However, the solvent capillary extension in relation to the gas capillary, the height of the

DESI emitter tip above the sample surface, and the desire for the best image resolution without jeopardizing signal intensity were all factors in determining the solvent flow rate.

2.4.3   Solvent Flow Consistency/Elimination of Bubbles

Bubbles in the solvent flow were a major impediment to obtaining good quality, consistent images. Bubbles came from a variety of sources.

The main source of bubbles was a leak in the Loctite 404 superglue that was supposed to seal the Prosolia solvent emitter from the high-pressure nitrogen gas within the Swagelok T. Since the nitrogen gas pressure was 160 psi, the superglue needed to be well cured for at least 24 hours and the entire Prosolia solvent emitter needed to be replaced every 3-4 months or whenever bubbles appeared. The Loctite 404 superglue was only methanol resistant, so over time, the flowing methanol solvent slowly broke down the superglue seal, allowing the high-pressure nitrogen gas a way to escape causing bubbles to form within the solvent. When supergluing the Prosolia emitter into the PEEK tubing, a drop of glue was carefully positioned at the location where the emitter was exiting the PEEK tubing and the emitter was immediately slid into the PEEK tubing approximately 3 mm to increase the surface area of the glue contact for a better seal.

The solvent syringe was another source of bubbles. When refilling the syringe before each tissue scan, all air needed to be pressed out before connecting the syringe to the DESI probe, or else the air would slowly be pressed out along with the solvent during the tissue scan. Bubbles caused gaps or holes in the mass spectral tissue images because consistent signal intensity was dependent on consistent solvent flow and electrical continuity. Even when all sources of bubbles were eliminated, the signal intensity was not always consistent. We were

unable to conclusively identify all sources of signal fluctuations, but known sources of fluctuations are discussed in other sections, such as improper grounding of the mass spectrometer and uneven tissue slices.

2.4.4 Solvent Tip/Prosolia Emitter

Major complications with obtaining a smooth and clean tip by simply scoring and snapping the polyimide coated fused silica capillary using a ceramic edge caused inconsistencies with the solvent spray and solvent spot coming from the DESI source. An inconsistent solvent spot caused fluctuating signal intensity and poor image resolution. We solved this problem by purchasing precision cleaved capillary emitters. They were 4 cm in length with 0.05 inch ID and 0.15 inch OD purchased from Prosolia Scientific (Indianapolis, IN, U.S.A.).

2.5 High Voltage

The high voltage power supply (Stanford Research Systems, Inc. Model PS350, Sunnyvale, CA, U.S.A.) was set at +5 kV or -5 kV, depending on whether positive ion mode or negative ion mode for the mass spectrometer was desired, respectively. One paper describing ideal settings for beginners using DESI showed that a capillary voltage of +3 kV was best for highest spectral quality using positive ion mode.[22] However, this same article claimed that -4 kV was ideal for testing marker using negative ion mode and -4.5 kV was best for liver tissue samples using negative ion mode.[22] The Fernandez lab applied +3.6 kV for positive ion mode DESI tissue imaging[11] and the Cooks research lab applied -5 kV for their negative ion mode DESI tissue imaging.[8] The most recent publication concerning the impact of the DESI sprayer geometry on performance used -4.5 kV for negative ion mode imaging of biological tissue.[7] Our experiments in the Farnsworth lab suggested that the high voltage setting was not as critical of a

parameter as the solvent and gas parameters for generating quality DESI images. Therefore, all mouse brain tissue images were recorded using negative ion mode with the high voltage power supply set to -5 kV. This setting was best for ionizing arachidonic acid (303 m/z) and other lipids and fatty acids in the 800-900 m/z range.

2.6 Mass Spectrometer Parameters

The mass spectrometer has a few voltage settings that can be tweaked for better signal intensity, better peak shape, a wider or narrower mass range, or a higher or lower mass range. The sniffer geometry design was studied with the hope of increasing signal intensity. The sniffer had two custom built modifications to help with stability and reproducibility of signal.

2.6.1 Mass Spectrometer Voltage Settings

Table 2.3: Mass Spectrometer Voltage Settings

Parameter	Setting
Capillary Exit	-150 V
Skimmer 1	-50 V
Hexapole 1	-23 V
Hexapole RF	315 Vpp
Skimmer 2	-22 V
Lens 1 Transfer	49 µs
Lens 1 Pre Pulse Storage	17 µs

The mass spectrometer (MS) voltage settings used for most of the tissue image runs are summarized in Table 2.3. A schematic of the MS voltage settings is shown in Figure 2.5. The

following list has MS voltage settings that are changeable depending on the sample and desired mass spectrum: capillary exit, skimmer 1, hexapole 1, hexapole RF, skimmer 2, lens 1 transfer, lens 1 pre pulse storage, and ion beam focusing lenses and TOF settings.
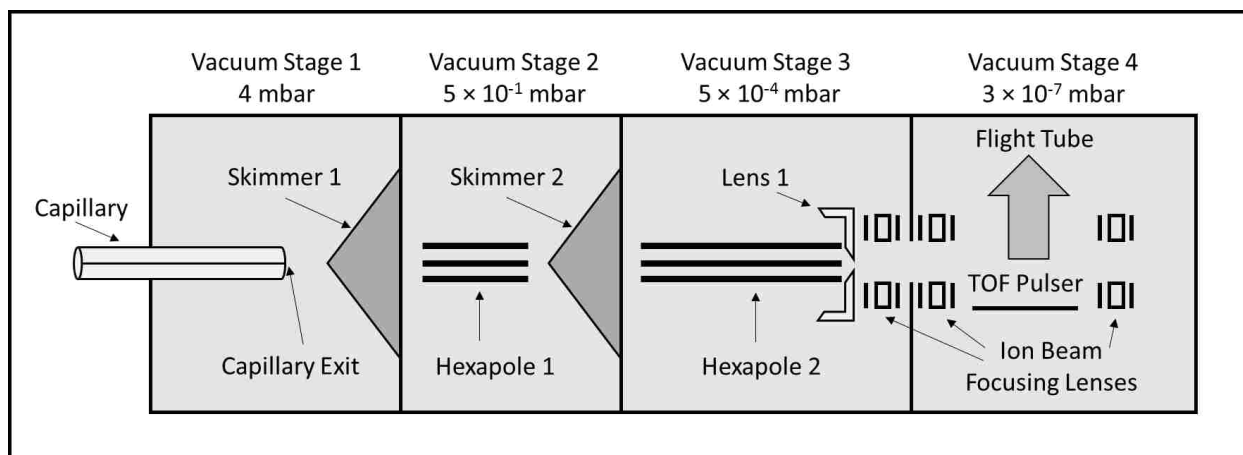
Figure 2.5: Schematic of the Mass Spectrometer Voltage Settings

The capillary exit voltage refers to the voltage applied to the end of the glass capillary that attracts ions from the sample surface through the sniffer into vacuum stage 1. The manufacturer recommends that the Skimmer 1 voltage be 1/3 of the capillary exit voltage and 10 V higher than the hexapole 1 voltage, but 30 V higher than the hexapole 1 voltage if the mass range is to be higher than 2000 m/z. Hexapole 1 voltage is not supposed to be changed since it does not have much sample dependency. Hexapole RF refers to the radio frequency voltage of both hexapole 1 and hexapole 2. Higher voltage setting of the hexapole RF allows higher m/z ions to pass through. Recommended settings for the hexapole RF are ~70 Vpp for 100 m/z, ~200-300 Vpp for 500 m/z and ~800 Vpp for 1500 m/z and higher. The hexapole RF was the most important voltage setting for determining the range of optimized m/z values.

Bruker recommends leaving the voltage applied to skimmer 2 unchanged, since it does not significantly affect the ions allowed to pass through. Lens 1 transfer is a time window that can be changed, depending on the m/z range desired. The longer the time window was set, the higher the m/z limit was for allowing ions to reach the TOF pulser. The recommended minimum value for the lens 1 transfer time is 10μs, and the maximum value is 10μs slower than the TOF pulse cycle or TOF Rep Time. Lens 1 pre pulse storage refers to the time allowed for the ions to collect in the TOF pulser before the pulser is turned on to detect the ions. In general, this pre pulse storage time allows for either more ions or fewer ions, depending on the time chosen, but the mass spectrometer manual also mentions that lower m/z ions can be seen when the storage time is increased. The recommended minimum lens 1 pre pulse storage time is 1 μs and the maximum time is 10 μs slower than the lens 1 transfer time. The ion beam focusing lenses and TOF settings are only optimized in Service Mode and are not to be touched based on sample ion optimization.

2.6.2   Sniffer Geometry Designs

Six custom sniffer designs were made by the Precision Machining Lab at BYU. The designs are included in Figure 2.6. A straight tube, an 18° blunt nose tube, a 10° blunt nose tube, an 18° tube with the tip cut to be parallel with the sample surface, an 18° tube with an angled tip, and an 18° tube with a squashed tip were the names to describe each of the six sniffer designs. From previous experiments, Wiseman et al. determined the optimum collection angle for maximum ion intensity to be 10° when the DESI spray angle was positioned between 55-75°.[8] Later, after computer simulations of the desorbed droplets in DESI, Costa et al. concluded that ions splashed off from the surface at angles ranging from 0 to 15°.[4]
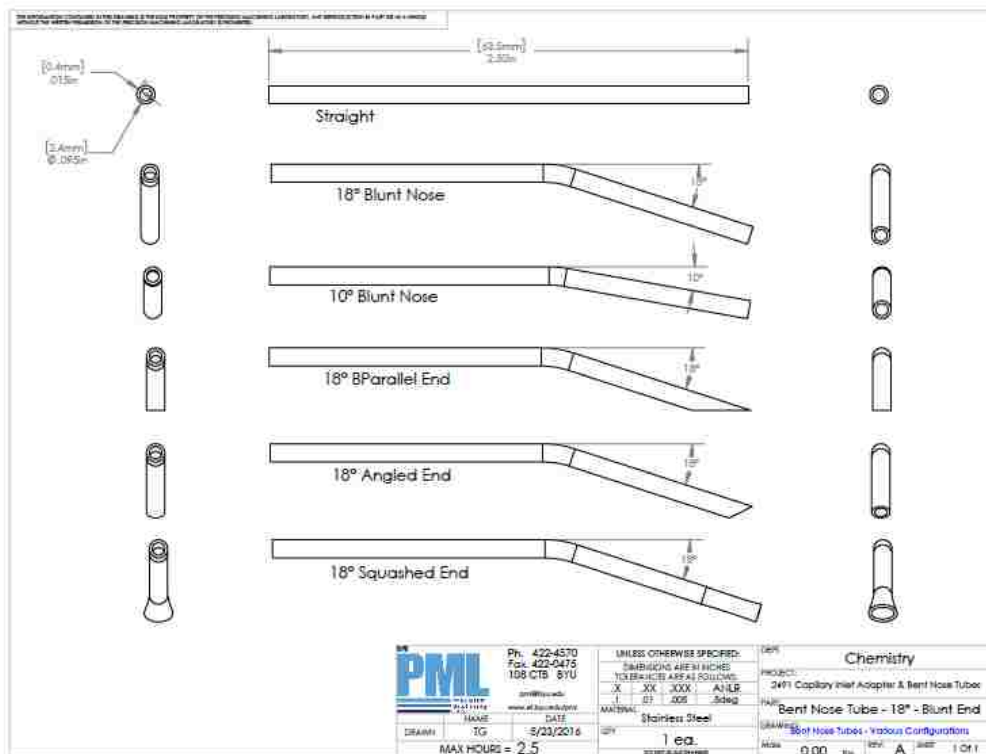
Figure 2.6: Sniffer Geometry Designs

When the six custom sniffer designs were tested to compare their performances, the differences were not as significant as they were predicted to be. The straight tube, however, resulted in signal intensities decreasing by half compared to the angled sniffers, so the straight tube was immediately eliminated from the sniffer options. The sniffer collection tip had more of an impact on signal intensity than the collection angle. The 18° tube with an angled tip and the 18° tube with a squashed tip both improved signal intensity by 25-30% when compared with signal intensity collected from the 18° tube with a blunt nosed tip. The improved signal intensity was attributed to more ions at the surface of the sample entering the wider entrance of the squashed sniffer tip and the larger entrance of the angled sniffer tip. The DESI spray angle was held constant at 55° for all comparative sniffer studies. With all angled sniffer designs, highest

28

signal intensity was achieved when the sniffer tip was as close to the sample surface as possible without scratching the tissue slice.

2.6.3   Capillary Bridge Support and Sniffer Clamp

The capillary bridge support (Figure 2.7) was designed and built to protect the glass capillary inlet of the mass spectrometer and to provide support and stability for the sniffer that slid onto the glass capillary. The sniffer clamp (Figure 2.8) was designed and built to prevent rotation of the sniffer because the sniffer was easily bumped when rastered across the tissue surface for a DESI scan. When the sniffer was bumped due to close proximity to the sample surface, the alignment of the DESI spray and the sniffer inlet was altered and the signal intensity decreased drastically.
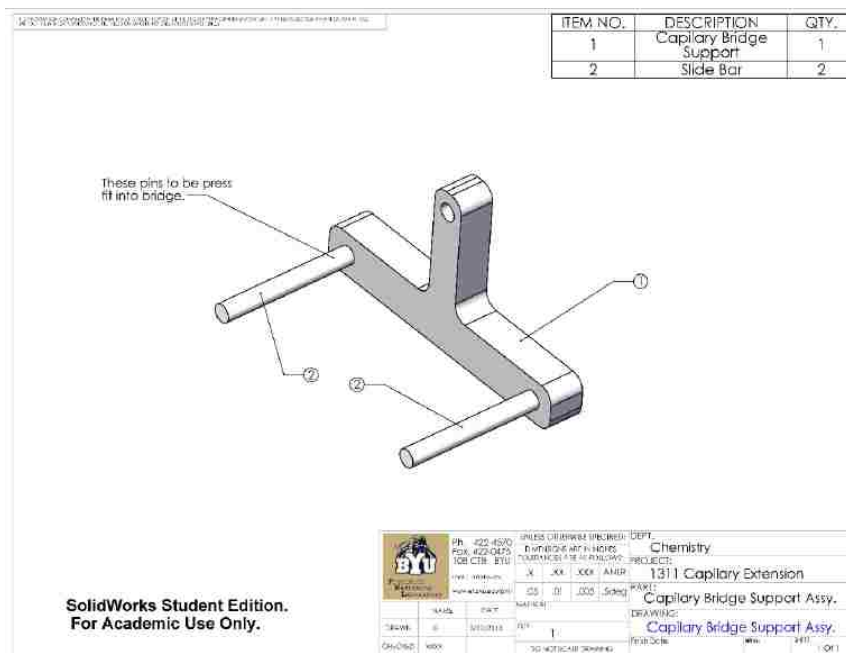
Figure 2.7: Capillary Bridge Support
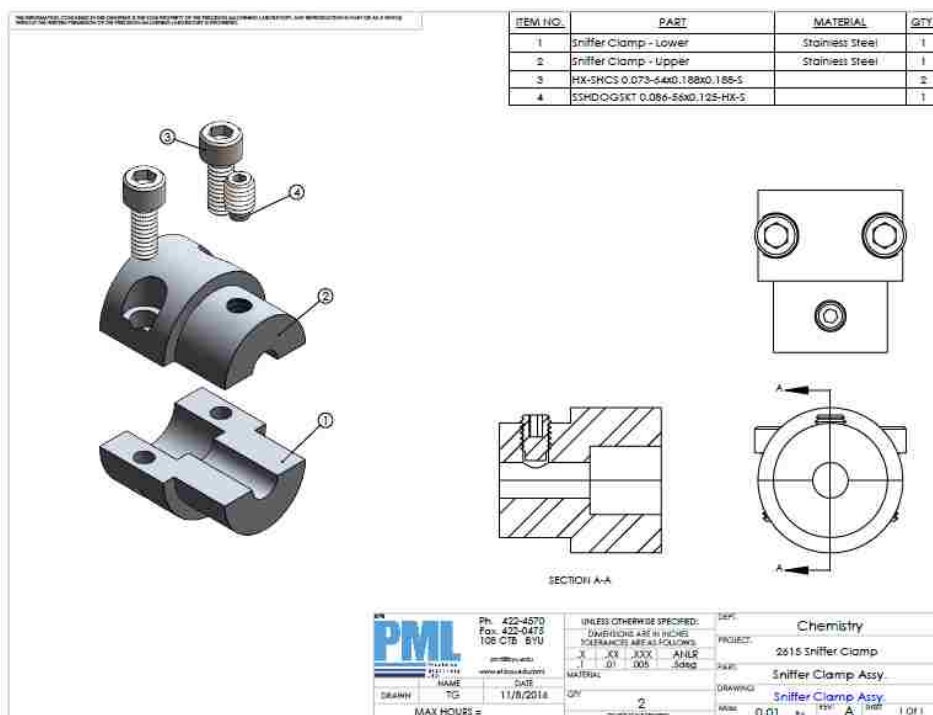
Figure 2.8: Sniffer Clamp

2.7 Imaging Parameters

Quality DESI images depended on stable signal intensity and good resolution, which were affected by the pixel size, solvent spot size and shape, and uniform surface charge. Pixel size was determined by the scanning rate of the sample beneath the DESI probe and the collection rate of the mass spectrometer. Solvent spot size and shape were dependent on the solvent and gas parameters described previously, such as the solvent flow rate, solvent capillary tip, gas pressure, and gas capillary tip. Uniform surface charge depended on proper grounding of the stage and sample holder.

2.7.1 Pixel Size/Scan Rate

The pixel size was determined by the motorized stage's scan rate and the programmed distance between row scans. The motorized stage scan rate was 75 µm/sec and the mass spectral acquisition rate was 1 Hz with a 2-spectra rolling average. Each row was separated by 150 µm, resulting in a pixel size of 75 µm × 150 µm. The solvent spot size was determined by the geometry parameters described in section 2.2 as well as the gas and solvent parameters described in sections 2.3 and 2.4, respectively. Minimizing the solvent spot size improved spatial resolution but sacrificed signal intensity. Therefore, a compromise was made between signal intensity and spatial resolution to have adequate DESI imaging capabilities.

2.7.2 Solvent Spot

The solvent spot was the best indicator of proper DESI optimization. The Nikon microscope eyepiece and Dino-lite camera were used to see the solvent spot on the tissue surface. Figure 2.9 shows how difficult the solvent spot was to see due to poor contrast with the mouse brain tissue. The perfect solvent spot was perfectly elliptical with stable solvent flow. A jumpy solvent spot or a nonsymmetrical ellipse were evidence of improper Taylor cone formation due to imperfect optimization of the following parameters: extension distance of the solvent capillary relative to the gas capillary, jagged edges of the gas capillary tip, improper gas pressure or solvent flow rate, clogging within either the gas or solvent capillaries, bubbles from a leaky solvent capillary, or unstable high voltage due to insufficient warmup time.
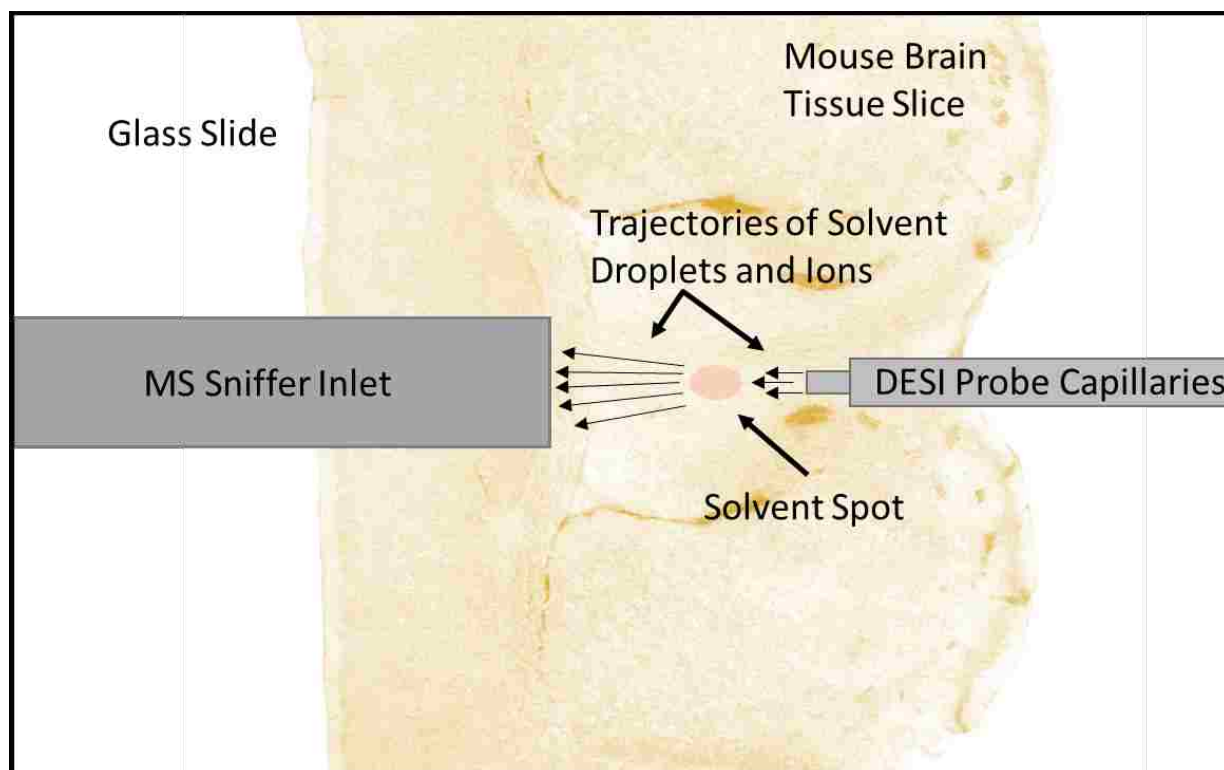
Figure 2.9: DESI Solvent Spot

2.7.3 Surface Charge Effects

After observations that static charge from a finger to the experimental table was enough to trigger the mass spectrometer to start or stop a scan, a more thorough investigation was taken to understand proper grounding techniques. Inconsistent and unreliable imaging was noticed as well due to the design and material of the glass slide holder.

A study was found by Gao et al. that focused on measuring the surface charge of DESI experiments in hopes of better understanding the ionization mechanism.[25] A custom built static charge measurement apparatus was used to measure the surface charge density to then model the

motion of the charged droplets. Gao concluded that pneumatic forces and vacuum suction were responsible for the movement of charged droplets toward the mass spectrometer inlet.

Knowing that surface charge was important for the DESI mechanism, we discovered that there needed to be uniform contact of the stainless steel slide holder to the glass slide. A drawing of one of the stainless slide holders is shown in Figure 2.10. Any holes in the stainless steel slide holder to reduce manufacturing costs caused a loss of signal when the DESI spray passed over that location so a solid metal slide holder was designed and built.
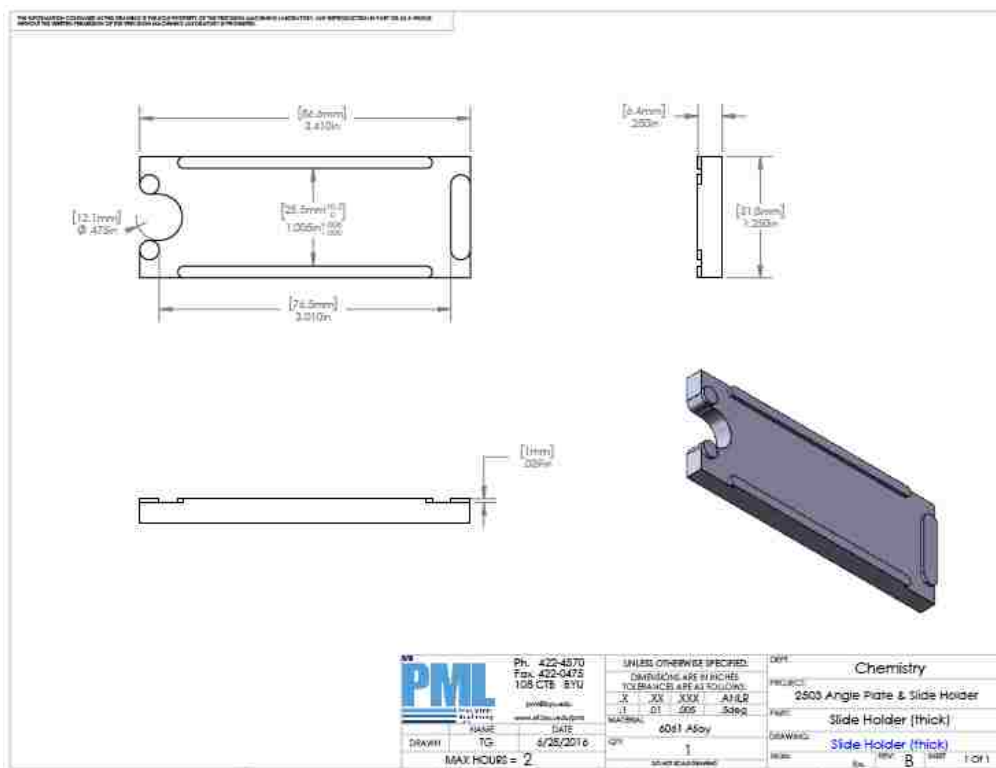
Figure 2.10: Slide Holder Design

Proper grounding was ensured by grounding the motorized stage and slide holder as well as the mass spectrometer and table to a common ground within the laboratory. Although an

33

occasional static charge still triggered the mass spectrometer, these grounding precautions greatly improved the consistency of the DESI imaging.

2.8   Steps for DESI Imaging with a Bruker MicrOTOF II Mass Spectrometer

The following routine was used to begin each DESI tissue scan. Details for why individual parameters were chosen are included in previous sections. Data processing after a tissue scan is discussed later in section 3.1.

1. Refill solvent syringe with pure methanol and push out any air pockets.

2. Set flow rate of syringe pump to 2.5 μL/min and push start then wait until solvent flows through the tubing and exits the DESI capillary tip.

3. Attach the sniffer inlet and support bridge to the mass spectrometer.

4. Turn on N_2 gas tank to 60 psi and wait for solvent spray to stabilize for 2-3 mins.

5. Slowly turn up N_2 gas to 160 psi.

6. Click 'operate' on MS computer screen for a negative ion mode DESI scan.

7. Turn on high voltage power supply to -5 kV.

8. Place glass slide with old brain tissue under DESI spray probe and sniffer inlet.

9. Raise sample stage up until MS sniffer inlet is < 1 mm from sample surface without scratching tissue.

10. Move DESI probe into position following the geometric parameters outlined in Table 2.2, being careful not to bump the solvent and gas capillaries since they are extremely fragile.

11. Check that the MS voltage settings match Table 2.3 and double check that all the DESI parameters match Table 2.1.

12. Lipid signal intensity for 303 m/z should rise at least to 1×10^4 but ideally to 1×10^5 or higher if DESI is optimized.

13. Once DESI signal is adequate and all settings are optimized, retrieve a tissue slice from the -80°C freezer.

14. Allow tissue slice to thaw under slight negative pressure for 20 minutes in portable desiccator.

15. Use a razor blade to remove any excess optimum cutting temperature (OCT) compound from around tissue to prevent edges peeling up and disrupting ion trajectories.

16. Replace test tissue glass slide with new tissue glass slide and repeat steps 10-13.

17. Position solvent spot at the bottom left of a tissue slice relative to the mass spectrometer as seen in Figure 4.2.

18. Open MATLAB program and 'run' the desimap program.

19. Prompts will ask for horizontal pixel size (75 μm), vertical pixel size (150 μm) and spectral rate (1 Hz).

20. After positioning at lower left as step 17 instructed, hit 'enter' on keyboard and then position at upper right corner of tissue slice and hit 'enter' again.

21. A few numerical values will appear relating to the final image size and predicted acquisition time. Remember the number of seconds each row will take.

22. Right click in the mass spectral window and select 'edit segment limit'. Type the number of seconds each row will take from step 21.

23. In the 'Mode' tab, click on the 'configure' button and double check that the mass spectrometer is in 'remote control' so that the MATLAB program can trigger the motorized stage and mass spectrometer to work together.

24. After all steps are complete and all settings are optimized, hit 'enter' on the keyboard one last time in the MATLAB window and the motorized stage should move the tissue slice back to the lower left starting position (step 17) and begin acquiring data for the DESI image by rastering across the tissue slice one row at a time.

25. When image is complete, turn off all parts of the DESI imaging setup.

3 SOFTWARE DEVELOPMENT OF THE MATLAB GUI IMAGE_INSPECTOR

3.1 File Conversions

During each DESI tissue scan, the Bruker MicrOTOF II mass spectrometer saved each row of tissue information to an individual file with a .d file extension. Free downloadable processing programs (msconvert[26] and imzML Converter[27,28]) were used to convert the .d original acquisition files to .mzML files and ultimately to a single .imzML file. Then this condensed .imzML file was converted into a MATLAB datacube using an adapted version of Georgia Tech's imzml_to_cube[29] MATLAB program. Paul Farnsworth created a program called image_inspector to allow users easy access to the mass spectral and image data in the data cube. His program incorporated some elements of another Georgia Tech MATLAB program.[29] Finally, I added the isotope ratio capability, statistical analysis, region of interest saver, and other features to Dr. Farnsworth's program to create the current version of image_inspector.

The following are required to make the file conversions from .d original mass spectral acquisition files to .mzML files then to a single .imzML file and then to a .mat MATLAB datacube.

1. Once the DESI tissue scan is complete, move all the .d files to a new file folder such as "new brain scan" with only those .d files in it.

2. Open the computer's command prompt in the start menu and do the following steps ignoring the quotation marks around what needs to be typed.

a. Type "D:" and hit 'enter'. This fetches the D drive on the computer.

b. Type "cd Data\Charlotte\new brain scan" or wherever the file folder is located from step 1 and hit 'enter'. This step finds the new folder created in step 1 with the .d files.

c. Type "msconvert *.d" and hit 'enter'. This step converts all the .d files to .mzML files and places them into that same folder. Wait 10-15 minutes for this step to finish.

3. Now on the Bruker mass spectrometer computer, open the imzML converter which should be in the imzML converter folder on the desktop.

a. Input the .mzML files by clicking the "Add" button and selecting all the .mzML files in the file folder created in step 1.

b. In the Image tab, make sure the button next to "continuous" is selected.

c. In the Scan tab, make sure the selections are "linescan left to right" and "flyback," which are instructions for how the DESI tissue scan was taken.

d. Click the "Convert" button, type in a filename for the final .imzML and .ibd files to be named, hit 'enter', and wait until the progress bar finishes.

4. Copy the final file folder which has .d, .mzML, .imzML, and .ibd files to the group drive.

5. On a computer with MATLAB installed, convert the .imzML and .ibd files to a final MATLAB file called a datacube. All detailed instructions for using the imzml_to_cube program and the image_inspector program are in Appendix A.

3.2   MATLAB datacube

The final datacube has four dimensions of data: x coordinate, y coordinate, m/z, and signal intensity. Mass spectral information was collected for each pixel for the entire brain tissue slice. For each x,y coordinate position, there is an entire mass spectrum which has signal intensity for each data point ranging from 200 to 900 m/z. Figure 3.1 demonstrates how the datacube can be imagined as a stack of ion intensity images for each m/z value.
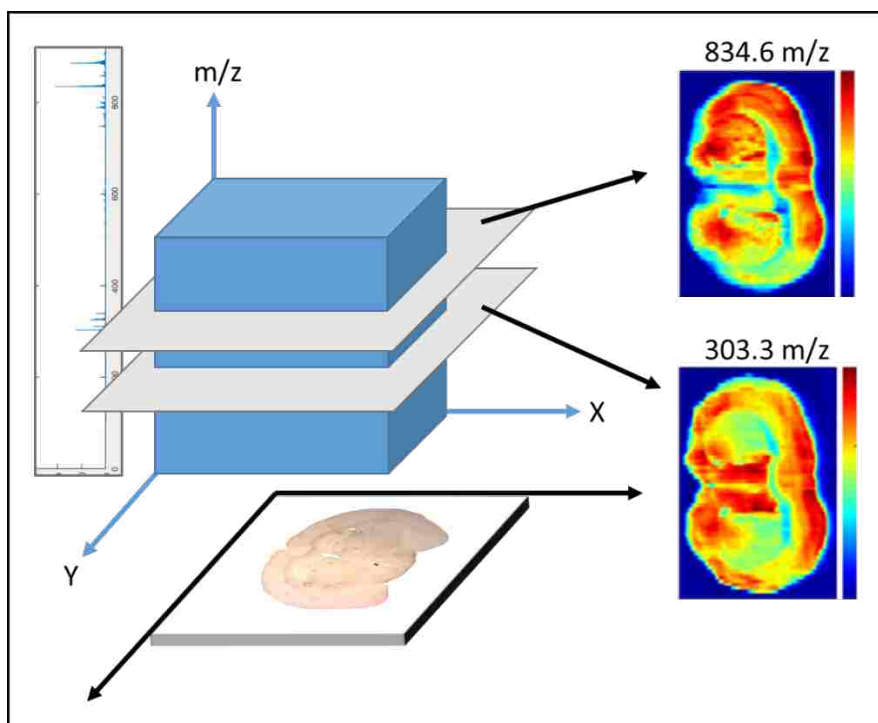
Figure 3.1: MATLAB Datacube

3.3   MATLAB GUI image_inspector

Detailed instructions for using the MATLAB graphical user interface (GUI) program image_inspector are included in Appendix A. Figure 3.2 shows a screenshot of the

image_inspector GUI program. Individual elements of the GUI program are described in further detail in this chapter.
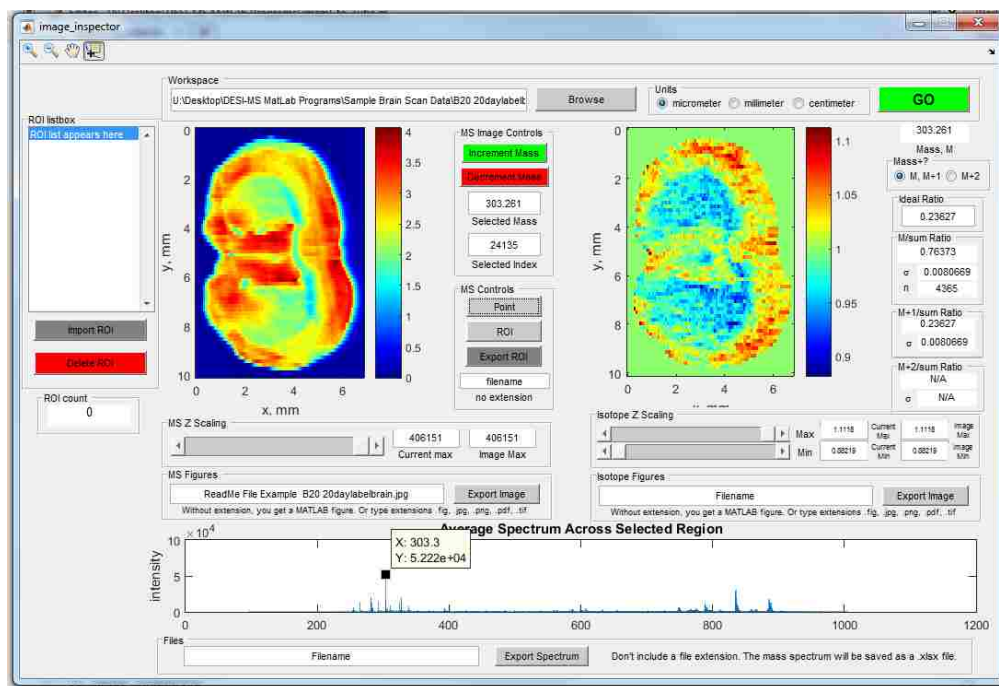
Figure 3.2: image_inspector Graphical User Interface (GUI)

3.3.1   Averaged Mass Spectrum

An averaged mass spectrum for the entire DESI scan appears at the bottom of the GUI as seen in Figure 3.2. When a region of interest (ROI) or a single pixel is selected, a new mass spectrum appears. In the case of a single pixel, the mass spectrum is for that pixel. For an ROI selection, the spectrum is the average of the spectra from the pixels within the ROI boundaries. Peaks in the averaged mass spectrum can be selected to show a concentration image of the entire brain scan at the selected mass.

40

3.3.2   Concentration Image

When a peak is selected from the averaged mass spectrum and the "Point" button is

clicked, a concentration image is generated on the left-hand side of the GUI. This concentration

image is created by summing the area beneath the selected peak for each individual pixel. The

area is calculated by summing the intensity of 12 points above and below the center of the

selected point as shown in Figure 3.3. The number of points to be included in the area was

determined by looking at the 303.3 m/z peak as well as the 834.6 m/z peak and ensuring the

entire peak area was included without including neighboring peaks.
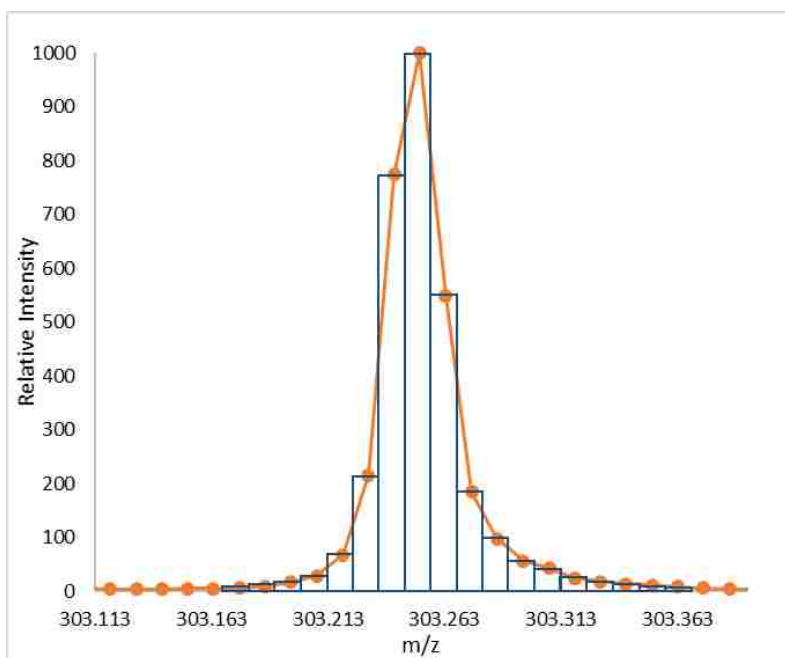
Figure 3.3: Calculating Area of Peak

The colormap is determined by setting the maximum pixel intensity to red and the lowest

pixel intensity to dark blue. "Jet" was the chosen among possible MATALB color schemes for

the colormap. The color scaling of the concentration image is manipulated by using the "MS Z scaling" panel which changes the maximum scale value corresponding to red.

3.3.3   Isotope Image

Creating the isotope ratio image on the right-hand side of the GUI was more complex than displaying a concentration map. The idea of the isotope ratio image came from wanting to see if deuterium was regioselectively incorporated by different lipids and fatty acids and to see if the rates of incorporation could be measured. Figure 3.4 and Figure 3.5 show the mass isotopomers of phosphatidylserine (40:6) (834.6 m/z) and an arachidonic acid isomer (303.25 m/z), respectively. As deuterium was incorporated into the body, the mass isotopomer pattern of the lipids changed due to the heavy nature of deuterium compared to hydrogen.
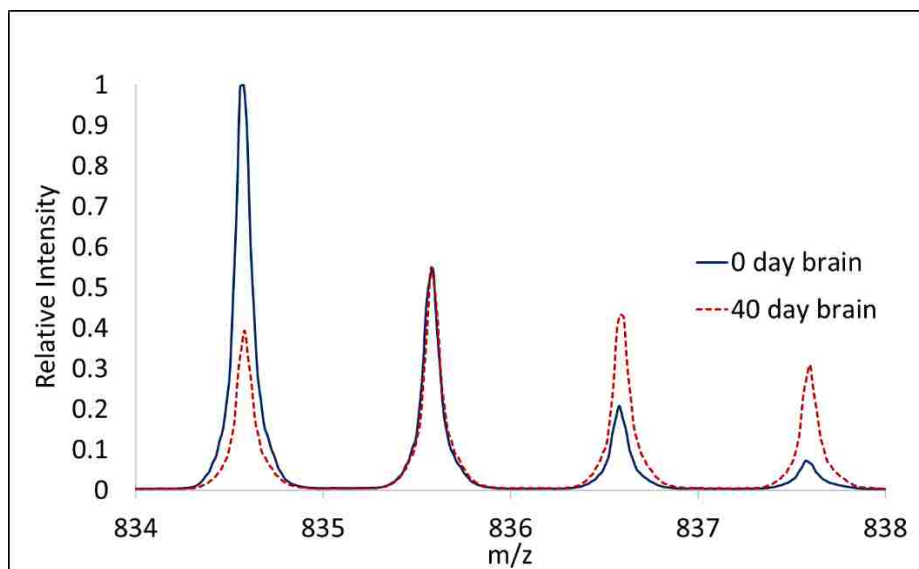
Figure 3.4: Mass Isotopomer of Phosphatidylserine at 834.6 m/z

42

As illustrated in Figure 3.4, the sample from a mouse that had been on a deuterium enriched diet for forty day has an isotopomer distribution shifted to higher masses compared to the unlabeled sample. Figure 3.5 shows a less noticeable change in the isotopomer distribution but still significant for the study. The isotope ratio image was designed to calculate the ratio of the M peak to the M+1 peak and show the isotope ratios visually for each DESI scan of brain tissue.
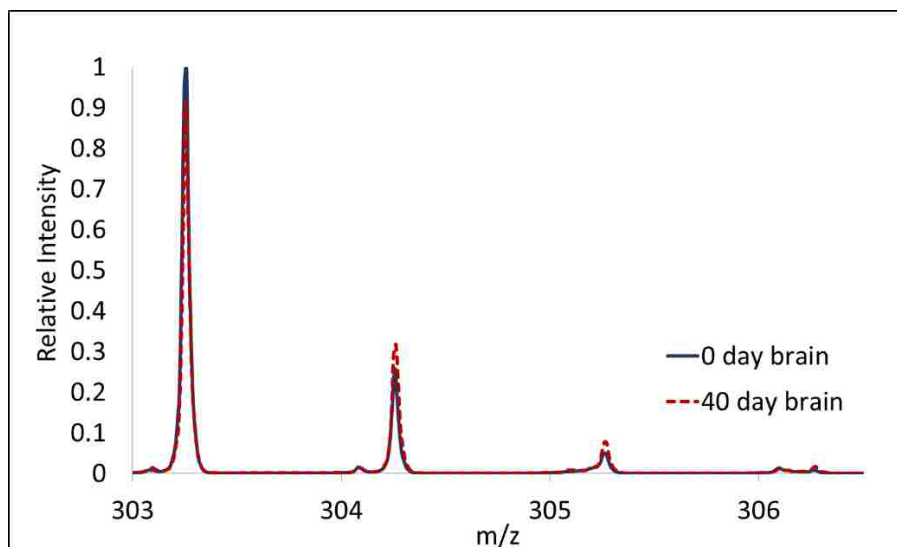
Figure 3.5: Mass Isotopomer of Arachidonic Acid Isomer at 303.3 m/z

Isotope ratios are included in an image based on the following criteria. The program calculates a pixel intensity for the M peak below which an isotope ratio will not be calculated. The threshold is arbitrarily set at the maximum intensity in the concentration image divided by seven. The corpus callosum region usually does not meet the threshold, since the concentration of most species in that region is low. Technically this threshold is different for each compound and brain scan. The lower the concentration in the brain for a specific compound, the lower the

threshold level is, leading to more potential interferences from background species in the calculation of the isotope ratio. Knowing that the mass spectral images were acquired at atmospheric pressure, background compounds present in the atmosphere could not be eliminated. For better results, the mass spectrometer should have been optimized for a specific lipid in a narrow m/z range. However, since the mass spectral range was broad in these studies to allow monitoring of multiple fatty acids simultaneously, the maximum intensities suffered and the background ions had a larger effect than desired.

After the threshold is determined, the isotope ratios of the M+1 peak divided by the sum of the M and M+1 peaks are calculated for each of the pixels that meets the concentration intensity threshold. An isotope ratio image is created using the same colormap and scaling approach that is used in the concentration image. The colormap of the isotope ratio image can be manipulated by using the "Isotope Z scaling" panel, which changes the maximum scale value corresponding to red or the minimum scale value corresponding to blue. The "Ideal Ratio" box in the GUI is used to create a more meaningful isotope ratio image. Changing this box to the (M+1)/sum average output changes the center value of the colormap so that deviations above and below this average are observed. A known ratio for a specific m/z can also be used for a specific compound to see deviations from the ideal.

3.3.4   Region of Interest Selection

The region of interest (ROI) button was designed initially to generate an averaged mass spectrum from only those pixels located within the ROI boundaries. Now that the isotope ratio image has been incorporated, the ROI button calculates an averaged isotope ratio and the standard deviation of that ratio for all the pixels within the ROI.

The "ROI listbox" located on the far left side of the GUI as seen in Figure 3.2 saves any regions of interest to be recalled at a later date. When a ROI is selected and uploaded, the isotope ratio is recalculated and the averaged mass spectrum is graphed. More details about using the ROI functions are in Appendix A.

4   INITIAL MOUSE BRAIN STUDY

4.1   Research Workflow

Collaborating with Dr. John C. Price's research group, we used DESI mass spectrometric imaging to measure spatially regulated *in vivo* metabolic rates in mice. We were responsible for the DESI imaging and isotope ratio processing. The Price lab was responsible for properly labeling the mice with deuterium by altering their water intake, reproducibly slicing brain and other tissue using a cryostat, thaw mounting the tissue slices to glass slides, and helping determine the incorporation rates of individual lipids after DESI imaging. The work flow of the research is outlined in Figure 4.1 with the Price lab responsible for step one and step six. Steps two through five were primarily our responsibility. The DESI source was optimized for mouse tissue imaging as described in Chapter 2, data conversion software was created to convert the mass spectrometer .d files to a MATLAB datacube as described in Chapter 3, and a MATLAB graphical user interface was designed to process the large quantities of mass spectral data acquired from each tissue scan as described in Chapter 3 and Appendix A. More details are provided in this section about key steps in the research workflow as well as an analysis on preliminary results found using our image_inspector program.
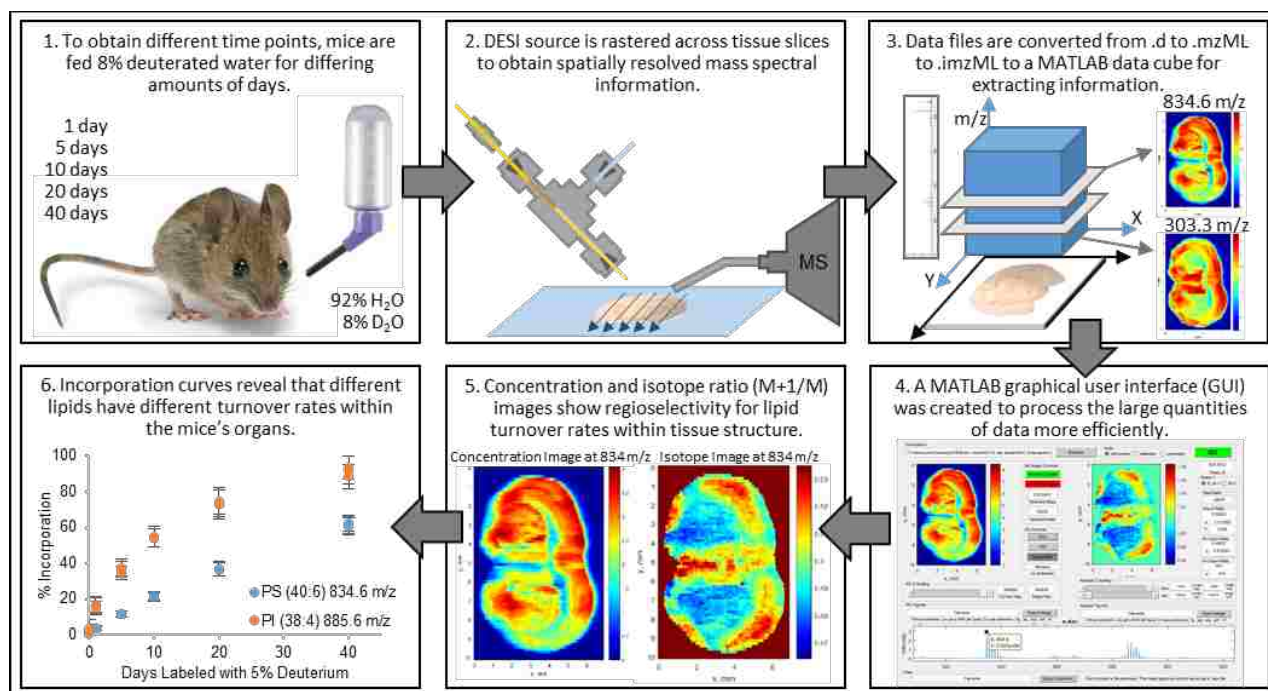
Figure 4.1: DESI Research Workflow

4.1.1 D$_2$O Labeling of the Mice

All mice in this study were treated and cared for at Brigham Young University (BYU) following the Public Health Service Policy on Humane Care and Use of Laboratory Animals. All experiments were approved by the Institutional Animal Care and Use Committees of BYU. Female mice, ranging in age from 13-16 months, were housed in groups of five. A few mice were saved as control mice. All experimental mice were given an intra-peritoneal (IP) injection of saline deuterium oxide (0.9% w/v NaCl, 99.8% D2O). 15μL of the saline solution was injected per gram body weight. After this initial IP bolus, mice were fed food and 8% deuterium enriched drinking water for the duration of the experiment as seen in Figure 4.1. Therefore, the mice experienced a 2 molar percent excess (MPE) initially and then their bodies rose to 5 MPE during the following 10 days. Ideally, the mice should have been given an initial IP injection that

spiked their bodies to 5 MPE but laboratory calculation errors forced us to measure the deuterium enrichment in each animal by collecting daily urine samples. Mice were humanely killed with carbon dioxide anesthetization and cardiac puncture at the end of days 1, 5, 10, 20, and 40. Brain tissue was immediately harvested, flash frozen on dry ice, and stored at -80°C. Blood cells from the plasma were centrifuged for 10 minutes at 800xG and 4°C and then stored at -80°C.

4.1.2   Tissue Preparation

The age of the tissue[30] and the surface properties[31] of the tissue have both been shown to have a negative effect on image quality and lipid signal intensity. When prepping the tissue and storing the tissue, temperature and time were both important factors that affected image quality. Dill et al.[30] examined the effects of storage time at -80°C, time left at room temperature before scanning, and the number of freeze/thaw cycles. Longer than 7 months of storage at -80°C caused a reduction in lipid signal intensity. Degradation of the tissue was noted when tissue was left out at room temperature for longer than 24 hours. Degradation was defined as an appearance of fatty acid dimers. Increasing degradation was also noticed after each freeze/thaw cycle of a tissue slice. Dong et al.[31] explored the effects of semi-quantitative detection of organic acids in grapevine stems. They concluded that variations in the tissue surface greatly affected the detection of the analyte and careful attention needed to be made when interpreting DESI imaging results because normalization strategies were not entirely effective. Although Dong's study was not on tissues from animals or humans, the conclusion from this study is still applicable for DESI imaging of animal tissue.

With the knowledge from these studies about tissue preparation and with guidance and recommendations from the Fernandez group,[11] we determined the following procedure to be best for our research methods. We coronally cut the mouse brains immediately after they were dissected and flash-frozen on dry ice. Then, the frozen forebrains were mounted to the chuck of a Thermo Scientific Microm HM550 cryostat with VWR Clear Frozen Section Compound and flash-frozen using liquid nitrogen. With the temperature of the cryostat set to -15°C, 50 μm thick sections were sliced and thaw-mounted onto VWR Superfrost Plus glass slides. Slices were re-frozen on dry ice and stored at -80°C until ready for DESI imaging. Before DESI imaging, tissue slices were thawed at room temperature under slight negative pressure for approximately 20 minutes as described by the Fernandez group.[11] Using a razor blade, the remaining mounting compound was sliced and peeled away from the brain slice to prevent the compound from drying out, lifting up, and blocking the ions from entering the MS inlet during a DESI tissue scan.

Careful attention was given during cryosectioning of the brains to prevent tissue slices from folding over onto themselves and from tearing. The cryostat blade was replaced before each brain was sliced. The glass slides were angled and slowly tilted to help the tissue slices thaw-mount slowly and smoothly without trapping bubbles or tearing. Ideally, two slices were placed on each glass slide. A less than perfect tissue slice was used to optimize DESI settings before running a scan on a better-looking tissue slice.

4.1.3   DESI-MS Imaging

A Bruker MicrOTOF II mass spectrometer coupled with our laboratory-constructed DESI source, described in Chapter 2, was used to acquire DESI images. Our motorized, programmable translational stage (Prior Scientific, Rockland, MA, U.S.A.) communicated with the mass

spectrometer to raster the tissue samples and obtain mass spectral data one pixel (75 µm × 150 µm) at a time as seen in Figure 4.2. A custom-machined glass slide mount was used to hold the tissue samples in place on the stage. The MATLAB code used to communicate with the stage and the mass spectrometer is included in Appendix B.
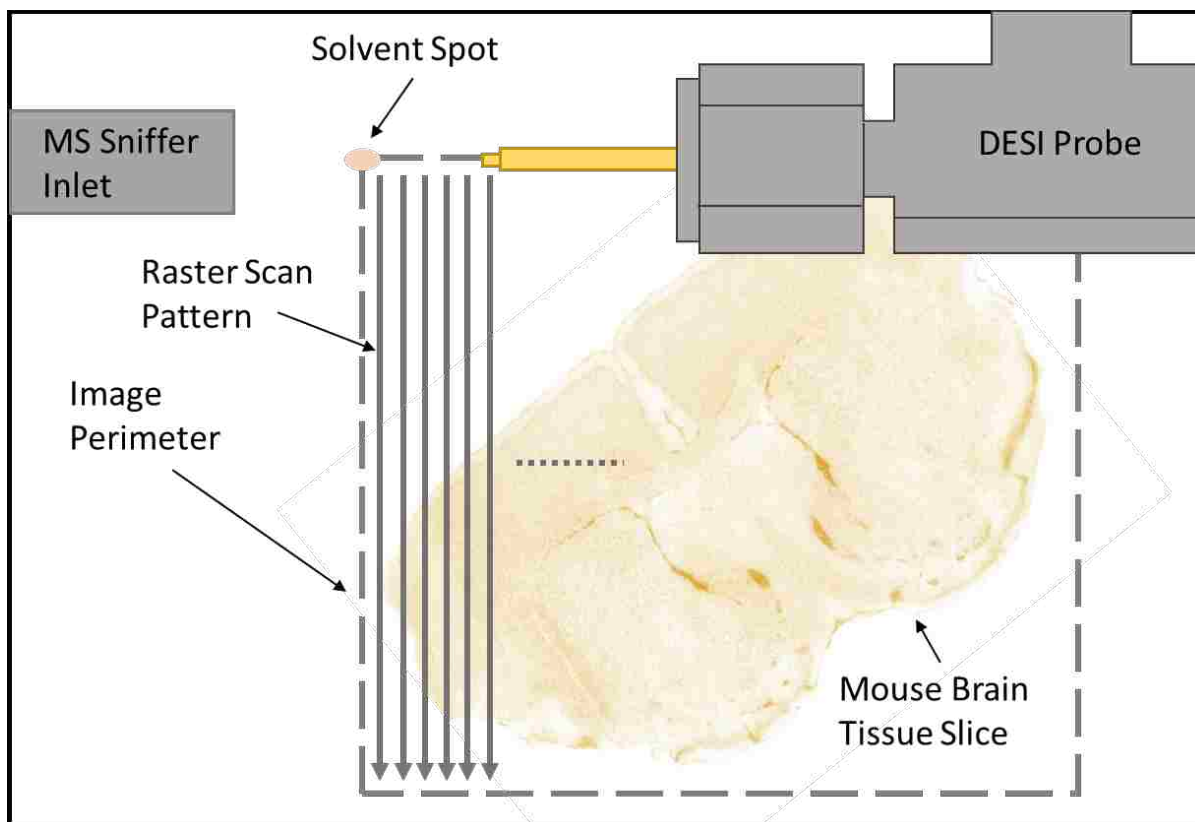

Figure 4.2: Raster Pattern for DESI Imaging

4.1.4   Image_inspector Analysis

After the DESI source was used to image the mouse brains, MATLAB was used to process the large mass spectral data files and create concentration and isotope ratio images with

color maps for visual appeal and clarity. Four lipids were selected for detailed study because they had the highest intensities in the mass spectrum, unique regiospatial concentration patterns, tentative assignments from another published research study,[8] and mostly clean M+1 peaks for monitoring isotope ratio changes. An arachidonic acid isomer (AA), docosahexaenoic acid (DHA), phosphatidylserine 40:6 (PS), and phosphatidylinositol 38:4 (PI) were the four lipids highlighted in this research study as seen in Figure 4.3, Figure 4.4, Figure 4.5, and Figure 4.6, respectively. The first two columns in these four figures contain isotope ratio images with burgundy backgrounds. The last column contains concentration images with a blue background.

Signal intensity in the DESI images for a chosen m/z value is directly related to the concentration of that particular compound. However, signal intensity can also be affected by the tissue type, optimization of DESI parameters, tissue surface roughness, and changes in the surrounding atmosphere during a DESI scan. Although many variables affected the consistency of the signal intensity, with variations particularly noticeable in the concentration images, the spatial distribution of the lipids was consistent with classical brain structures for each of the four targeted lipids. For instance, the signal intensity of PS (Figure 4.5, right column) in the DESI images for all the different time points of the experiment showed that the relative concentration of PS was higher in the cerebral cortex and caudoputamen and lower in the corpus callosum.

When comparing the changes in the signal intensities in the concentration images with the changes in the isotope ratios for the four lipids, we noticed they are not necessarily linked, particularly for AA, PS, and PI (Figure 4.3, Figure 4.5, Figure 4.6). If we look at the isotope ratio images that have been scaled linearly for the entire 40-day-long experiment (global scaling), we see a change in color for the entire brain, suggesting that new lipid is being synthesized throughout the entire organ. Looking at the isotope ratio images that are scaled to emphasize

52

variations within each image (independent scaling), we notice small but measurably faster turnover rates in different parts of the brain for individual lipids. The symmetry of each isotope ratio image resembles the structure of a typical mouse brain, which reduces the possibility that transient fluctuations are responsible for the changes. The isotope ratio images are much more robust than the concentration images because ionization efficiency does not affect the isotopomer distribution ratios. Heavy and light versions of each lipid are chemically identical to one another and therefore respond the same during DESI imaging.

AA (Figure 4.3) was observed to have relatively high concentrations everywhere in the brain tissue except for parts of the caudoputamen region and the corpus callosum. Lipid turnover rates were observed to be slower in the caudoputamen and corpus callosum regions as well. This correlation suggests that AA is synthesized and degraded locally.

DHA (Figure 4.4) was found mostly in the cerebral cortex. Unlike the other three lipids studied here, DHA had a very small change in the isotope ratio suggesting that lipid turnover is minimal throughout the entire brain. DHA is considered conditionally essential in the diet and so these results were not surprising. Noisy isotope ratio images, particularly noticeable in the global scaling column, were partially caused by a background peak interfering with the M+1 peak. When the background peak varied in intensity from scan to scan, the linearity of the global scaling for the isotope ratio images was noticeably affected.

Looking at the independent scaling of the isotope ratio images for PS (Figure 4.5), there was a small but measurably faster turnover rate in the septal nucleus and a subsection of the cerebral cortex. Slightly slower turnover was observed in the caudoputamen region and corpus callosum. The concentration images revealed relatively high concentrations of PS throughout the entire brain except for the corpus callosum.

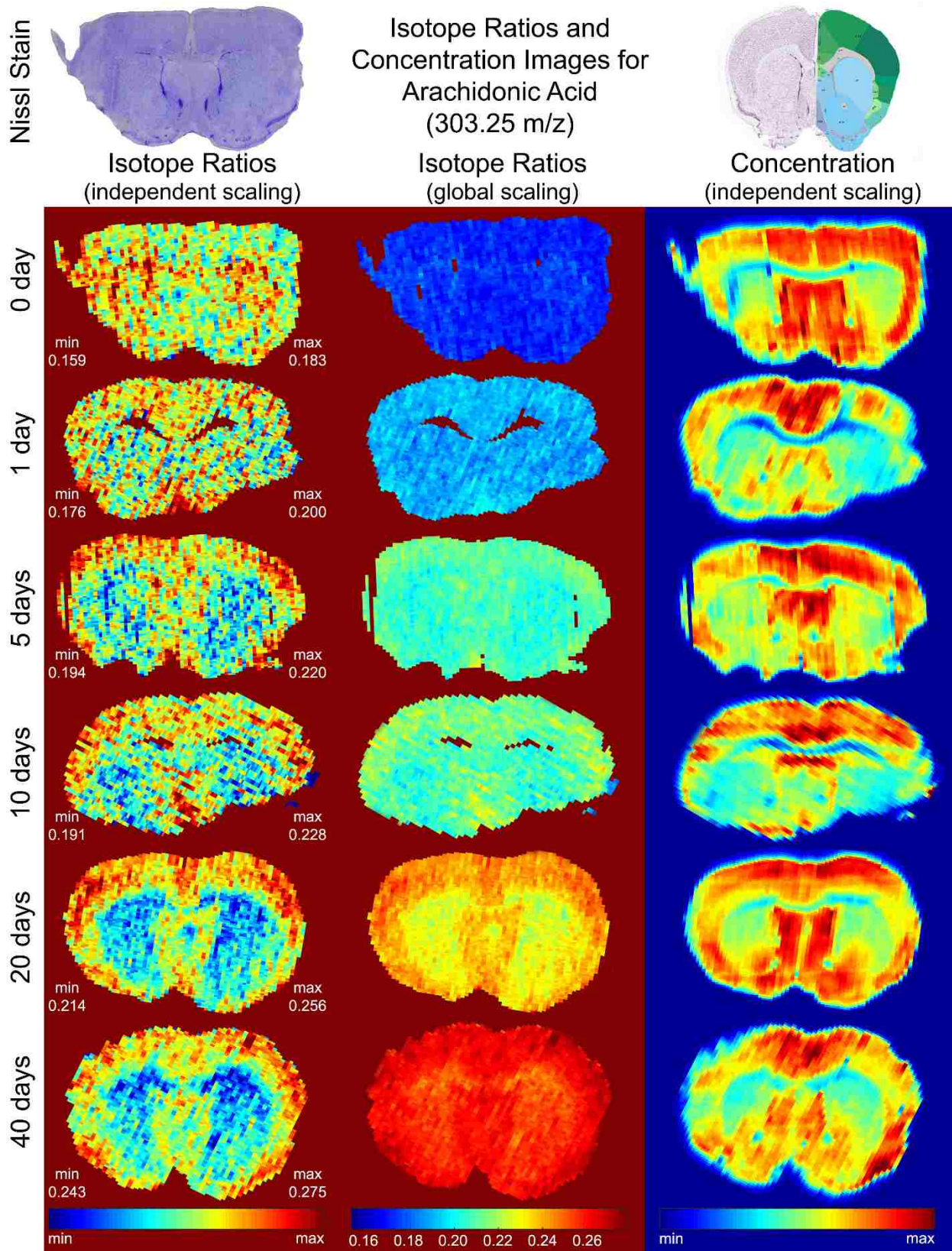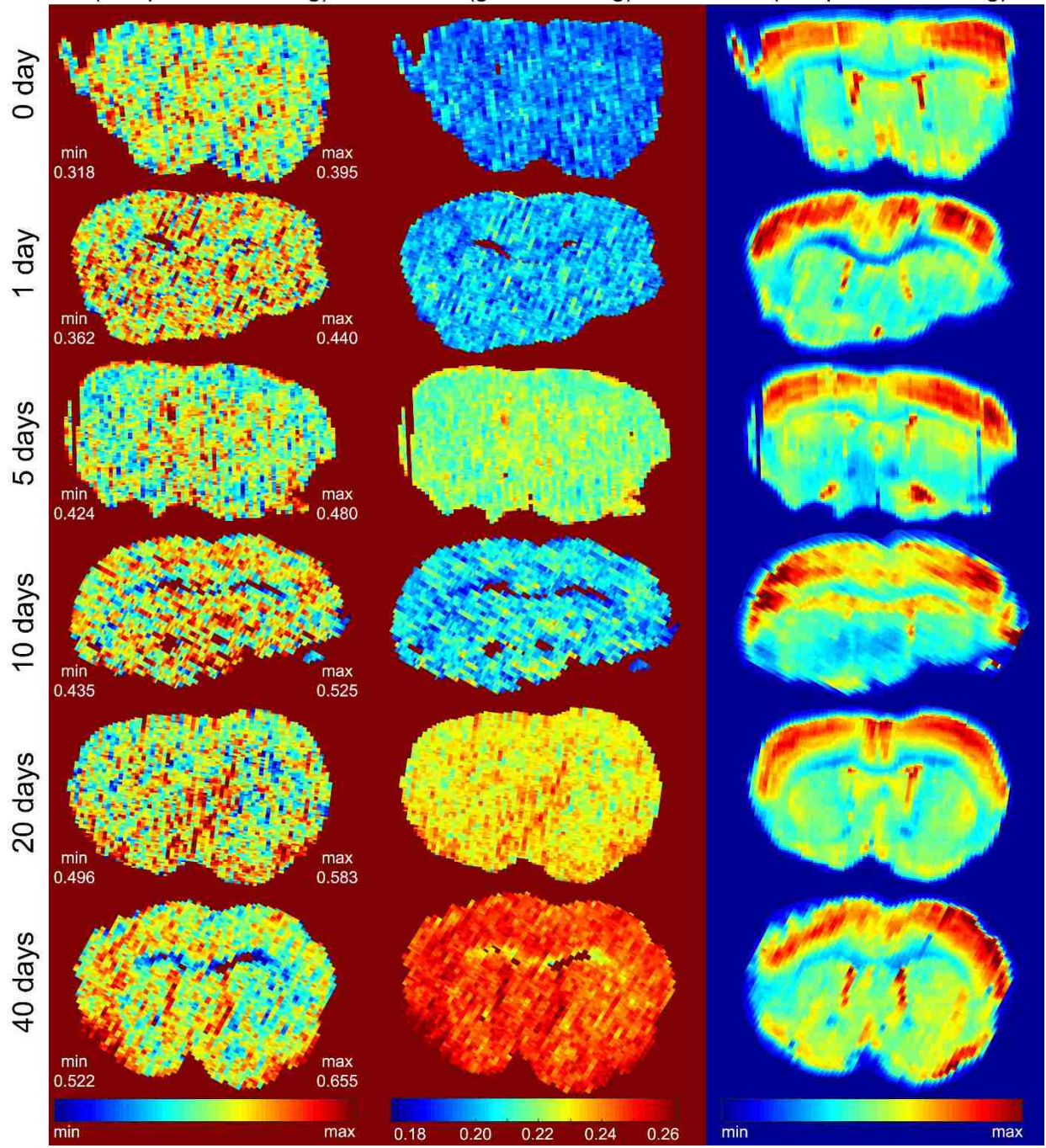*Figure 4.3: Concentration and Isotope Ratio Images for 303.25 m/z*

Figure 4.4: Concentration and Isotope Ratio Images for 327.3 m/z
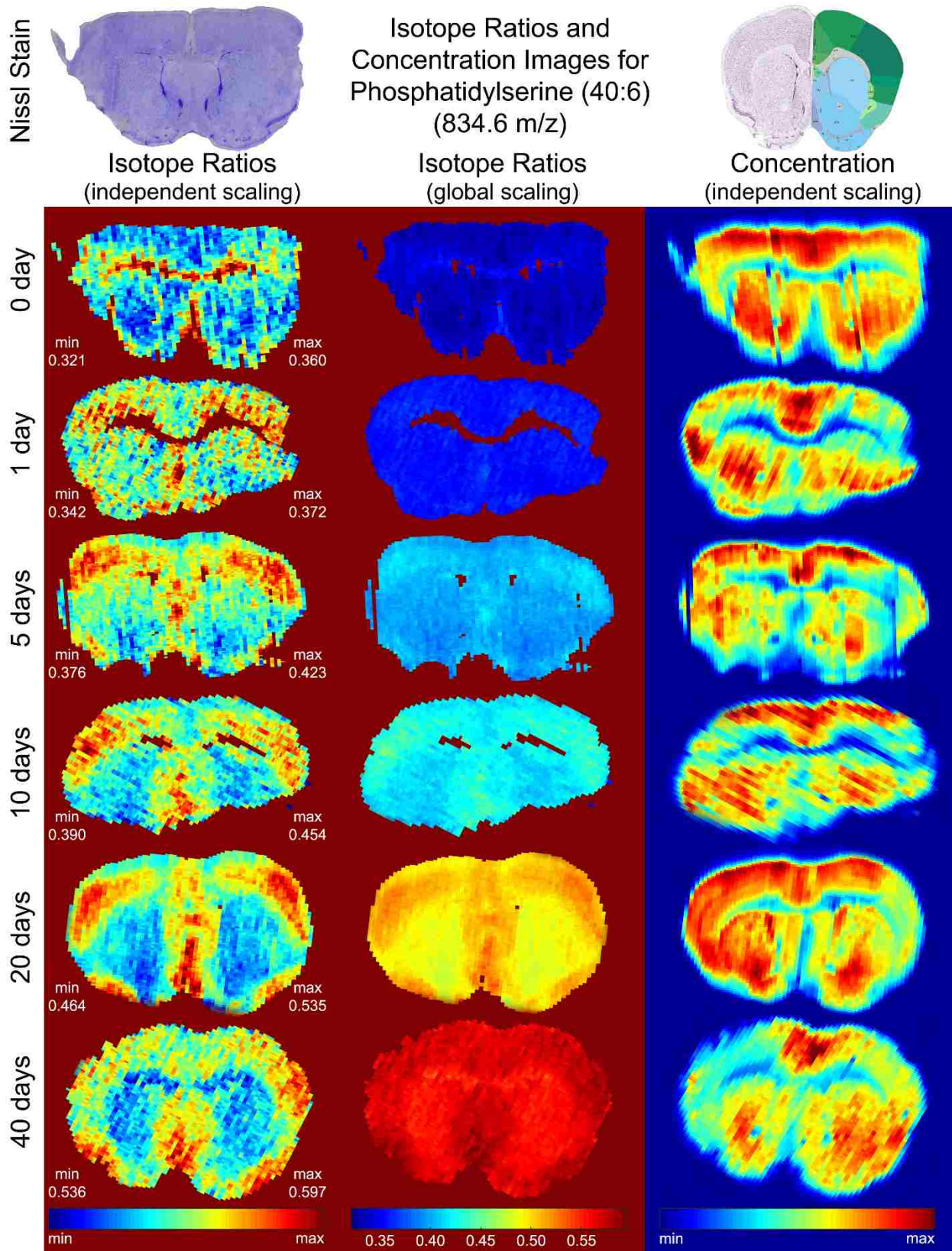
Figure 4.5: Concentration and Isotope Ratio Images for 834.6 m/z
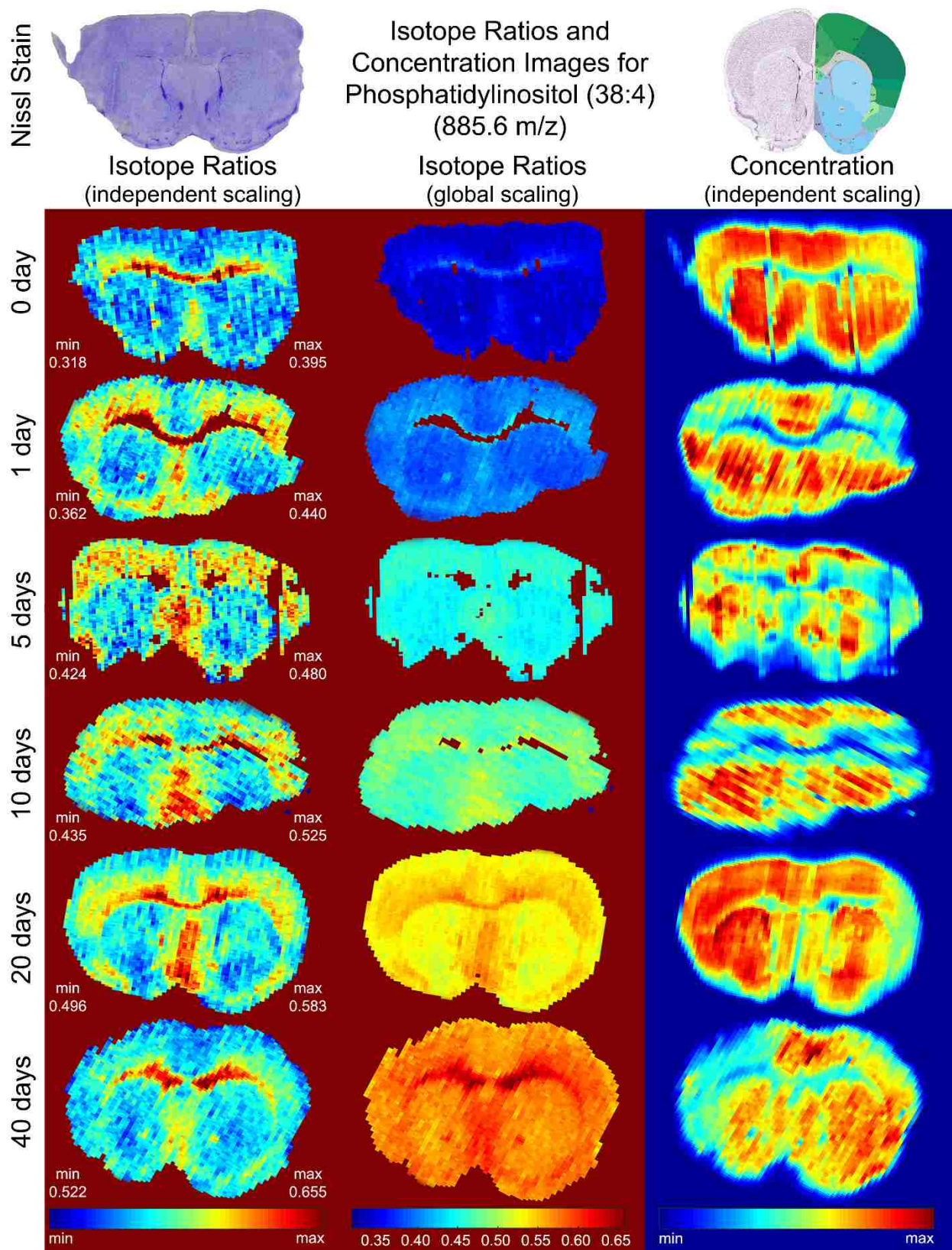
Figure 4.6: Concentration and Isotope Ratio Images for 885.6 m/z

PI (Figure 4.6) was observed to have similar concentration images to PS. Relatively high PI concentrations were found throughout the entire brain except for the corpus callosum. However, the isotope ratio images for PI varied dramatically from the isotope ratio images for PS. The fast turnover occurred in the corpus callosum where the concentration was relatively low. Therefore, the body must either synthesize and immediately degrade this lipid locally in the corpus callosum or the body synthesizes and distributes this lipid to the surrounding areas from the corpus callosum.

4.1.5   Incorporation Curves

Figure 4.7, Figure 4.8, and Table 4.1 were created by Richard Carson and Dr. John C. Price. These figures and this table are used with permission to explain how DESI imaging was used to measure *in vivo* metabolic rates.

Figure 4.7 shows how the experimental and simulated mass isotopomer distribution changed over time as more deuterium was incorporated into a mouse's lipids. The initial isotopomer distribution pattern at time point zero days came from the natural isotope abundances of carbon, nitrogen, oxygen, and hydrogen. Over time, the main mass peak (M0) intensity decreased and the M+1 (M1) and M+2 (M2) peak intensities increased as more deuterium was incorporated from the deuterium enriched drinking water. We calculated the number of covalent deuteriums sites (*n*) for each lipid (Table 4.1) after we measured the D_2O enrichment in the mice and optimized the isotopomer simulation to match the experimental data. AA, PS, and PI each had a single best *n* value that minimized the deviation between the experimental and theoretical isotopomer distributions, as previously described.[19,32] We could not determine a unique *n* value

for DHA because this lipid had a small overall change in the isotopomer distribution and had interferences from nearby molecules.
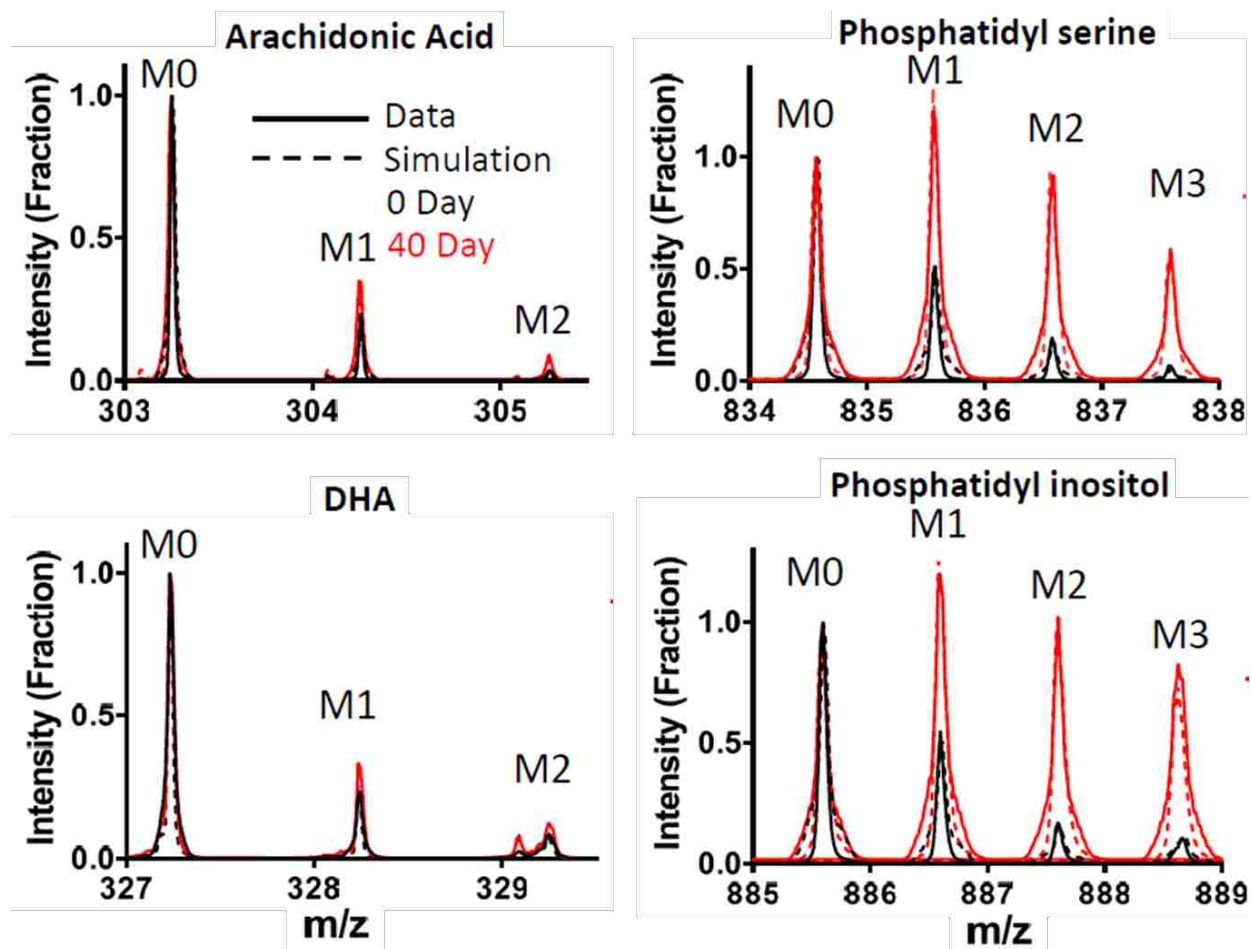
Figure 4.7: Comparison of Experimental and Optimized Simulations of Lipid Isotopomers

High-resolution mass spectra were used to measure independent turnover rates (k) for multiple lipids simultaneously. These calculations were previously described for peptides by Price[32,33] and others,[34,35] but this was the first time lipid turnover rates were measured using DESI-MS. Turnover rates (k) for the cerebral cortex (CO) and caudoputamen (CA) regions of the

brain were calculated by averaging the mass spectra in those regions using our image_inspector program and using the scipy package in python for the recursive, non-linear regression fit. Differences in the calculated k values for the CA and CO regions were statistically significant for AA, DHA, and PS as seen by the asterisks in Table 4.1.

Figure 4.8 shows the kinetic curves for each of the four major singly-charged ions observed in our DESI mass spectra. The kinetic curves show that lipids vary in their turnover rates as well as their percentages of biosynthesized lipid compared to dietary lipid. As lipids are biosynthesized within the body, protons and deuteriums are incorporated from the water available within the body. The number of deuteriums incorporated depends on the deuterium enrichment of the body water at that time, which was measured from the urine and plasma of each mouse. Table 4.1 summarizes the common lipid name, observed ionic mass, elemental composition, number of deuterium sites, calculated turnover rates for the CA and CO regions, and the percentage of biosynthesized compared to dietary lipid for the four lipids in this study.

More details on calculating the *n* values and *k* values for each of these four lipids can be obtained from Richard Carson and Dr. John C. Price. A brief summary has been provided here in this thesis to help describe the collaborative efforts of using DESI-MS imaging for measuring spatially regulated *in vivo* metabolic rates.
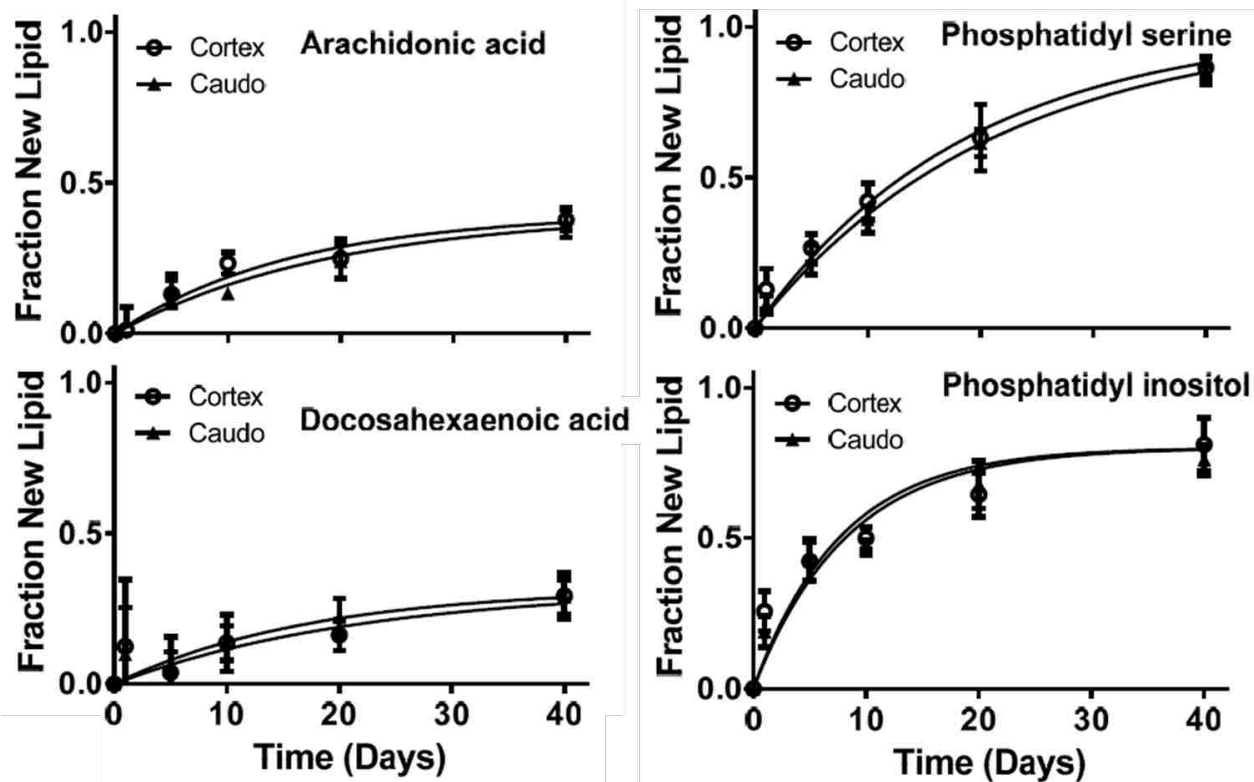
Figure 4.8: Kinetic Curves for the Four Lipids: AA, DHA, PS, and PI

Table 4.1: Common Name, Observed Ionic Mass, Elemental Composition, Number of Deuteriums, Turnover Rates, and Percentage of Biosynthesized Lipid for the Four Major Singly Charged Ions Observed in our DESI-MS Spectra

Lipid	m/z	Formula	n	k in CA	k in CO	%
Arachidonic Acid*	303.25	$C_{20}H_{32}O_2$	6	0.051±0.005	0.063±0.007	40
Docosahexaenoic Acid*	327.25	$C_{22}H_{32}O_2$	~8	0.057±0.019	0.045±0.010	32
Phosphatidylserine*	834.6	$C_{46}H_{77}NO_{10}P$	21	0.053±0.003	0.047±0.001	100
Phosphatidylinositol	885.6	$C_{47}H_{82}O_{13}P$	27	0.121±0.012	0.129±0.016	76

4.2 Nissl Staining

A protocol, copyrighted from Viapiano Lab in 2007, was used for cresyl violet staining or "Nissl staining" of the mouse brain tissue slices. The protocol involved using 100% methanol as

the volatile fixative and then dipping and rinsing the slide in the following solvents: 10 mM

phosphate buffered saline (PBS), double distilled water (ddH$_2$O), Nissl stain, 90% ethanol, 95%

ethanol, 100% ethanol, and 100% xylene. The Nissl stain was composed of 0.1 g cresyl violet

acetate, 100 ml ddH$_2$O, and 250 µl glacial acetic acid. Permount mounting medium (Fisher

Scientific, Pittsburgh, PA, U.S.A.) or a similar mounting compound was used to preserve the

Nissl stained tissue slices before analysis under a microscope. Figure 4.9 is an example of a Nissl

stained mouse brain tissue slice. DESI imaging did not have a noticeable effect on the tissue

quality after two tissue slices of mouse brain, one of them DESI imaged and one not, were

stained and compared under a microscope.

Figure 4.9: Nissl Staining of a Mouse Brain Tissue Slice

4.3   Lipid Identification

Other research labs using DESI for mass spectrometric tissue imaging have published multiple articles with lists of identified compounds in negative ion mode.[8,36] Our lab used these lists for tentative assignments of lipids and fatty acids in our mass spectra and then confirmed the assignments using fragmentation patterns from tandem mass spectrometry (MS/MS) on an Agilent quadrupole time of flight (QTOF) mass spectrometer.

4.3.1   Previous Research Studies

The first published study of 2D molecular imaging using DESI examined fatty acids and lipids in a rat brain in the mass range of 200-900 m/z.[8] Fatty acids in the lower mass range in negative ion mode (m/z < 400) consisted of palmitic acid (255 m/z), oleic acid (281 m/z), stearic acid (283 m/z), arachidonic acid (303 m/z), docosahexaenoic acid (327 m/z), and many others. In the higher mass range (m/z > 700), lipids consisted of sulfatides, phosphatidylserines, and phosphatidylinositols. Lipid assignments were made using tandem mass spectrometry, lipid standards, and comparison to previous ESI mass spectra. A summary of all their peak assignments is included in the supporting information.[8] This summary helped us initially identify peaks in our DESI mass spectra of mouse brain.

One DESI imaging study focused on comparing lipid content in diseased and normal tissue because important biological roles of lipids are disrupted in diseases such as cancer and Alzheimer's disease.[36] Lipids and fatty acids in positive and negative ion mode were detected and identified from rat brain tissue. Tandem mass spectrometry was used to confirm lipid assignments. These lipid assignments were helpful for our initial tentative assignments as well.[36]

4.3.2   QTOF MS/MS Fragmentation

An Agilent quadrupole time of flight (QTOF) mass spectrometer was used to obtain MS/MS fragmentation patterns of our lipids of interest to confirm our tentative lipid assignments obtained from previously published research articles. Our targeted lipid species were 303.25, 327.3, 834.6, and 885.6 m/z. Fragments of our targeted lipid species were observed in negative ion mode at three different collision energies (10 eV, 20 eV, and 40 eV). Fragment identifications in the following figures, created by Richard Carson, were assigned using Metlin.Scripps.edu and LipidMAPS.org online databases. Blue diamonds in the following figures indicate the parent ions and all fragments are [M-H]$^-$ ions unless otherwise indicated.

The targeted lipid species at 303.25 m/z was confirmed to be an arachidonic acid isomer (AA, m/z = 303.25, $C_{20}H_{32}O_2$) with fragments identified in Figure 4.10, Figure 4.11, and Figure 4.12. The prominent peaks at 61.9890, 89.0251 and 183.0128 m/z could not be conclusively assigned. Although other groups have claimed this peak to be arachidonic acid (C20:4 $\Delta^{5,8,11,14}$, m/z = 303.25, $C_{20}H_{32}O_2$), comparison to an arachidonic acid standard (Sigma-Aldrich, St. Louis, MO, U.S.A.) shows a disagreement in the fragmentation pattern so we can only conclude it to be an isomer of arachidonic acid.

The targeted lipid species at 327.3 m/z was confirmed to be docosahexaenoic acid (DHA, C22:6 $\Delta^{4,7,10,13,16,19}$, m/z=327.3, $C_{22}H_{32}O_2$) with fragments identified in Figure 4.13, Figure 4.14, and Figure 4.15. The 96.9642 and 281.2570 m/z fragment peaks are listed in the Metlin, Scripps database as characteristic of DHA but no fragment structures accompanied these peaks. The 69.0365, 89.0276, 153.8448, 185.0161, and 199.0253 m/z peaks could not be conclusively assigned.

The targeted lipid species at 834.6 m/z was confirmed to be phosphatidylserine (PS, C40:6, m/z=834.6, $C_{46}H_{77}NO_{10}P$) with fragments identified in Figure 4.16, Figure 4.17, and Figure 4.18. At 10 eV collision energy, the parent ion is the only peak seen with no other identifiable fragments because the fragmentation energy was too low. The prominent 89.0254 m/z peak could not be assigned in the 20 and 40 eV collision energy mass spectra. This 89.02 m/z peak appeared in all MS/MS runs of the samples as well as the standards so we believe it is a contaminant of unknown identification and structure.

The targeted lipid species at 885.6 m/z was confirmed to be phosphatidylinositol (PI, C38:4, m/z=885.6, $C_{47}H_{82}O_{13}P$) with fragments identified in Figure 4.19, Figure 4.20, and Figure 4.21. The parent ion could not be fragmented at 10 or 20 eV collision energy. A mechanistic study was published to characterize phosphatidylinositol using electrospray ionization tandem mass spectrometry.[37] Key fragments and fragmentation pathways are described there.

Figure 4.10: Fragmentation Pattern for 303.25 m/z at 10 eV Collision Energy

Figure 4.11: Fragmentation Pattern for 303.25 m/z at 20 eV Collision Energy

Figure 4.12: Fragmentation Pattern for 303.25 m/z at 40 eV Collision Energy

Figure 4.13: Fragmentation Pattern for 327.3 m/z at 10 eV Collision Energy
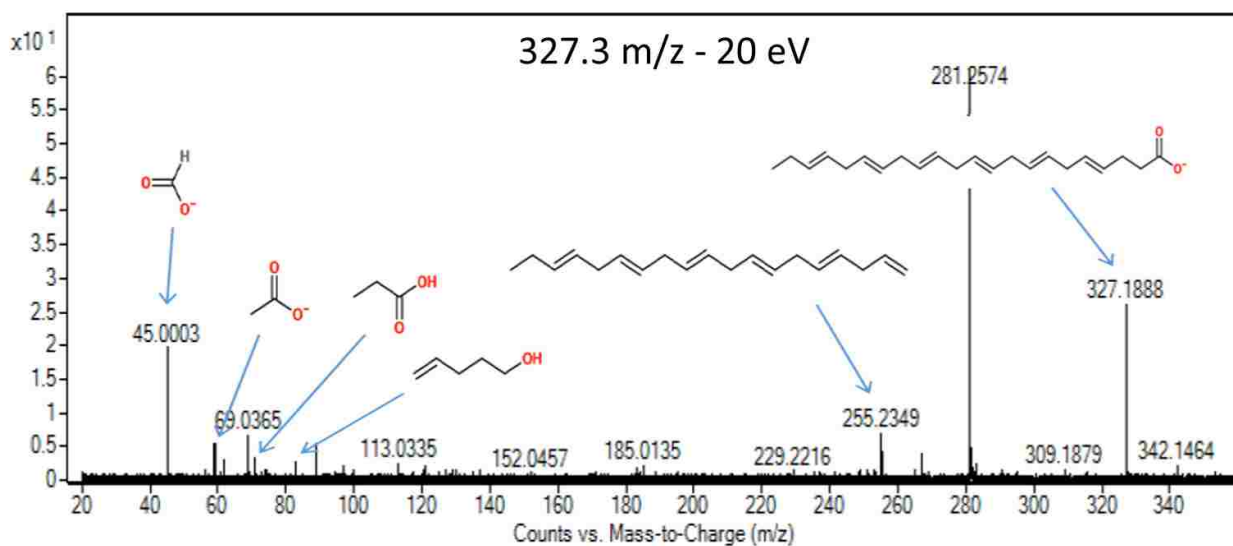
Figure 4.14: Fragmentation Pattern for 327.3 m/z at 20 eV Collision Energy
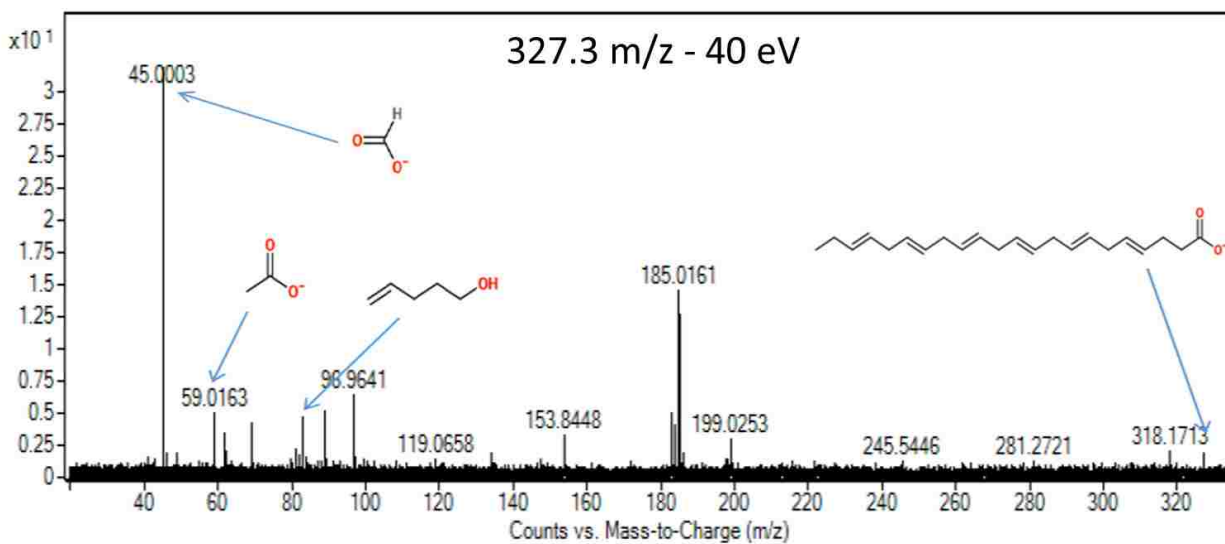
Figure 4.15: Fragmentation Pattern for 327.3 m/z at 40 eV Collision Energy
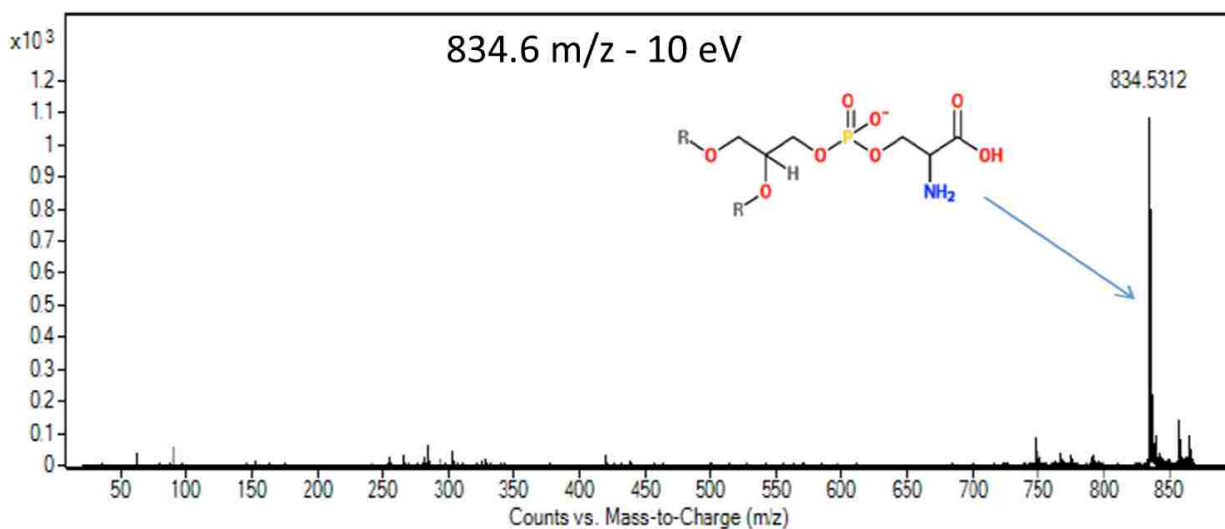
Figure 4.16: Fragmentation Pattern for 834.6 m/z at 10 eV Collision Energy
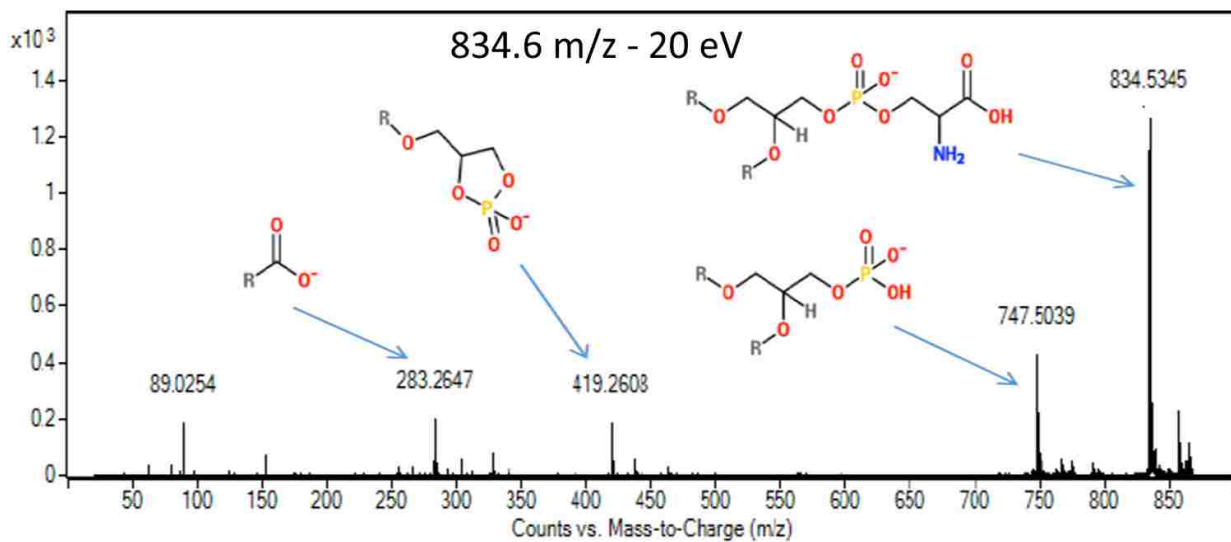
Figure 4.17: Fragmentation Pattern for 834.6 m/z at 20 eV Collision Energy
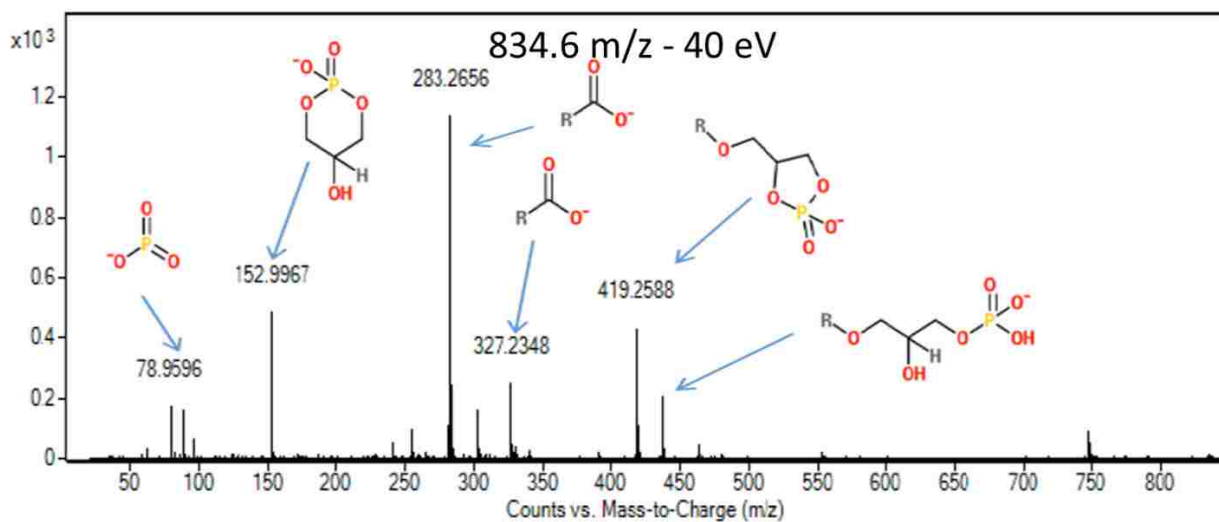
Figure 4.18: Fragmentation Pattern for 834.6 m/z at 40 eV Collision Energy
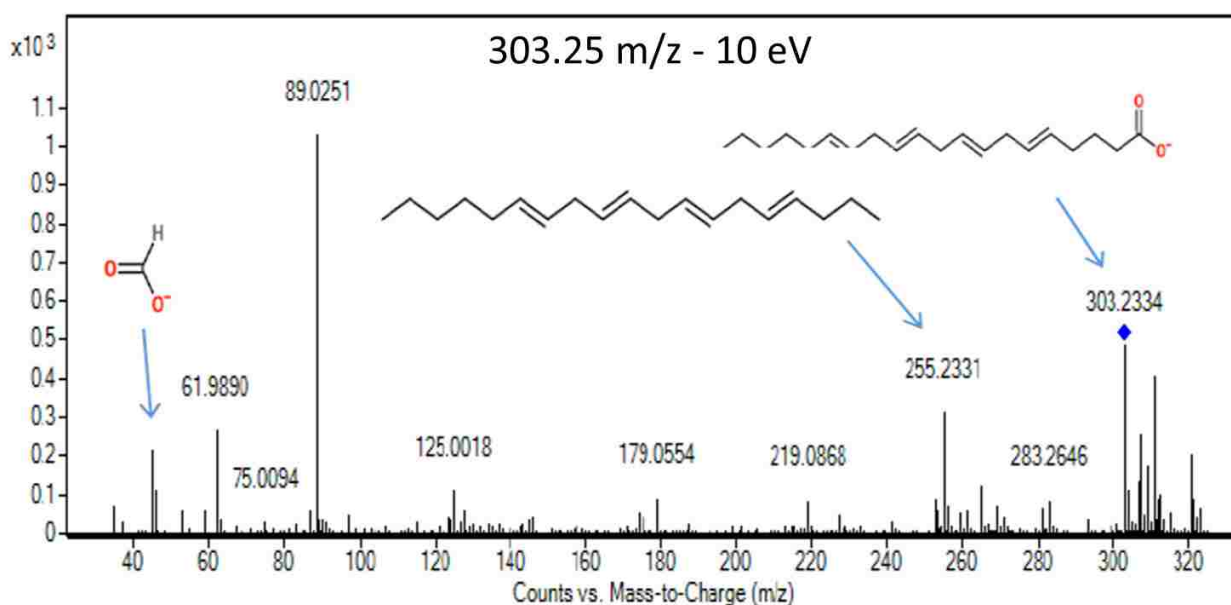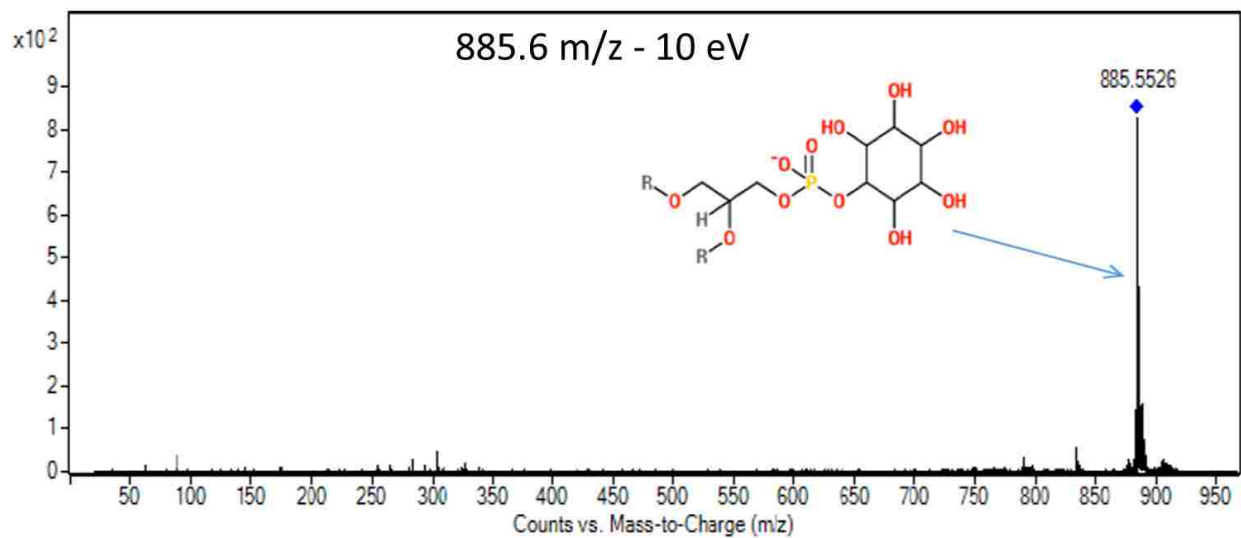
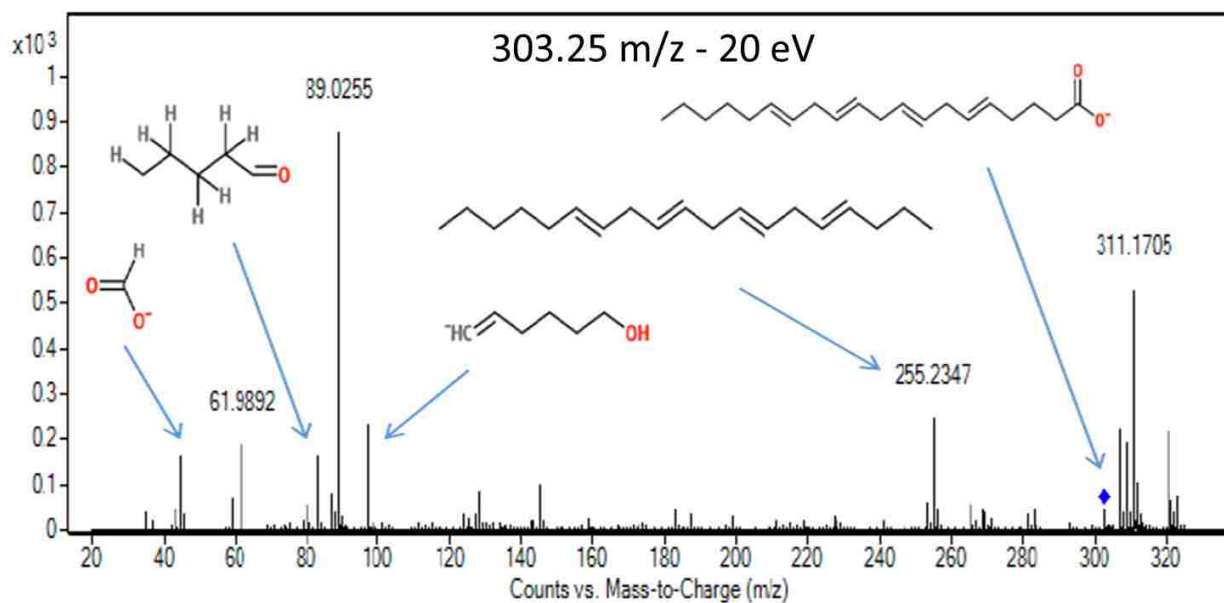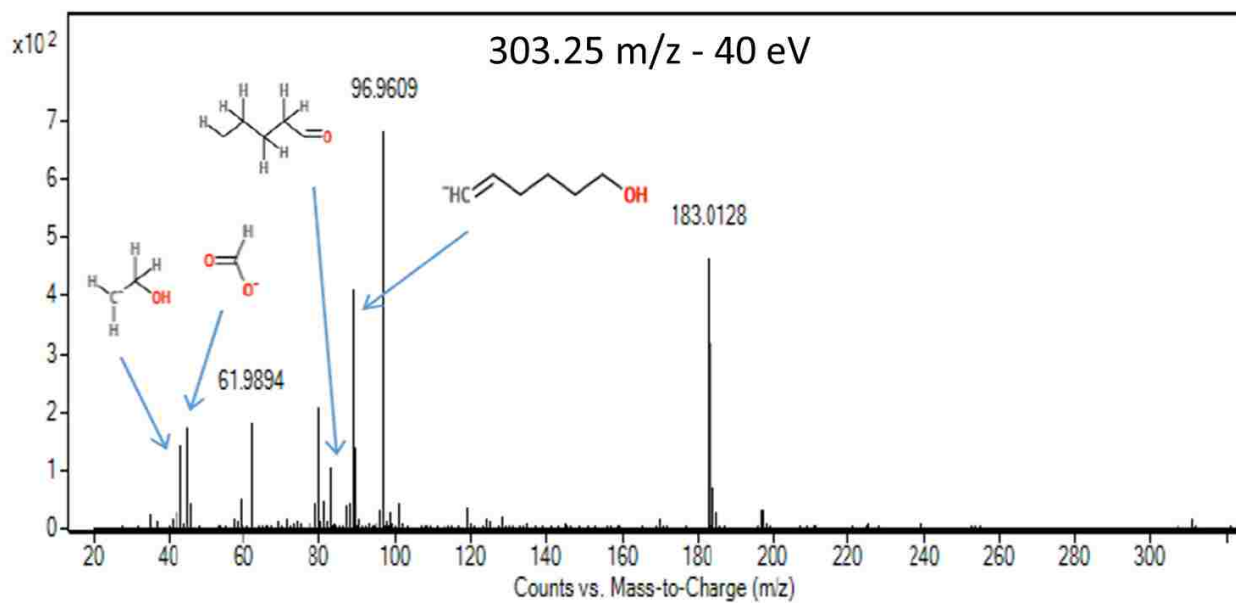*Figure 4.19: Fragmentation Pattern for 885.6 m/z at 10 eV Collision Energy*
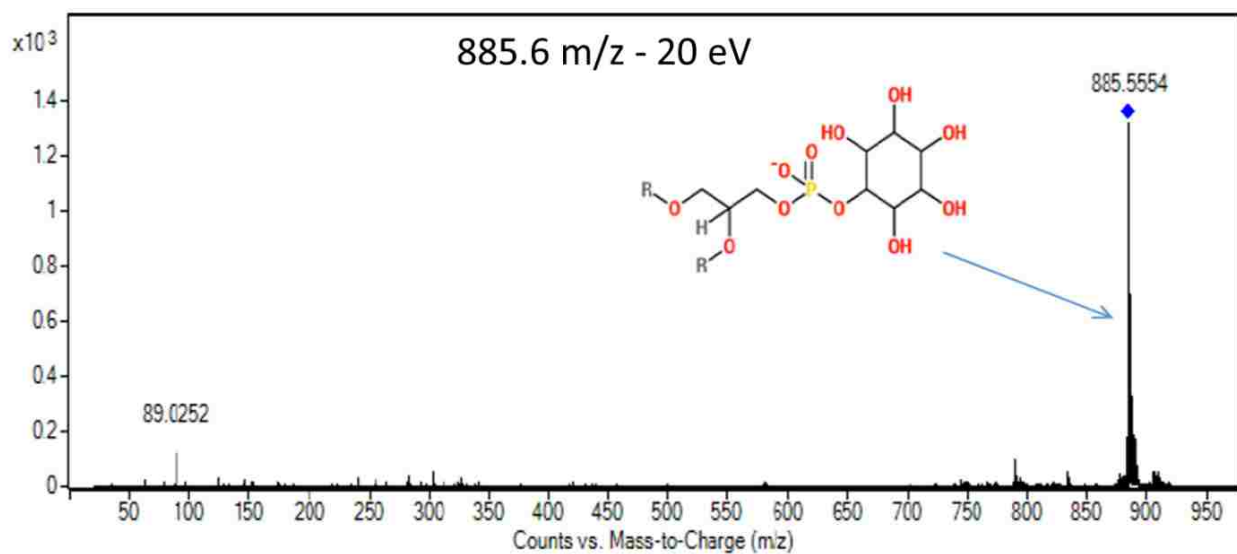
Figure 4.20: Fragmentation Pattern for 885.6 m/z at 20 eV Collision Energy

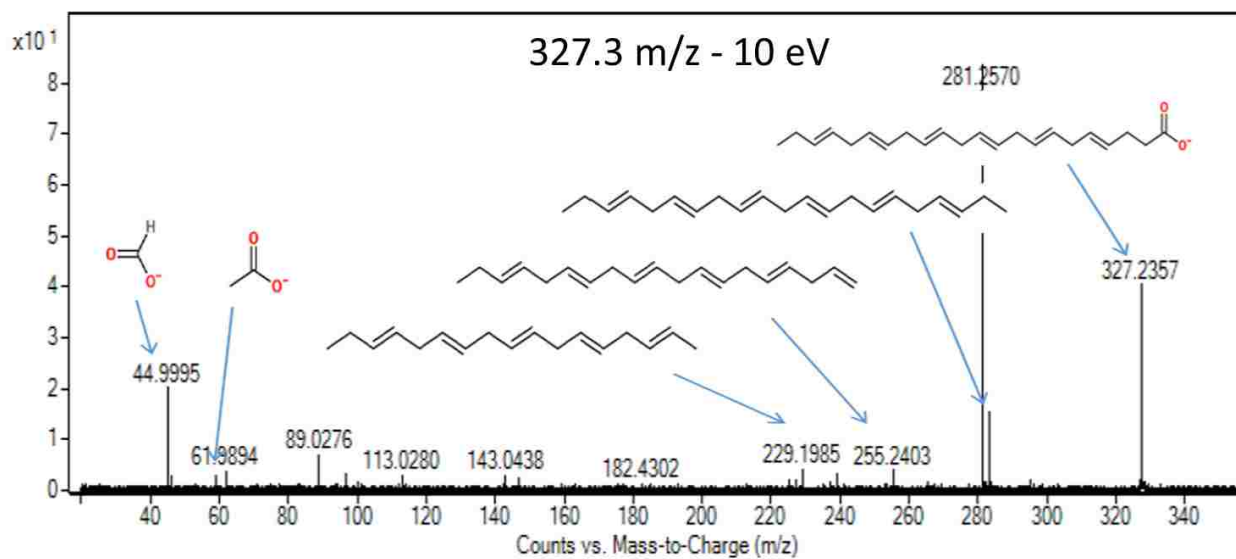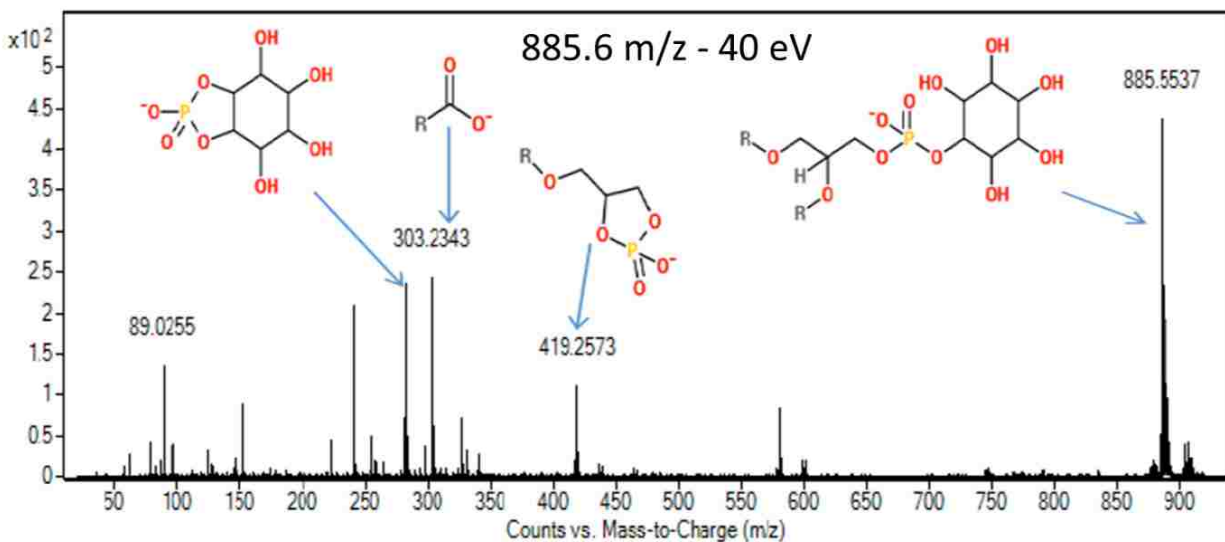*Figure 4.21: Fragmentation Pattern for 885.6 m/z at 40 eV Collision Energy*

4.4 Attempts at Washing the Tissue

A study using negative ion mode MALDI mass spectrometry imaging demonstrated that aqueous washes at various pHs during sample preparation enhanced lipid sensitivity.[38] Washing the adult mouse brain tissue with aqueous buffers of ammonium formate (pH 6.4) or ammonium acetate (pH 6.7) increased signal intensity up to five-fold as well as increased the total number of detectable analytes (S/N > 5). Washing was performed by dipping the tissue slices mounted on glass slides into a series of fresh buffer solutions (4 °C) for 5 seconds at a time. Washing lengths of 5, 10, 15, and 30 seconds were evaluated and 15 seconds was found to be the optimal length of time. The enhanced sensitivity for lipid detection was attributed to either the formation of adducts or by removing sample components that may interfere with lipid ionization.

The first application for this washing step in DESI-MS imaging was performed by Rachel Bennett Stryffler in unpublished work summarized in her dissertation.[24] She confirmed that washing tissue samples in ammonium formate buffer prior to positive ion mode imaging

71

improved lipid imaging by removing salts on the tissue surface, which favored the formation of $[M+H]^+$ ions rather than $[M+Na]^+$ and $[M+K]^+$ ions. Mass spectral analysis was simplified when sodiated ions that interfered isobarically with other protonated lipid species were eliminated. Washing prior to negative ion mode tissue imaging did not change adduct formation because most ions were already $[M-H]^-$ ions. However, higher lipid signal intensities were observed. Stryffler not only claimed that washing removed endogenous species from the sample surface that interfered with lipid ionization but also proposed that washing increased the surface wetness to possibly help the kinetic mass transfer of the lipids. She stated that desiccating the washed tissue was important to remove excess buffer but warned against drying for extended lengths of time. Excess drying caused tissue degradation.

In our DESI imaging experiments, we attempted washing a few tissue slices with 50 mM ammonium formate buffer for a total of 15 seconds, 5 seconds at a time. We observed cleaner peak shapes and a slight decrease in the number of background ions. The 303.25 m/z peak increased in intensity by approximately 25% but the 834.6 m/z peak decreased in intensity by 25%. We never observed a lipid signal intensity increase of five-fold as mentioned in the MALDI imaging study.[38] We did not pursue washing the tissue as a new standard protocol for sample preparation before DESI imaging because we did not see significant enough improvements in lipid signal intensity for us to justify increasing our sample preparation time. Further investigation in the future for washing tissue might yield different results.

4.5 List of Problems and Parameters Known to Affect Tissue Imaging

Here is a list of many problems and parameters that have either been hypothesized or confirmed to have an impact on DESI imaging quality, sensitivity, reproducibility and repeatability. This list should help identify possible reasons for DESI imaging malfunctions.

- Tissue slicing procedure

- Roughness/jaggedness of tissue slices

- Temperature of storage freezer

- Length of time in storage freezer

- Length of dessication time before DESI imaging

- Length of time at ambient temperature

- Ambient temperature and humidity during DESI imaging

- Solvent type and flow rate

- Gas pressure

- Sniffer tip proximity to sample surface

- DESI probe height above glass

- Distance between DESI probe and MS sniffer inlet

- DESI probe angle and MS inlet angle

- Solvent capillary extension and angle relative to gas capillary

- Polishing of gas capillary

- Solvent capillary superglue in PEEK tubing

- Presence of bubbles in solvent capillary

- Electrical contact between MS sniffer and MS glass capillary inlet

- Metal stage slide holder needs to be properly grounded

- Surface material of the slides used for tissue slices

- Grounding of the table/stage setup

- High voltage settings and proper contact to the no-dead-volume connector

- MS voltage settings and proper polarity chosen

- Complete removal of the OCT glue before imaging of a tissue slice

- Location of the brain slice on the glass slide

- Structures present in the brain slice and age of the brain

- Levelness of the glass slide relative to DESI probe for controlling stable signal intensity

- Solvent spot size and shape

- Pixel dimensions and speed of the motorized stage

4.6 Anatomical Structures of a Mouse Brain

Understanding the anatomy of a mouse brain helped us identify structures we observed in our DESI images. Different lipids were found in higher concentrations in different regions. Figure 4.22 and Figure 4.23 are both screenshots of coronal slices of a mouse brain from atlas.brain-map.org. This interactive website provides a tour of the mouse brain, one slice at a time. We approximated where in the brain our tissue slice came from based on comparison of structures in our images with similar anatomical structures in the library. In the following

figures, the greenish blue region marked with CTX is the cerebral cortex. The light green region

marked HPF in Figure 4.22 is the hippocampal formation. The light pink region labeled TH in

Figure 4.22 is the thalamus. The red region labeled HY in Figure 4.22 is the hypothalamus.
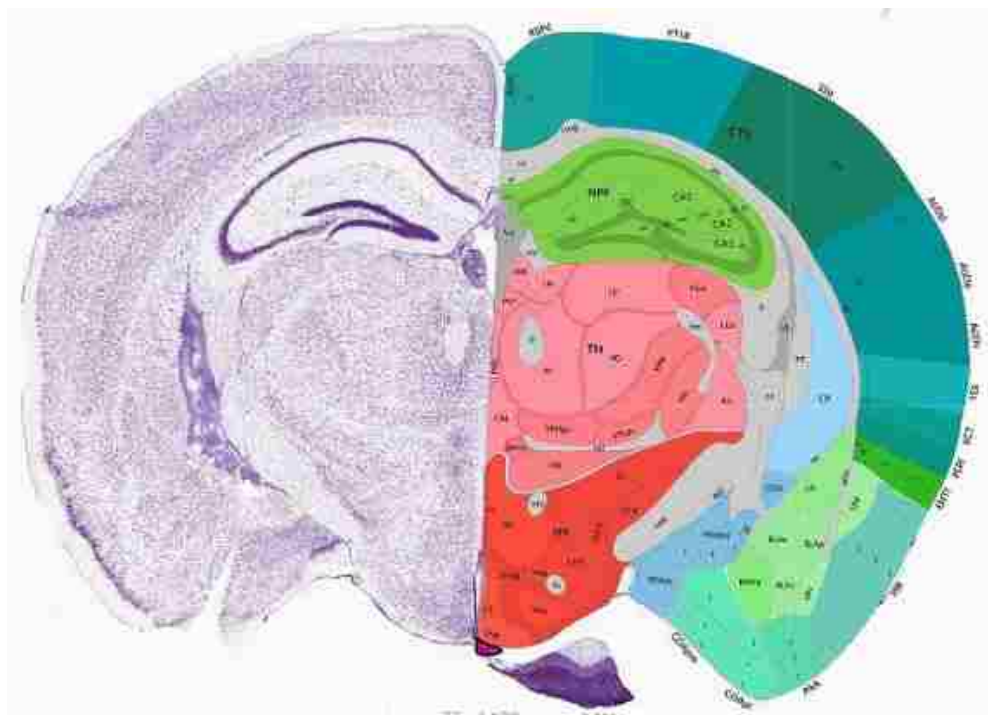
Figure 4.22: Coronal Slice of a Mouse Brain

The brain slice in Figure 4.23 resembles the structures seen in most of the brain slices we

DESI imaged for our metabolic rate study. The light blue region marked CP in Figure 4.23 is the

caudoputamen, which is part of the striatum. The other light blue region labeled ACB in Figure

4.23 is the nucleus accumbens which is also part of the striatum. The two darker blue regions in

the center of the brain labeled MS and NDB in Figure 4.23 are the medial septal nucleus and the

diagonal band nucleus, respectively. The grey region that separates the green and blue regions is

the corpus callosum. Most lipids we observed in the brain either had comparatively high

intensity in the corpus callosum relative to the cerebral cortex or relatively low intensity in the corpus callosum relative to the cerebral cortex. The corpus callosum is known to be a region in the brain with the largest amount of white matter, which allows for communication between different parts of the brain. Various lipid concentrations in gray matter, white matter, and myelin in the human brain have been studied using chromatography.[39] The purpose and location of every lipid in the brain is still outside the realm of human knowledge but the more we develop new techniques to study lipids, the more knowledgeable we become.
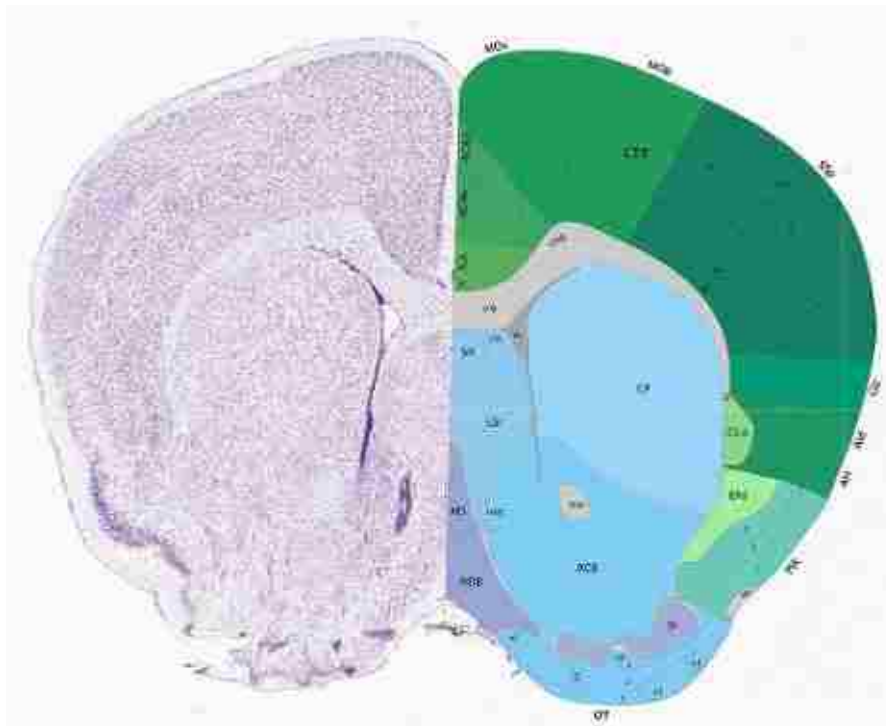
Figure 4.23: Another Coronal Slice of a Mouse Brain

4.7   Conclusion

Although DESI-MS is considered a robust technique, good quality images are only achieved when the samples are prepped, stored, and analyzed properly and good signal intensity is only achieved when the DESI probe geometry is optimized. The research workflow involved labeling the mice with deuterium enriched water, properly slicing the brains, imaging the brains using our DESI setup, analyzing the mass spectral data using our image_inspector program, confirming the identities of lipids using MS/MS fragmentation patterns, and calculating turnover rates with incorporation curves. Problems and key parameters were addressed to help future users of DESI-MS identify causes and possible fixes. Anatomical structures of the brain were identified using atlas.brain-map.org.

5 CONTRIBUTION TO PUBLICATION

A paper is currently in the process of being published with the title "Imaging Regiospecific Lipid Synthesis in Mouse Brain with Desorption Electrospray Ionization – Mass Spectrometry." We are hoping for the Journal of Lipid Research (JLR) to accept it. The authors that contributed to this publication were Richard H. Carson, Charlotte Lewis, Mercede N. Erickson, Anna P. Zagieboylo, Bradley C. Naylor, Kelvin W. Lee, Paul B. Farnsworth, and John C. Price. Richard Carson and I contributed equally.

My contribution to this paper included much of the DESI imaging, image_inspector program development, isotope ratio image analysis, fragmentation pattern determination, and multiple figure creations. I studied previously-published research and optimized the DESI source to image mouse brain slices. Then I imaged the mouse brains provided by the John C. Price research group. I updated Dr. Farnsworth's image_inspector program by adding isotope ratio capability, statistical analysis, and other features to create the current version described in Chapter 3, Chapter 4, and Appendix A. I converted the mass spectral DESI imaging data into MATLAB datacubes to be used by the image_inspector. I used atlas.brain-map.org to help identify key anatomical features of the mouse brain. I identified that differing turnover rates existed for different lipids in various regions of the brain. I found previously published articles[8,37] to help with our lipid identification process and helped identify key fragments in the MS/MS fragmentation data. With assistance from Mercede Erickson, I compiled the key DESI

image figures, containing the concentration and isotope ratios images of the mouse brains, for the

publication (Figure 4.3, Figure 4.4, Figure 4.5, and Figure 4.6). I also created the DESI

schematic figure (Figure 1.1) and the workflow figure (Figure 4.1) used in the publication.

6 ALZHEIMER'S DISEASE BRAIN STUDY

Mouse models of Alzheimer's disease that have been deuterium-labeled will be imaged using DESI to identify regions affected by plaque formation within the brain. Abnormal and differing metabolic rates are expected in these plaque regions because plaque is predicted to affect the metabolic pathways that are responsible for the constant synthesis and degradation of lipids and fatty acids within the brain. The metabolic turnover rates of the Alzheimer's mouse models will be compared to the healthy control models to gain a better understanding of how Alzheimer's disease affects the lipids and fatty acids within the brain. This research study is still being conducted but the results should be enlightening to the Alzheimer's disease research community.

6.1 Background on Alzheimer's Disease

The Alzheimer's Association shares valuable information on their website, alz.org, to inform the public about the definition, symptoms, stages, and current research regarding Alzheimer's disease. The following information was found on their website. Alzheimer's disease is a specific type of dementia that is characterized by memory loss, thinking problems, and behavioral changes. Patients with Alzheimer's disease slowly lose their memory and ability to care for themselves because it progressively worsens with time. No current cure is known but treatments are available to temporarily improve or slow down the side effects. Research is being

conducted constantly to help find ways to treat the disease, delay the onset, or prevent the development altogether. The nerve cells in the brain are affected by two abnormal structures: plaques and tangles. Plaques are formed from the build-up of beta amyloids (Aβ), unique protein fragments that interfere with the spaces between nerve cells. Tangles are defined as bundles of hyperphosphorylated tau protein that accumulate within the brain. The role of plaques and tangles in the brain, in regards to Alzheimer's disease, is still not known but it is believed that these formations disrupt nerve cell communication. This loss of communication is hypothesized to cause nerve cells to die, leading to memory loss, personality changes, and ultimately a loss of self-reliance.

A review article, published in 2004 by Mark P. Mattson, focuses on Alzheimer's disease and current progress in understanding the neuron degeneration responsible for loss of memory and changes in cognitive abilities.[40] Mattson mentions that drugs have been developed to temporarily improve memory, but no treatments have been discovered to stop, reverse, or prevent the neurodegenerative disease yet.

Many studies have been done linking lipids to Alzheimer's disease. Oxidative stress within the brain causes lipid peroxidation, which contributes to Alzheimer's disease because lipid peroxidation in a recent mouse brain study has been shown to precede amyloid plaque formation.[41] Low levels of docosahexaenoic acid (DHA) within the brain and the presence of Aβ-dependent lipid peroxidation has been hypothesized to disrupt actin filaments, ultimately increasing cognitive deficits for patients with Alzheimer's disease.[42] Increasing DHA consumption is suggested to reduce the risk of Alzheimer's disease but mechanisms and potential for therapeutic treatment have not yet been fully studied.[42]

Cholesterol is a lipid that ranges from 7% to 21% of the dry weight of the brain's gray matter, white matter, and myelin.[39] Cholesterol regulates both the production and removal of the β-amyloid protein (Aβ).[43] Alzheimer's disease is characterized by abnormal accumulation of this Aβ protein within the brain and increased levels of cholesterol within the brain have been shown to increase the Aβ content.[43] Drugs that prevent the synthesis of cholesterol have shown to decrease the Aβ accumulation by twofold within the brain, revealing a possible approach for reducing the risk of Alzheimer's disease.[44]

6.2   Reactive DESI for Detecting Cholesterol

Cholesterol has a possibly strong link to the development and progression of Alzheimer's disease.[45] Identifying where cholesterol is located within the brain and how cholesterol concentrations and metabolic turnover rates are affected by the presence of Aβ plaques and neurofibrillary tangles might provide better insights for understanding cholesterol's connection to Alzheimer's disease. One study so far has published the ability to use reactive DESI for spatially detecting cholesterol within mouse brains.[46] However, our efforts at reproducing their results have not been successful thus far.

Wu et al. described using betaine aldehyde (BA) as the additive to the DESI solvent system to selectively react with the alcohol group of the cholesterol molecules in rat brain.[46] The solvent system, ACN/H$_2$O/DMF (8:3:1), contained 65 ppm BA. BA ([C$_5$H$_{12}$NO]$^+$, elemental mass: 102.092) supposedly reacts with cholesterol (C$_{27}$H$_{46}$O, elemental mass: 386.355) through a nucleophilic addition to form a hemiacetal salt ([BA+Cholesterol]$^+$, 488.45 m/z, Figure 6.1). Reactive DESI was used to record spatial 2D images of phospholipids and cholesterol simultaneously. After background subtraction, a peak at 488.5 m/z, assigned as

[BA+Cholesterol]$^+$, was the only prominent peak in the 300-700 m/z range. Several other phospholipid peaks were seen in the 750-950 m/z range. When the solvent was not doped with 65 ppm BA, the 488.5 m/z peak disappeared.
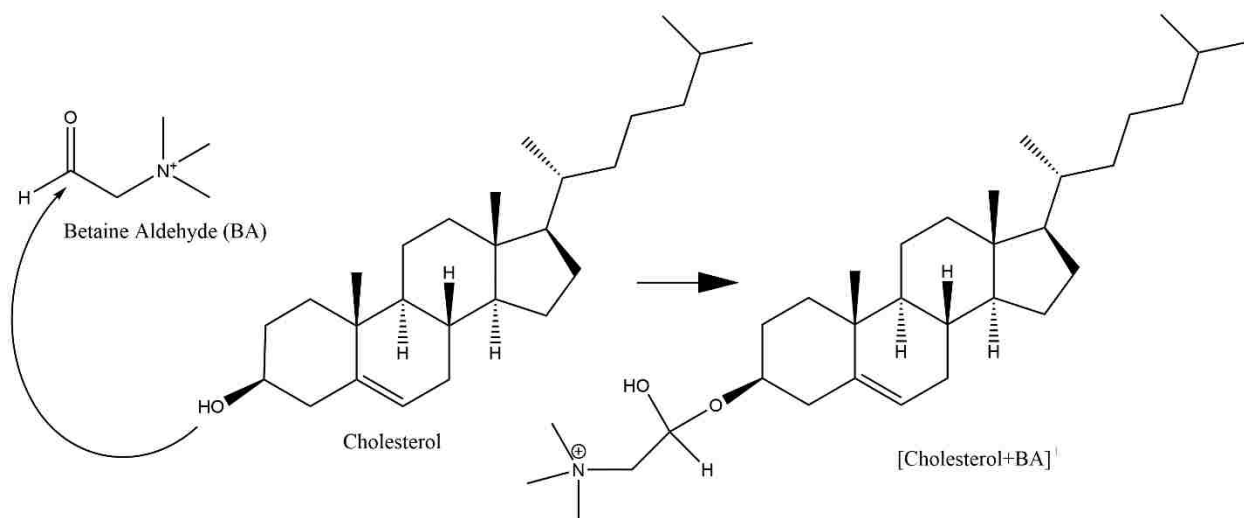
Figure 6.1: Betaine Aldehyde Reaction with Cholesterol for Reactive DESI

We replicated their experimental procedures in positive ion mode with an attempt at reproducing their 2D images of cholesterol within a mouse brain. We attempted their solvent system, ACN/H$_2$O/DMF (8:3:1), without 65 ppm BA and had difficulty seeing the prominent phospholipids peaks shown in their mass spectra. We observed a noisier background compared to the solvent system of 100% methanol and we also observed strong contamination from the tissue mounting compound when using ACN/H$_2$O/DMF (8:3:1). We tried ACN/DMF (4:1) instead and saw improved background and higher phospholipid signal intensity. After adding 65 ppm BA to our ACN/DMF (4:1) solvent, we observed a strong peak at 414.1 m/z (signal intensity 8×10^4) that overwhelmed the spectra (Figure 6.2), but we did see a small

[BA+Cholesterol]$^+$ peak appear at 488.45 m/z. The 488.45 m/z peak had a maximum intensity of 5×10^3. We confirmed that this peak came from the native cholesterol within the mouse brain tissue by observing the disappearance of the peak when we moved the DESI probe away from the brain tissue. The following day we used the exact same tissue and same solvent, and we saw a dramatic fourfold increase in signal intensity (2×10^4) of the 488.45 m/z peak. We were unsure why using a previously sprayed tissue slice a second time gave an increase in the [BA+Cholesterol]$^+$ signal intensity.
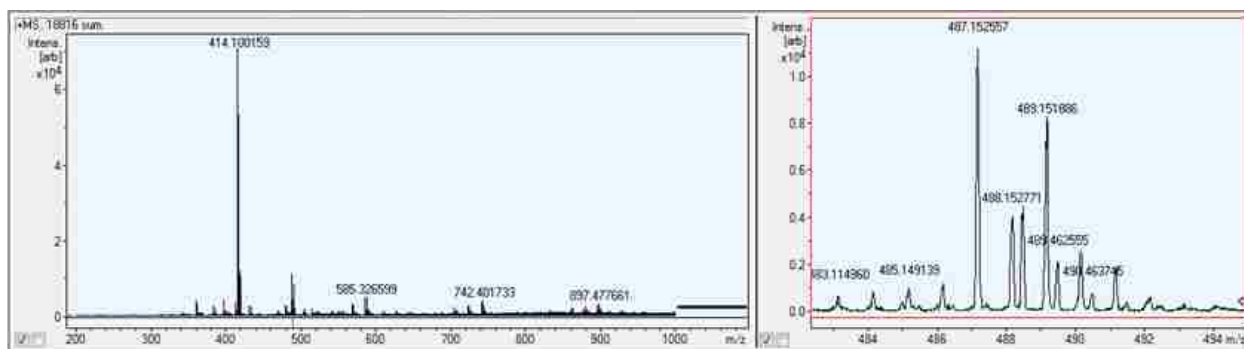
Figure 6.2: First Attempt at Seeing [BA+Cholesterol]$^+$ on a Brain Tissue Slice

We decided to try their ACN/H$_2$O/DMF (8:3:1) solvent once again with 65 ppm BA. We dipped a glass slide in a 1:1 methanol:chloroform solution of 500 µg/mL cholesterol. When the solvent evaporated, a visible thin film of crystallized cholesterol was left on the slide. We observed a kinetic time-dependent behavior of the [BA+Cholesterol]$^+$ signal intensity. An initial raster scan across the brain tissue gave a signal intensity of 2×10^4. Then when the DESI probe was returned to the initial starting spot of the first raster scan, the signal intensity increased by threefold on average to 7×10^4. At times, the signal would spike to 1.5×10^5. This time dependent observation that the BA needed time to react with the cholesterol helps explain why

we observed an increase in the [BA+Cholesterol]$^+$ signal intensity on the second time imaging a previously scanned brain tissue slice.

After emailing the authors of the initial paper on reactive DESI used to image cholesterol in rat brains, they provided a few suggestions to help us.[46] They first confirmed that the ACN/H$_2$O/DMF (8:3:1) solvent system caused a significant (order of magnitude) drop in phospholipid signal intensity compared to 50:50 methanol:water or pure methanol, but methanol reacts strongly with BA so this alternative solvent system provided the best [BA+Cholesterol]$^+$ signal. Second, they said that no experiments were performed regarding the kinetics of BA reacting with cholesterol. They suggested that increasing the BA concentration or making fresh BA doped solvent might help with our low signal intensity. Third, they suggested reoptimizing the DESI alignment to improve signal. We tried all these suggestions and still only saw a maximum intensity of 6×10^4 for the 488.45 m/z peak on the glass slide with concentrated cholesterol after a third time rescanning the same area. Future experiments need to be conducted to further understand how to reproducibly image cholesterol in mouse brains using reactive DESI.

6.3   Future Goals

Although our efforts thus far have been unsuccessful for imaging cholesterol in mouse brain tissue, Mercede Erikson, an undergraduate in Dr. Paul B. Farnsworth's lab, is continuing the DESI imaging project. Imaging cholesterol within the mouse brain is one of the top priorities. Next we plan to use DESI imaging to locate Aβ plaques within deuterium labeled brains from transgenic mouse models with Alzheimer's disease. We hope to observe abnormal and differing metabolic rates in these plaque regions because plaque is predicted to affect the metabolic

pathways that are responsible for the constant synthesis and degradation of lipids and fatty acids within the brain. We plan to compare the metabolic turnover rates of the Alzheimer's mouse models to the healthy control models to gain a better understanding of how Alzheimer's disease affects the lipids and fatty acids within the brain.

7   CONCLUSIONS

This thesis highlighted our recent advancements for DESI mass spectrometric imaging including optimization of DESI parameters, spatial detection of lipids and fatty acids in mouse brains, and future disease analysis using spatially resolved *in vivo* metabolic rates focusing primarily on Alzheimer's disease. We developed a MATLAB program, image_inspector, to help us view and understand data acquired from DESI imaging. We measured metabolic rates of lipids and fatty acids within the brain by observing changes in isotopomer patterns. We confirmed lipid assignments using MS/MS fragmentation patterns. We created incorporation curves from data measured in the isotope ratio images and determined the number of exchange sites for multiple lipids. We hope our progress in DESI mass spectrometric imaging can contribute in the future to the application of DESI imaging in the various fields of neuroscience, pharmacology, clinical pathology, and oncology.

APPENDIX A.   README FILE FOR MATLAB IMAGE_INSPECTOR

A.1   Introduction

This appendix was adapted from the README file of the MATLAB image_inspector tutorial originally designed and written by Mercede Erikson. Edits were made by Dr. Paul B. Farnsworth and Charlotte Reininger.

The programs, imzml_to_cube and image_inspector, were created to process data from DESI-MS brain tissue scans. Files are first converted from their original acquisition format of .d files (Bruker data format) to .mzML files, then to .imzML files, using the free/downloadable programs msconvert[26] and imzML Converter[27,28]. A condensed .imzML file is then processed into a MATLAB datacube, by a direct adaptation of Georgia Tech's imzml_to_cube program, which contains substantial modifications made by Dr. Paul B. Farnsworth and Charlotte Reininger. Data are then extracted from the datacube using the image_inspector MATLAB code, which also contains major modifications by Dr. Paul B. Farnsworth and Charlotte Reininger.

A.2   Required Material

- MATLAB must be installed on your computer. The version used in this tutorial is R2015a.

- Download the folder of MATLAB programs to a local network/drive. This folder, titled "DESI-MS MatLab Programs", can be accessed by contacting my advisor, Dr. Paul B.

Farnsworth at Brigham Young University, if you are interested in DESI imaging and data processing.

- Obtain either sample datacubes provided or personal data to be processed. The sample datacubes are in the folder "Sample Brain Scan Data" within the "DESI-MS MatLab Programs" folder.

A.3   imzml_to_cube conversion instructions

Open the MATLAB program from your computer. Once open, click on the "Browse for Folder" icon in the top left corner (the open, yellow folder with a green arrow on it) which is highlighted with a red box in Figure A.1.

A window will pop-up prompting you to select a folder. Select the "DESI-MS MatLab Programs" folder, which contains the imzml converter and image_inspector programs. Click the "Select Folder" button on the bottom right as seen in Figure A.2. Clicking will close the window.
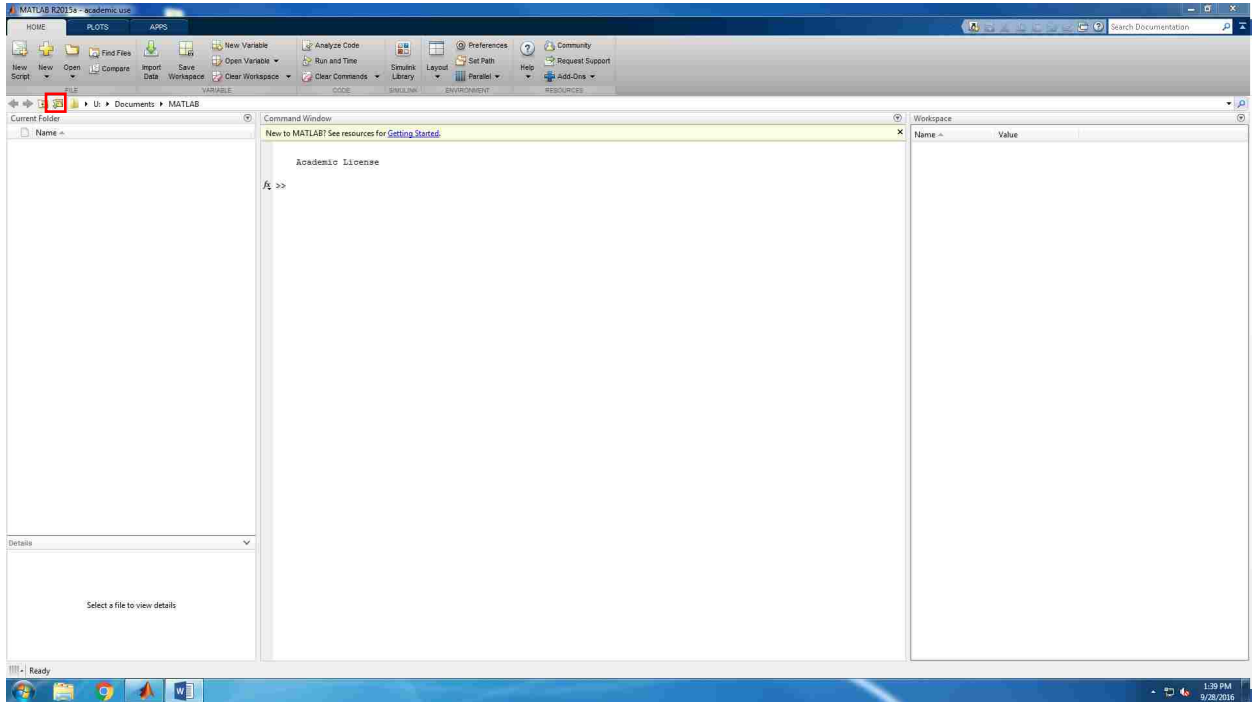
Figure A.1: Browse for Folder Screenshot
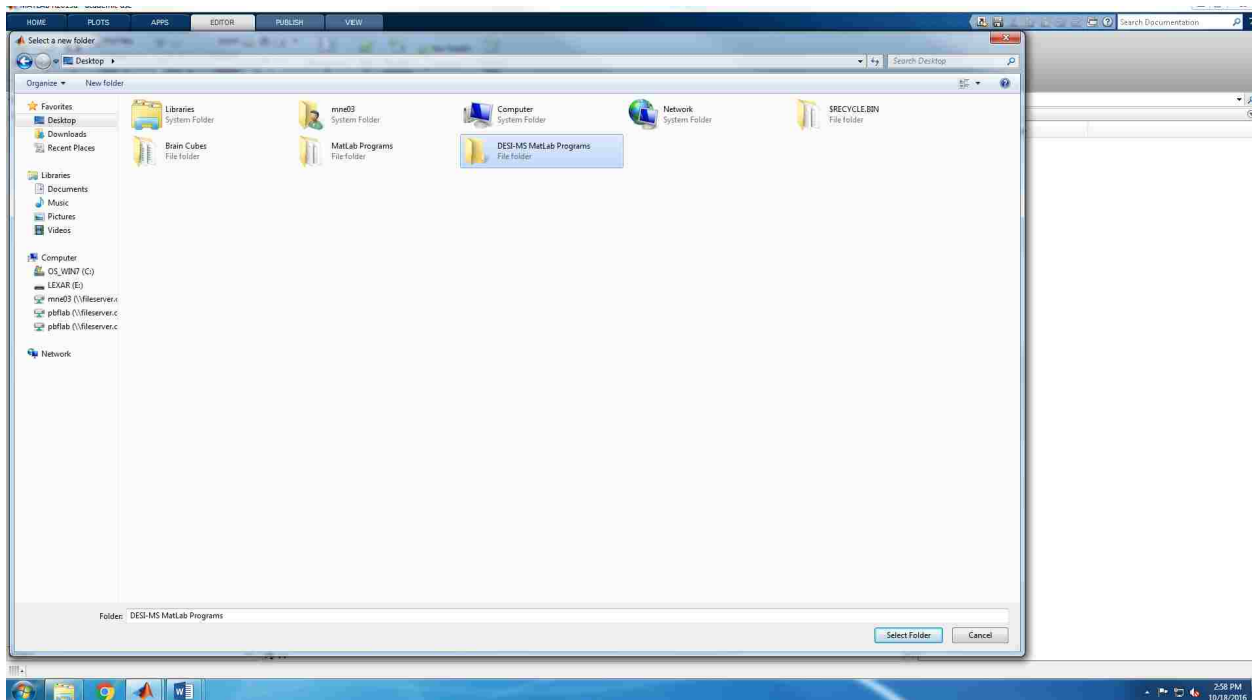
Figure A.2: Selecting a Folder Screenshot

Under the "Current Folder" window in MATLAB, you should find two image_inspector

programs (one .fig and one .m) and two imzml_to_cube programs (one .fig and one .m). Red

boxes highlight the "Current Folder" window and the aforementioned files in Figure A.3.
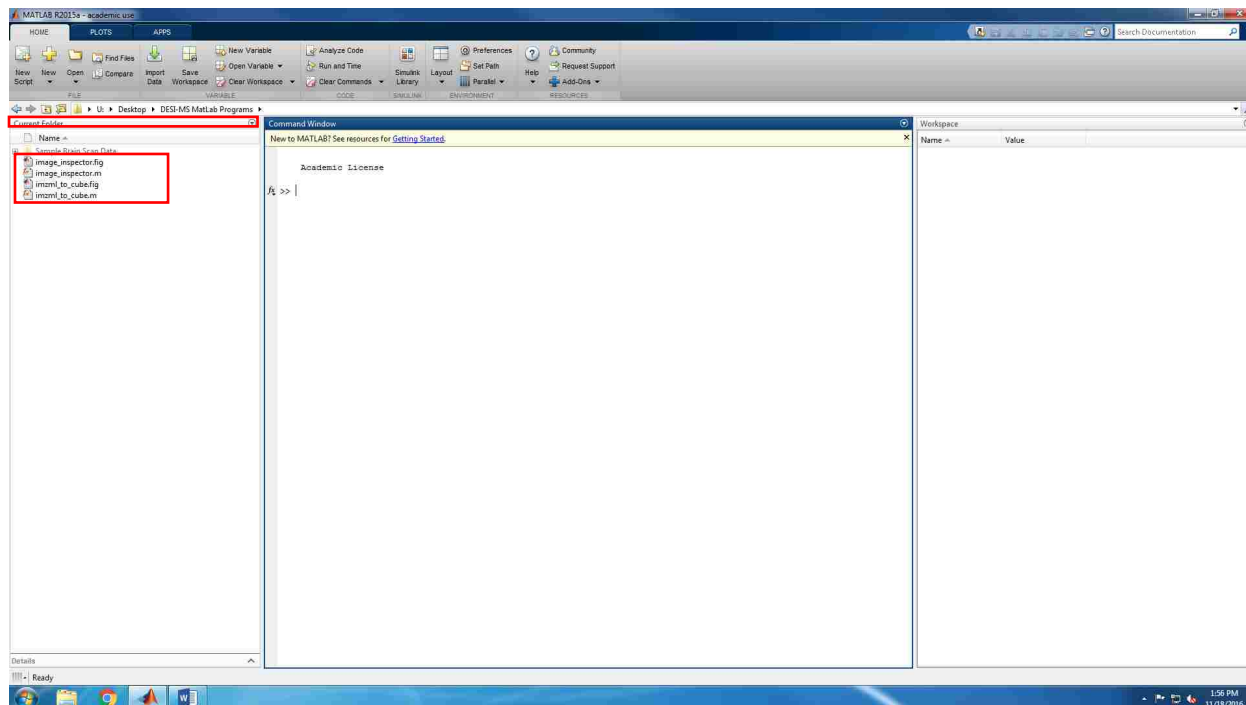
Figure A.3: File Location Screenshot

In the "Command Window", type "imzml_to_cube" and press enter. A window will

appear, as seen in Figure A.4, prompting you to enter various dimensions associated with your

brain file. Start by clicking the "Browse" button and loading the .imzML file of your desired data

set. If you are using the provided example data, choose the file "B20 20daylabelbrainsec 6-10-

16.imzML" located in the Sample Brain Scan Data folder. For the example data, the pixel width

is "75 µm"and the pixel height is "150 µm". These pixel dimensions depend on your DESI setup

and your mass spectrometer settings. For all of our sample data, these parameters are constant, but for other labs, these numbers will vary. Press the green"GO" button. Once the file is converting to a datacube, the File Properties will appear in the boxes on the right, along with the conversion progress in the bottom right corner. The progress output only reports in increments of 100, so to determine when the file is finished, a message will appear in the Command Window of MATLAB, highlighted with a red box in Figure A.4, describing the amount of time it took to convert.

Figure A.4: imzml_to_cube MATLAB GUI Screenshot

While the file converts, a warning message in MATLAB may appear in orange text as seen in Figure A.4. In files from the Bruker MicrOTOF II, the number of pixels in a row varies by one or two due to a lack of synchronization between the internal clock in the mass
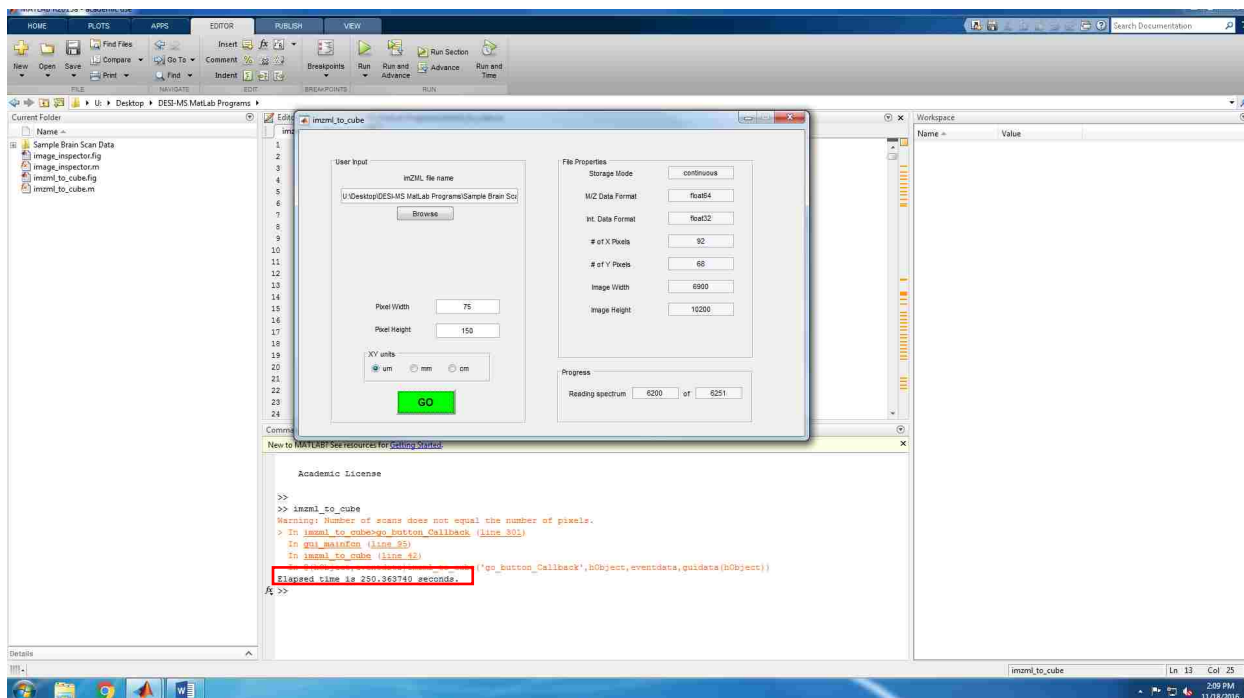
spectrometer and the external trigger that starts each scan. The warning reflects the variable

number of pixels. Missing pixels are filled with zeros, and the warning is not cause for concern.

Once the conversion is complete and the "Elapsed Time" message appears in the Command

window, the MATLAB datacube file will be saved in the same folder/location as the .imzML

file. Once complete, exit the imzml_to_ cube graphical user interface (GUI) window. The

MATLAB datacube file now contains four MATLAB arrays with the following variable names:

imgX, imgY, imgZ and img.

A.4   image_inspector Instructions

Next, we will process the MATLAB datacube file into mass spectral files, concentration

map images, and isotope ratio map images for selected compounds found within the brain tissue.

A.4.1   Running the image_inspector Program

Type "image_inspector" in the command window and press enter. A MATLAB graphical

user interface (GUI) window will appear. To import your datacube file, find the "Browse" button

on the top of the GUI as seen in Figure A.5 and use the pop-up file-finder window to find the

desired cube for processing (if you are using the example data, it will be the "B20

20daylabelbrainsec 6-10-16" cube that you just converted above, which should be saved into

your Sample Brain Scan Data folder). Click "Open" once the file is selected. You will see the

location and name of the file you selected in the "Workspace" box to the left of the "Browse"

button of the GUI. Also, ensure that in the "Units" bar to the right of the Browse button,

"micrometers" is selected. "Micrometers" is the default option. These key buttons and locations

are highlighted by red boxes in Figure A.5.

96

To call up the file you selected, you must click the green "GO" button in the right corner as seen in Figure A.5. It may take a few minutes to load so do NOT press the "GO" button again even if you think it is not working. As this is processing, check to make sure no red error messages appear in the "Command Window" of MATLAB.
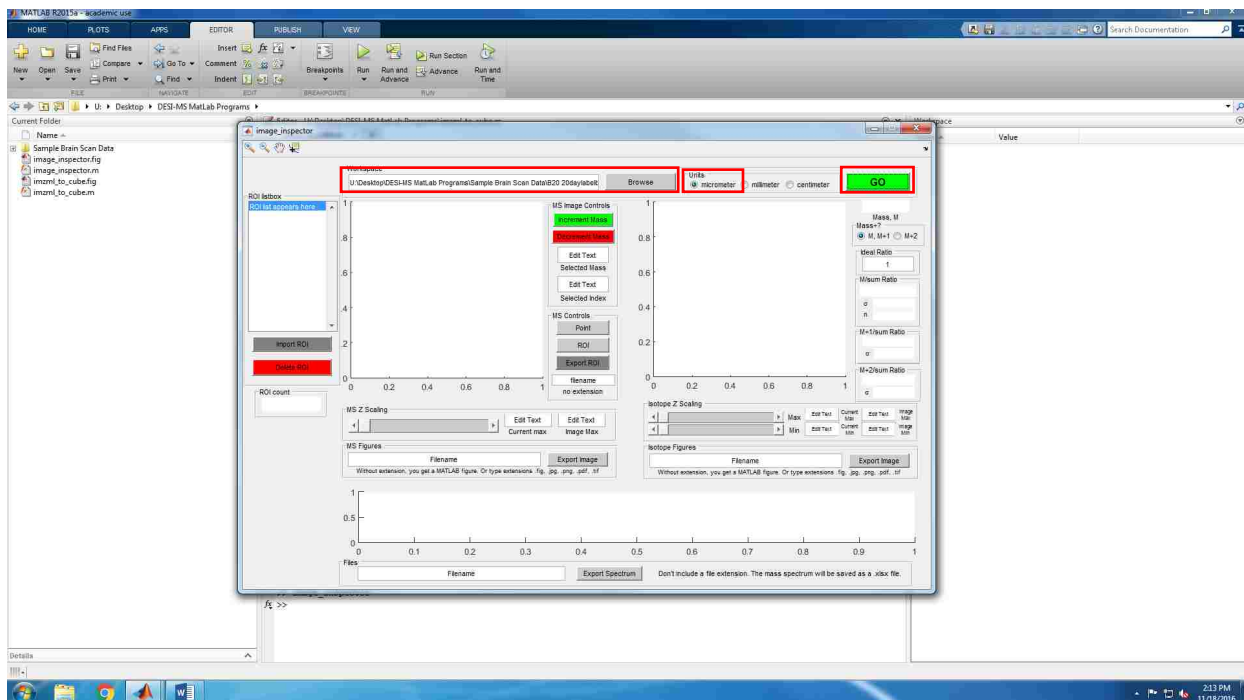
Figure A.5: MATLAB image_inspector Program Screenshot

A.4.2 Processing the Image

Once the datacube is imported, the left image panel will appear dark blue with random light blue pixels as seen in Figure A.6. This panel displays the concentration of an arbitrary m/z peak but since a meaningful mass has not yet been selected, the initial image will be meaningless.
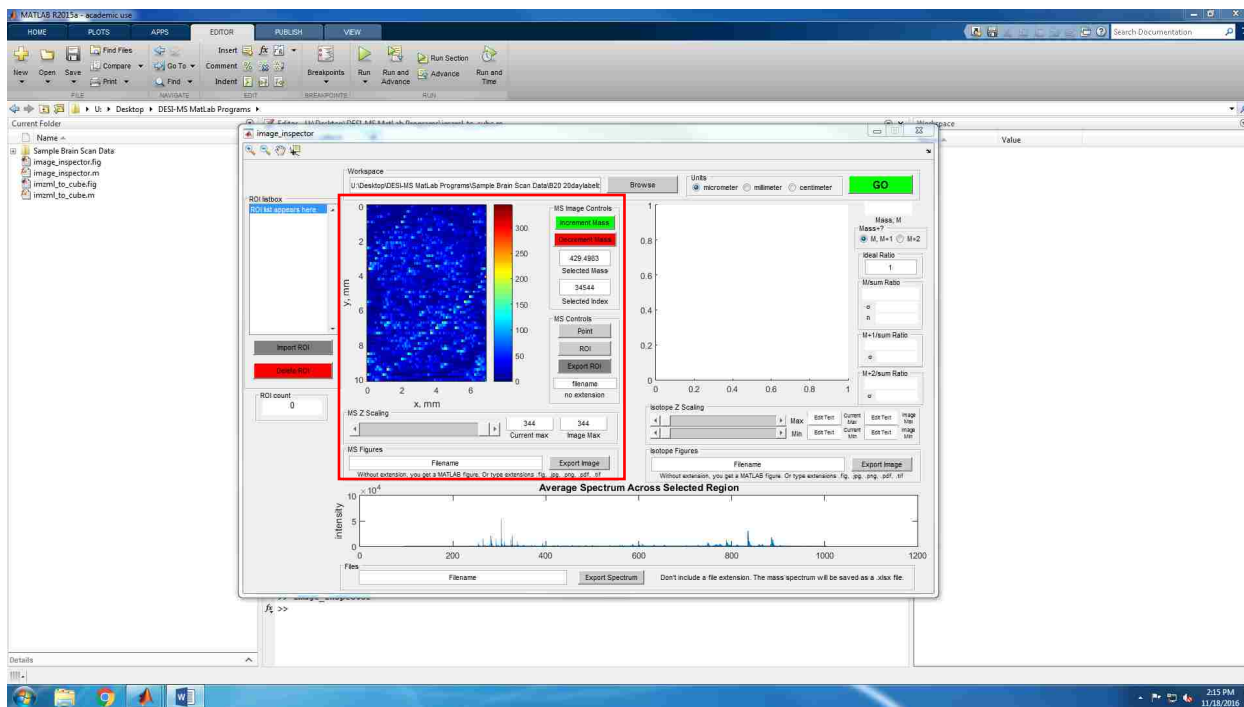
Figure A.6: Initial Import of the Datacube Screenshot

A.4.3   Mass Spectrum and Tool Bar

To view the concentration map of a selected mass, we first have to become familiar with the four tool buttons in the top left corner and the mass spectrum panel, located along the bottom of the GUI window labeled "Average Spectrum Across Selected Region". Both regions are highlighted with red boxes in Figure A.7. The average mass spectrum is displayed on an x-axis of m/z and a y-axis measuring the intensity of the m/z peaks. The initial spectrum in this window is averaged over the entire image. Below the spectrum window, there is an export option. To export a spectrum, type a file name to save the spectrum under (excluding any extension), and then click the "Export Spectrum" button. This will create an .xlsx file of the average mass spectrum data for the image you are processing. The spectrum presented in this window can be

changed to reflect the mass spectrum of a region of interest (ROI) in the image ranging in size from a single pixel to the entire image.
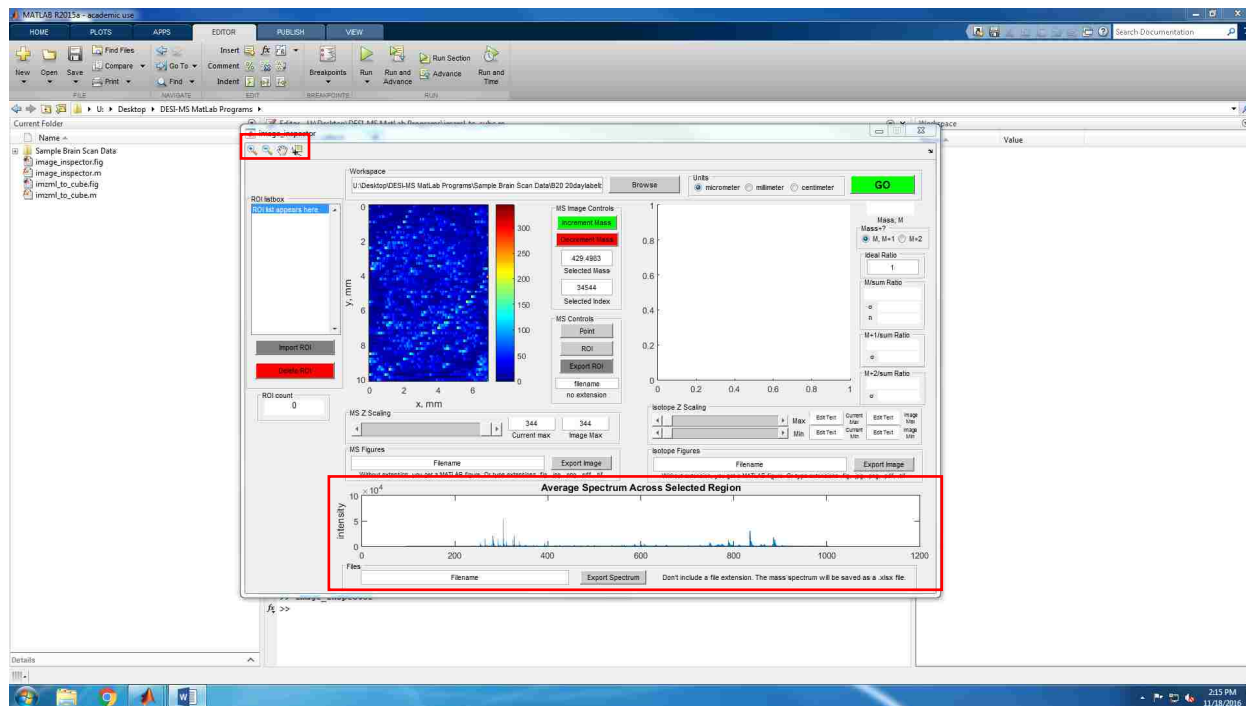
Figure A.7: Mass Spectrum and Tool Buttons Screenshot

The four buttons at the top in Figure A.7 are the selection tools used in the Mass Spectrum panel as well as in the concentration image on the left side of the GUI. There is a Zoom-In tool, Zoom-Out tool, a Pan tool, and a Data Cursor tool. To use the Zoom-In tool, click on the button and move your mouse to an area in the mass spectrum you want to zoom in on. You will create a rectangle around that area as seen in Figure A.8. Click where you want a corner of the rectangle to be placed, and while holding down the mouse, drag the rectangle around the desired region of the mass spectrum, then release.
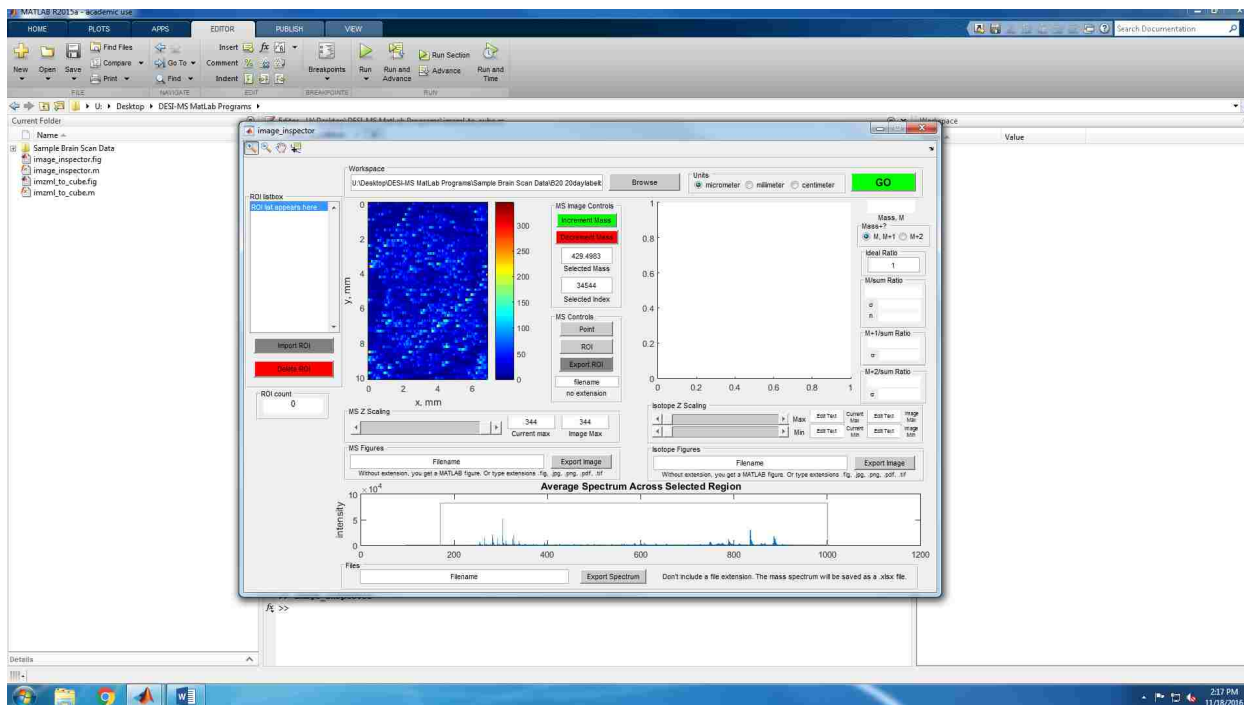
Figure A.8: Zoom-in Tool for Mass Spectrum Screenshot

To zoom out, simply select the zoom out tool and click anywhere within the mass spectrum window. The zoom functions are helpful when you are trying to select individual peaks that may be too small or that are hard to identify when the spectrum is zoomed out.

The Pan tool (resembles a hand) allows you to click and drag the spectrum so you can view different regions of a spectrum, or move a zoomed-in spectrum instead of having to zoom back out. To use, simply click and hold down your mouse, dragging the spectra in any direction.

The Data Cursor, the furthest right of the four tools, is the selection tool for a specific m/z peak in the mass spectrum. Select the icon, find a specific peak you want to analyze, and click on the top of that peak. A box will appear, as seen in Figure A.9, describing the peak m/z (X) and the intensity at the point you selected on the m/z peak (Y). The right and left arrow keys on your keyboard cause the point to move along the mass axis, tracking the intensity. Using the arrows,

100

you can confirm that you selected the top of the peak when the intensity is the largest number for that m/z value.
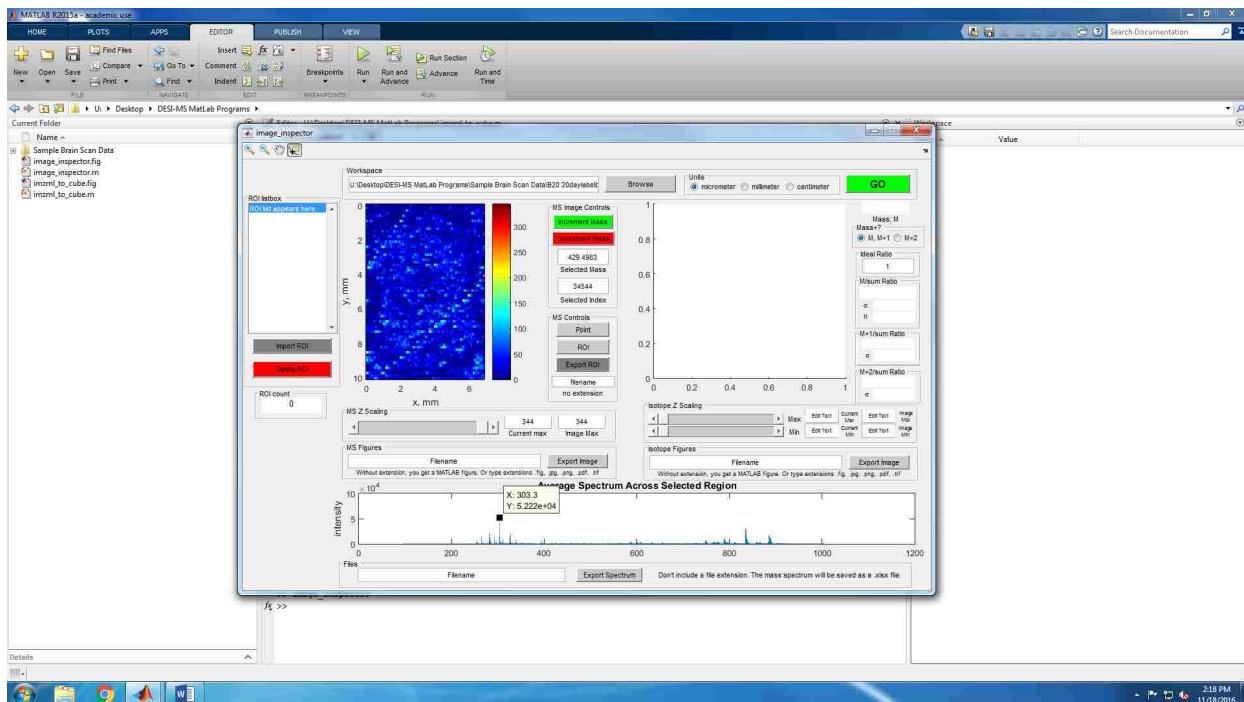
Figure A.9: Identifying a Peak in the Mass Spectrum Screenshot

After selecting a peak, click the "Point" button under the "MS Controls" panel which is highlighted with a red box in Figure A.10. This will display the concentration map of your image in the left of the two graph axes. This image is created by measuring the area under the chosen peak, which is accomplished by summing 12 points above and below each side of the center of the selected point. To select a different peak, simply click on a new m/z, and click "Point" again. You can repeat this process for any peak, and each peak will provide a unique concentration map of the brain for the compound or fragment, giving rise to the peak. You can also select a point on

101

the concentration image instead of the mass spectrum, which will output the mass spectrum for only that selected pixel.

The colors on the concentration map image range from blue to red as seen in Figure A.10, blue corresponding to the least intensity for an individual pixel and red corresponding to the highest intensity.

Figure A.10: Pick Point Selection Screenshot

A.4.4   Concentration Image Panel

To the right of the concentration image (left graph axes) there is a panel labeled "MS Image Controls". In this panel, there is a green button labeled "Increment Mass" and a red button labeled "Decrement Mass". These buttons move the mass of the m/z peak you selected up or

down as if you were moving the data cursor in the mass spectrum left or right by one data point at a time, and the concentration map then changes accordingly. Below these buttons are the "Selected Ma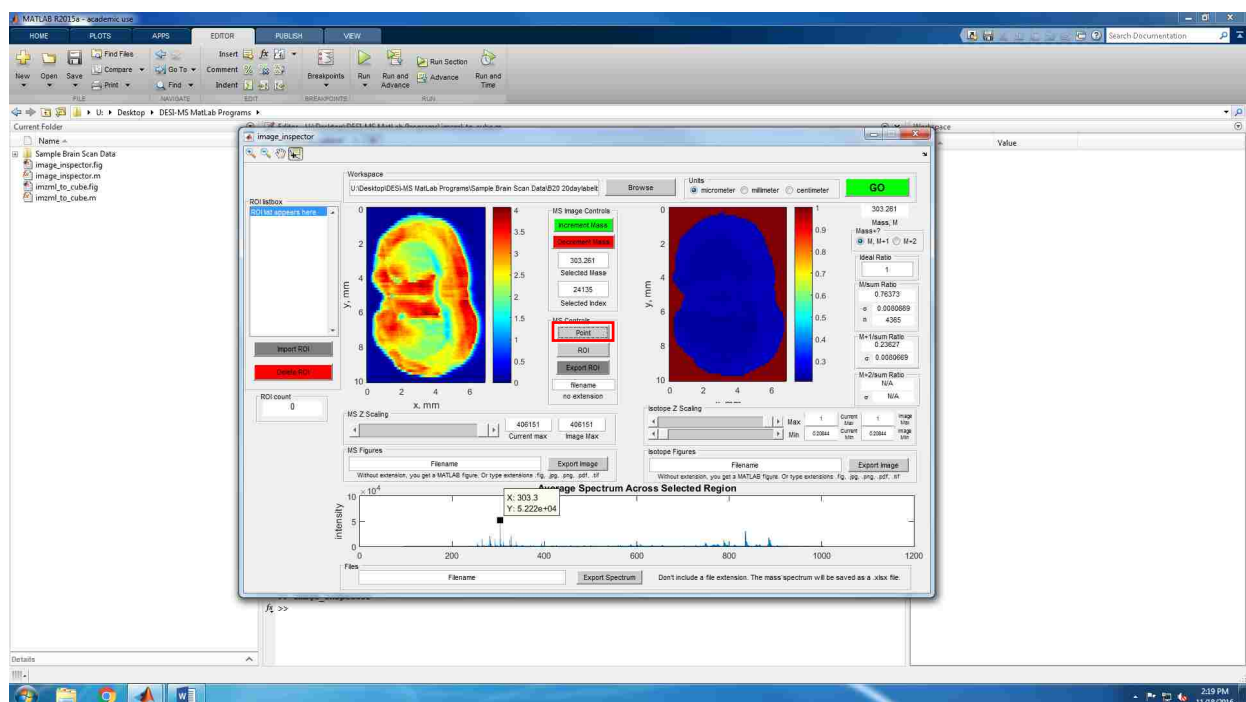ss" and "Selected Index" outputs. "Selected Mass" reads out the mass of the peak you have selected, and the "Selected Index" gives the corresponding data point index number from the datacube. If you think of the datacube as a stack of images, the index is the number up from the bottom of the stack. You can also select either a mass or an index by entering numbers directly in these boxes.

The next panel below the "MS Image Controls" is the "MS Controls". This is where the "Point" button for loading the concentration map for a selected m/z peak from the mass spectrum is located. There is also a button named "ROI", which is an acronym for Region of Interest. There will be instructions for how to select an ROI, along with how to use the "Export ROI" button later in this tutorial.

Underneath the concentration image is the "MS Z Scaling" panel and the "MS Figures" panel. The "MS Z Scaling" allows you to manipulate the concentration scaling located to the right of the concentration image. By sliding the scale to the left as seen in Figure A.11, you can watch the scale values change, changing the color and look of the image. Next to the sliding bar, the values for the current max and the image max are displayed. If you exceed the image maximum or minimum by sliding the bar too far in either direction, the brain image will become distorted and an error will appear in the running MATLAB code.
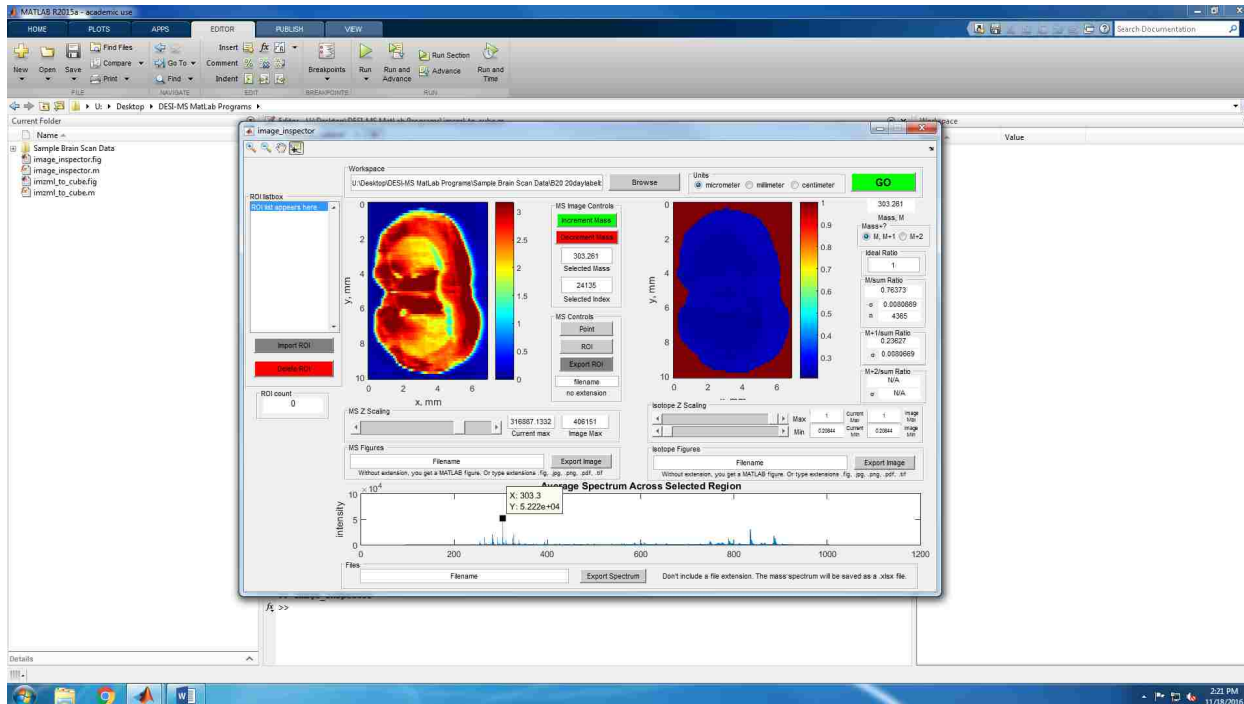
Figure A.11: MS Z Scaling of the Concentration Image Screenshot

The "MS Figures" panel, highlighted by a red box in Figure A.12, allows you to export

a .fig, .jpg, .png, .pdf, or .tif of the concentration image with a label of its m/z peak and the scale

bar. To export, type a desired file name for the image, and include the extension type

corresponding to the desired image format. Then click the "Export Image" button to the right of

the filename box. You can save and resave the image with as many different extensions you

desire. Just change the extension and press "Export Image" again. The image will then be saved

in the folder you have open in MATLAB.
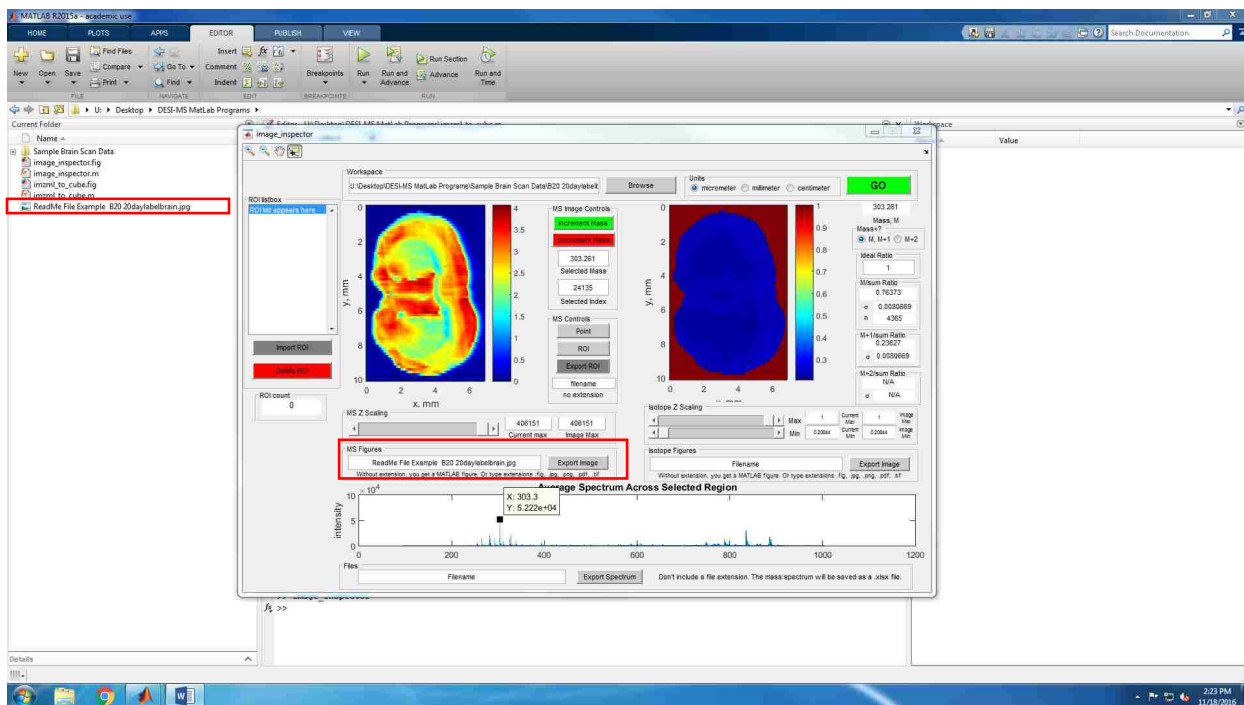
Figure A.12: MS Figures Panel Export Function Screenshot

A.4.5   Isotope Image Panel

The dark blue image with a burgundy background to the right of the concentration image is the isotope ratio image. The isotope image pixels are created from dividing two different peak areas to give a ratio. Peak areas include 12 points above and below the chosen peak. However, there is also a threshold for this image which causes some pixels to be excluded creating the burgundy background. The default threshold for each pixel to be included in determining the isotope ratio is the maximum intensity of the concentration image divided by seven. The threshold can be changed in the MATLAB code if desired.

To the right of the isotope ratio image are a variety of controls highlighted by a red box seen in Figure A.13. At the very top right corner, the mass of the currently selected m/z peak is

105

displayed. Underneath that, there is an option of choosing either the "M, M+1" or the "M+2" buttons. This gives you the option of choosing to include the M+2 peak for calculating isotope ratios. A reason not to include the M+2 peak would be if there are interfering neighboring peaks in the mass spectrum that overlap with your peak envelope. The isotope ratios are calculated for the individual peaks, M, M+1, and M+2 (if the "M+2" button is chosen) over the sum of the peaks. If the "M, M+1" button is chosen (the default option), then the sum is the sum of the peak areas of only the M and M+1 peaks. If the "M+2" button is chosen then the sum is the sum of the peak areas of the M, M+1, and M+2 peaks. For all our data processing we used the "M, M+1" peak option to avoid interference of overlapping peaks.
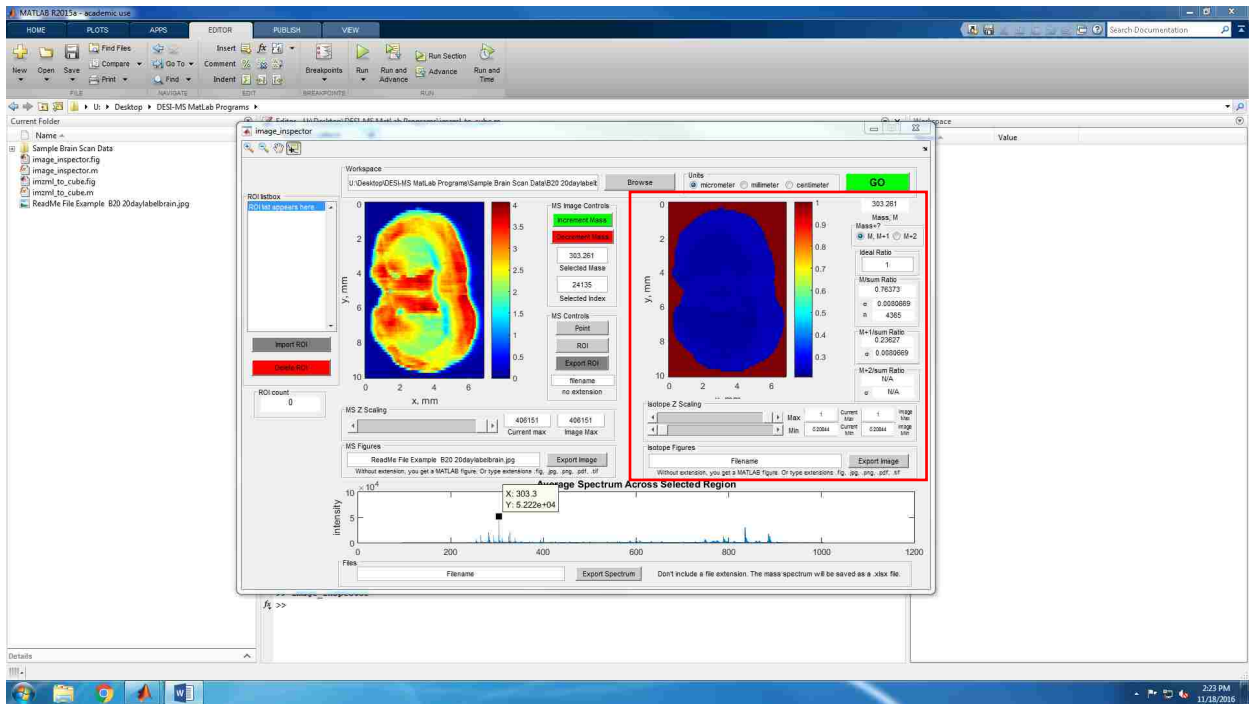

Figure A.13: Isotope Image Controls Screenshot

The next output is the "Ideal Ratio", which we will touch on after we cover the controls below it: the "M/sum Ratio", the "M+1/sum Ratio", and the "M+2/sum Ratio" outputs. Depending on which "Mass+?" option you chose from above, the "M+2/sum Ratio" outputs might read N/A. In our case, the "M+2/sum Ratio" output reads not applicable (N/A) since we chose the "M, M+1" button so we chose to ignore the M+2 peak altogether. The "M/sum Ratio" in this case provides the ratio of the M peak area over the sum of M and M+1 peak areas, since we chose not to include the M+2 peak. It also displays the standard deviation and the n value. The n value is the number of pixels averaged to calculate the displayed isotope ratios. If a region of interest was not selected, then the n value counts all the pixels in the entire isotope image with intensities above the threshold displayed to the immediate left of these ratio output boxes. If a region of interest was selected on the concentration image map to the far left in the GUI, then only the pixels within this ROI were used to calculate the isotope ratios. The standard deviation is simply the calculated standard deviation of the sample of the "n" pixels selected. The "M+1/sum Ratio" outputs the ratio and the standard deviation for the M+1 peak divided by the sum of the peaks, and the "M+2/sum Ratio" displays the ratio of the M+2 peak divided by the sum of the peaks (if the "M+2" button was selected) and standard deviation accordingly.

In the "Ideal Ratio" box you can input values that will affect the isotope ratio image scaling as seen in Figure A.14. The isotope ratio image always displays the M+1/sum values for each pixel. To see a more meaningful isotope ratio image, you can type the value for the M+1/sum peak into the "Ideal Ratio" box. This will make the center of your color map the average isotope ratio so that you can see deviations above and below this average. You can also type a known ratio if you know what the compound is at the specified m/z. Once you have typed a value, click the "Point" button that is in the "MS Controls" panel near the concentration image

on the left. If you want to change the ideal ratio, then simply type a new ratio in the "Ideal Ratio" box and select the "Point" button again.
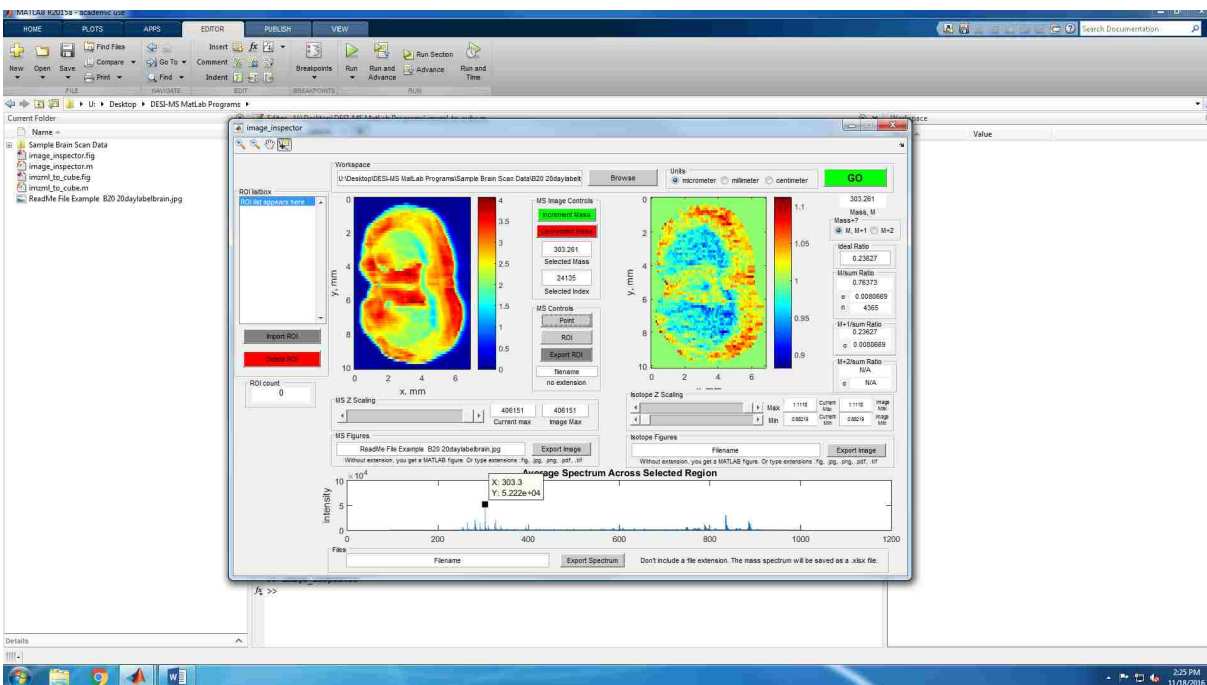
Figure A.14: Isotope Ratio Image Screenshot

This isotope image, as seen in Figure A.14, displays the different isotope ratios found in the various regions of the brain. Similar to the scaling for the MS image on the left, the higher isotope ratios will be the darkest red and the lower isotope ratios will be the darkest blue. From this isotope ratio map, we can analyze and discover where the highest and lowest isotope ratios for a specific lipid are located within the brain. For example, in the sample brain we are working on, the higher concentrations of our M+1 peak ratio are found in the upper ridge, named the cerebral cortex, whereas very low M+1 peak ratios are found in the two center sections, called the caudoputamen. This means the lipid turnover rates between these two brain structures could

be significantly different. The isotope ratio differences only occur for this brain image because this mouse was fed deuterated water for 20 days. If this were an unlabeled brain, there would be no systematic variations in the isotope ratios in different regions of the brain.

Again, we can adjust the scaling as seen in Figure A.15 similar to how we did for the concentration image, but the isotope panel has two adjustable bars, one for the maximum and one for the minimum. We can also export the image in the same manner as we previously did for the other image. Name the file, add the desired extension, and then click the "Export Image" button. This will export and save the image in the same folder you have open in MATLAB.
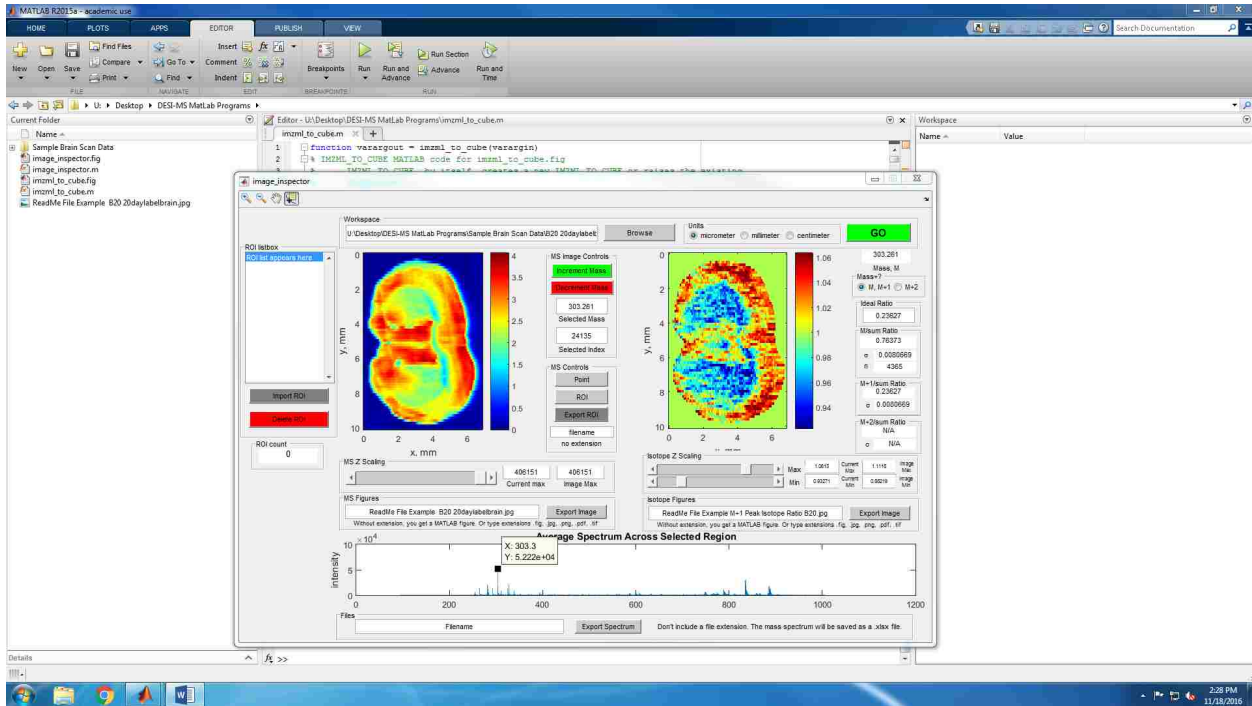
Figure A.15: Scaling Isotope Image Screenshot

A.4.6   Region of Interest and Exports

A region of interest (ROI) can be beneficial when trying to compare the concentrations of two separate structures of the brain. An ROI is created by selecting the "ROI" button, holding down your mouse, and then tracing around a certain area of the brain on the concentration image at the left of the GUI that you want to analyze. When you are tracing the region, be sure to cross your mouse path back over where you started. Only once you have done that can you release your mouse. If you do not cross the path with the mouse, a straight line from the start and end points will be automatically created to make an enclosed ROI. As soon as you let go of the computer mouse, you will see your region of interest appear on the brain, and the isotope ratios and mass spectrum will change. Figure A.16 has the top caudoputamen region selected.
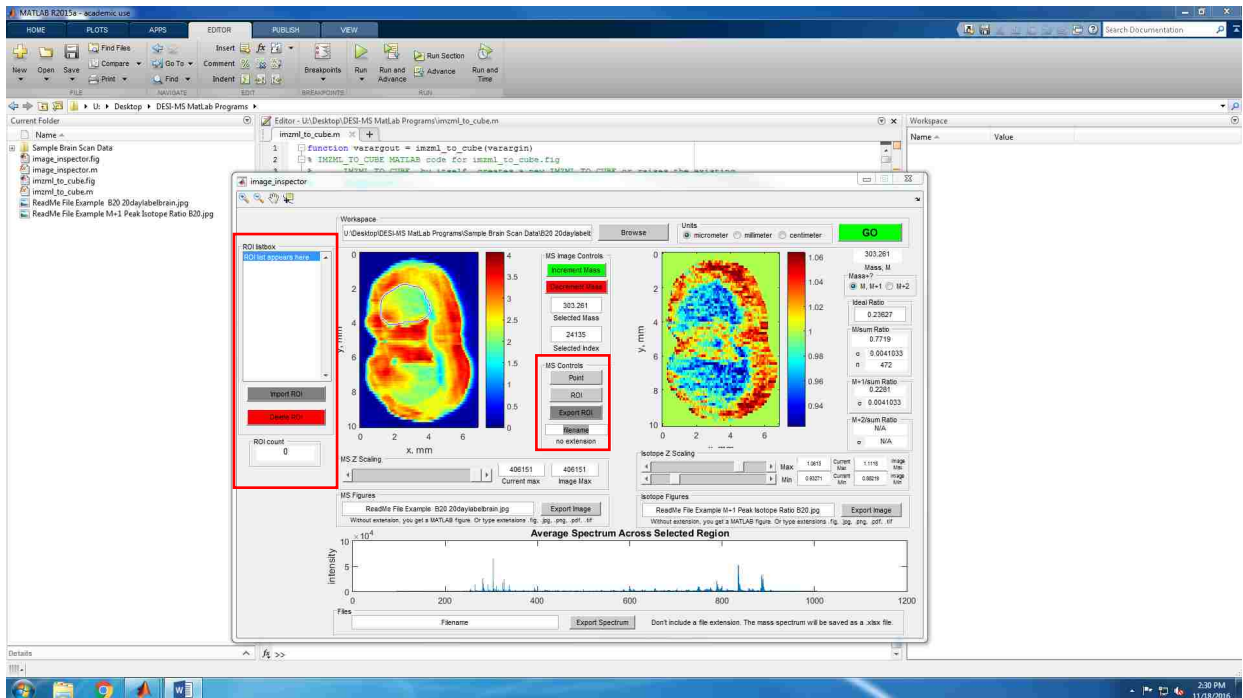
Figure A.16: Region of Interest Selection Screenshot

If you accidently select a region you do not want, you cannot undo the ROI you created, however you can restart by using the "Data Cursor"/selection tool in the top left of the GUI window, selecting a peak from the mass spectrum, clicking "Point", then choosing the "ROI" button and selecting your region once more.

On the very far left of the GUI window, you will see the "ROI listbox". This is where you can save the ROI you create for a brain, and later pull those regions and their corresponding data back up without having to redraw the ROI you selected. At this point, the list box should be empty other than the highlighted row that says "ROI list appears here". Underneath the list box lies an "Import ROI" button and a "Delete ROI" button. Below those is an "ROI count", which lets you know how many regions of interest are saved for that brain ("0" at the moment).

To save an ROI, you must first trace a region of interest as described a few paragraphs previously. Next, input a filename in the window below the "Export Region" button. Do not include a file extension. Finally, click on the "Export Region" button, which will save the highlighted region of the brain and its data to the file that shows up in the ROI listbox. Also note that you now have "1" under the "ROI count". The "ROI" and "Export ROI" buttons are highlighted with red boxes in Figure A.17.
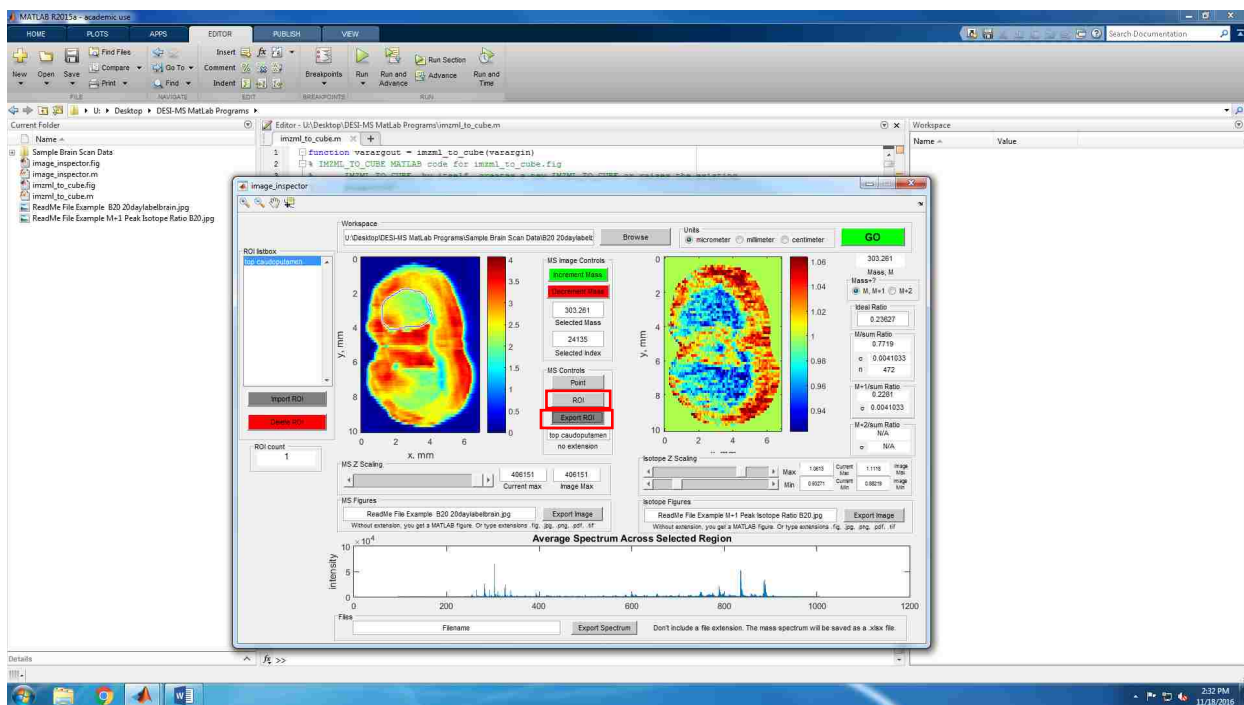
Figure A.17: Saving a Region of Interest Screenshot

To create another ROI, simply click the "ROI" button and trace another region as seen in Figure A.18. However, if you want to export that region/save it, be sure to change the filename, or else it will save with the previous filename directly below the previous ROI and you will have duplicate names representing two different regions of interest selected.

To delete an ROI from the list box, select the ROI filename, and click the "Delete ROI". To import a previous ROI so you can view the region, mass spectrum, and data, select the file name in the list box, and click the "Import ROI" button. If you want to remember what the regions of interest looked like, then click on the names in the listbox and outlines of the regions of interests will appear on the concentration image. However, only if you click the "Import ROI" button, will the isotope ratios and mass spectrum reflect the chosen ROI.
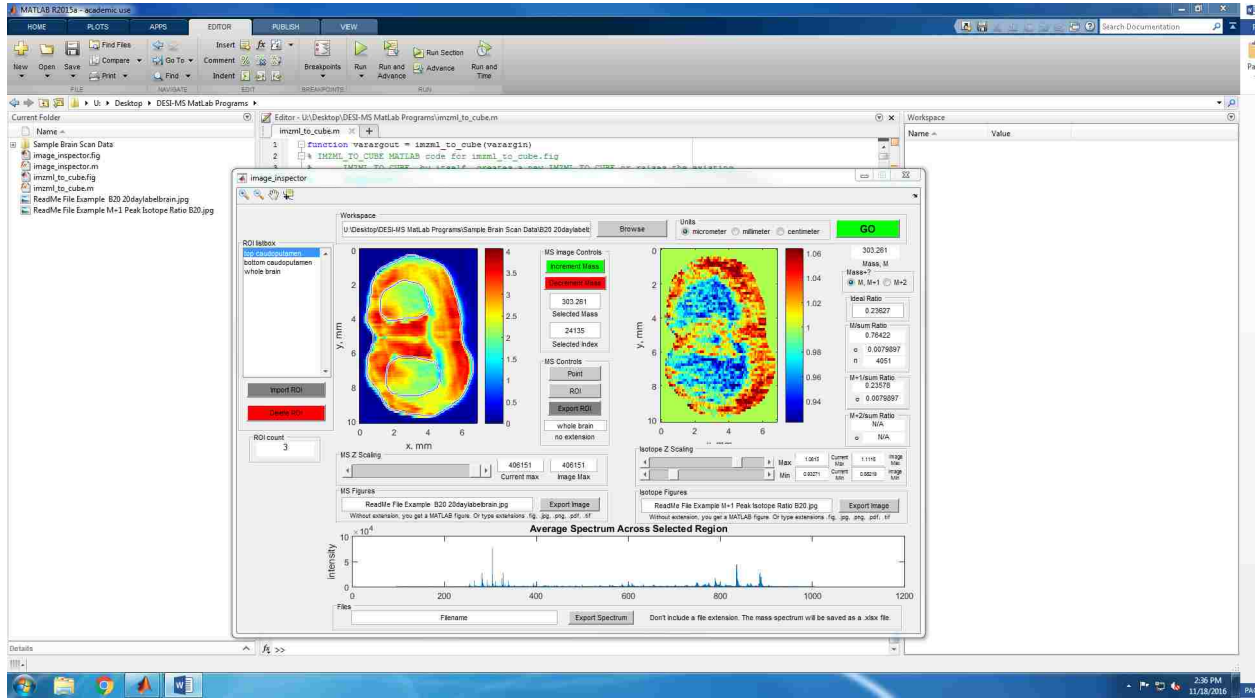
Figure A.18: Selecting Multiple Regions of Interest Screenshot

APPENDIX B.   MATLAB CODE FOR PROGRAMMABLE STAGE

```matlab
%Control Program for Prior Proscan II Stage

%Get everything closed and cleaned up
clear all;
close all;

%set up strings for stage communication

response = '';

%Open the com port

s = serial('com4','BAUD',9600,'Terminator',13);
fopen(s);

%Set the stage to compatibility mode. In this mode, the stage does not
%respond until a command is completed, so there is not a problem with
%commands piling up.

response = stage_cmd(s,'COMP 1');

%Set the timeout to 10 minutes. This is necessary because some commands
%(the scanning of a row, for example) may take a long time to execute.

set(s,'Timeout',1200);

%Set up the scan parameters

xres = input('Enter the desired horizontal pixel size in microns ');
yres = input('Enter the desired vertical pixel size in microns ');
AcqRate = input('Enter the spectrum acquisition rate in spectra/sec ');

%Define the area to be imaged

input('Position the stage at the lower left corner of the image area and then
press Enter ')
%This command defines the lower-left corner of the image as the origin
response = stage_cmd(s,'PS 0 0');
```

```matlab
input('Position the stage at the upper right corner of the image and then
press Enter ')
%This command defines the upper-right corner of the image and reads the
%stage coordinates in microns.
fprintf(s,'PS');
URcorner = fscanf(s,'%d,%d');

%Calculate the rate at which the stage will move during a line scan
% and convert the number to a string
% The value 560.71 is derived from calibration of the stage timing
% and differs from the value of 625 that the Prior tech support
% gave to Manan Dhunna
H_scan_rate = xres*AcqRate*560.71;
IH_scan_rate = round(H_scan_rate);
SH_scan_rate = ['SMS ',num2str(IH_scan_rate,'%d'),' I'];

%Calculate the number of pixels in a row
NumX = round(URcorner(1)/xres);
FNumX = double(NumX);
xlimit = NumX*xres;
S_xlimit = ['GX ',num2str(xlimit)];

%Calculate the number of rows
NumY = round(-URcorner(2)/yres);
FNumY = double(NumY);

%Calculate the necessary scan time for the mass spec
RowTime = FNumX/AcqRate;

%Estimate the total image time
ImageTime = RowTime*FNumY/60;
fprintf('The image will be %d rows x %d columns\n',NumY+1,NumX);
fprintf('Set the row acquistion time to %8.2f seconds\n',RowTime);
fprintf('Total acquisition time is about %8.2f minutes\n',ImageTime);

%Return the stage to the origin to start acquistion
response = stage_cmd(s,'SMS 100');
response = stage_cmd(s,'G 0 0');
input('Start the DESI spray and hit Enter to begin acquisition ')

%This loop rasters the image
for ii= 0 : NumY
    fprintf('You are now on row #%d \n',ii+1);
    row_pos = -ii*yres;
    %This section positions the stage at the start of a new row
    S_row_pos = num2str(row_pos);
    response = stage_cmd(s,['GY ',S_row_pos]);

    %This section sets the slow scan speed, triggers the mass spec
    %and begins scanning a row
    response = stage_cmd(s,SH_scan_rate);
    response = stage_cmd(s,'TTL 1 1');
    response = stage_cmd(s,'TTL 1 0');
    start_time = clock();
    response = stage_cmd(s,S_xlimit);
```

```matlab
        elapsed_time = etime(clock(), start_time);
        fprintf('it took %d seconds\n', elapsed_time);
        %This section sets the speed to max, and retraces the stage,
        %first to the bottom of the image, then to the left-hand side.
        response = stage_cmd(s,'SMS 100');
        response = stage_cmd(s, 'GY 0');
        response = stage_cmd(s,'GX 0');

end
%This is necessary to reset the com port.  If the program is aborted
%for any reason, this step must be done on the command line, or the
%program won't run again.
delete(s);
```

REFERENCES

1.   Takats, Z.; Wiseman, J. M.; Gologan, B.; Cooks, R. G. Mass spectrometry sampling under ambient conditions with desorption electrospray ionization. *Science* **2004**, *306*, 471-473.

2.   Brunelle, A.; Touboul, D.; Laprevote, O. Biological tissue imaging with time-of-flight secondary ion mass spectrometry and cluster ion sources. *J. Mass Spectrom.* **2005**, *40*, 985-999.

3.   Caprioli, R. M.; Farmer, T. B.; Gile, J. Molecular imaging of biological samples: Localization of peptides and proteins using MALDI-TOF MS. *Anal. Chem.* **1997**, *69*, 4751-4760.

4.   Costa, A. B.; Cooks, R. G. Simulation of atmospheric transport and droplet-thin film collisions in desorption electrospray ionization. *Chem. Commun.* **2007**, 3915-3917.

5.   Wiseman, J. M.; Puolitaival, S. M.; Takats, Z.; Cooks, R. G.; Caprioli, R. M. Mass spectrometric profiling of intact biological tissue by using desorption electrospray ionization. *Ange. Chem. Int. Ed.* **2005**, *44*, 7094-7097.

6.   Takats, Z.; Wiseman, J. M.; Cooks, R. G. Ambient mass spectrometry using desorption electrospray ionization (DESI): instrumentation, mechanisms and applications in forensics, chemistry, and biology. *J. Mass Spectrom.* **2005**, *40*, 1261-1275.

7.   Tillner, J.; McKenzie, J. S.; Jones, E. A.; Speller, A. V. M.; Walsh, J. L.; Veselkov, K. A.; Bunch, J.; Takats, Z.; Gilmore, I. S. Investigation of the Impact of Desorption Electrospray Ionization Sprayer Geometry on Its Performance in Imaging of Biological Tissue. *Anal. Chem.* **2016**.

8.   Wiseman, J. M.; Ifa, D. R.; Song, Q. Y.; Cooks, R. G. Tissue imaging at atmospheric pressure using desorption electrospray ionization (DESI) mass spectrometry. *Angew. Chem. Int. Ed.* **2006**, *45*, 7188-7192.

9.   Lanekoff, I.; Burnum-Johnson, K.; Thomas, M.; Cha, J.; Dey, S. K.; Yang, P. X.; Conaway, M. C. P.; Laskin, J. Three-dimensional imaging of lipids and metabolites in tissues by nanospray desorption electrospray ionization mass spectrometry. *Anal. Bioanal. Chem.* **2015**, *407*, 2063-2071.

10.   Eberlin, L. S.; Ferreira, C. R.; Dill, A. L.; Ifa, D. R.; Cooks, R. G. Desorption electrospray ionization mass spectrometry for lipid characterization and biological tissue imaging. *BBA-Mol. Cell Biol. L.* **2011**, *1811*, 946-960.

11.   Bennett, R. V.; Gamage, C. M.; Fernandez, F. M. Imaging of Biological Tissues by Desorption Electrospray Ionization Mass Spectrometry. *J. Vis. Exp.* **2013**.

12.   Abbassi-Ghadi, N.; Jones, E. A.; Veselkov, K. A.; Huang, J. Z.; Kumar, S.; Strittmatter, N.; Golf, O.; Kudo, H.; Goldin, R. D.; Hanna, G. B.; Takats, Z. Repeatability and reproducibility of desorption electrospray ionization-mass spectrometry (DESI-MS) for the imaging analysis of human cancer tissue: a gateway for clinical applications. *Anal. Methods* **2015**, *7*, 71-80.

13.   Calligaris, D.; Caragacianu, D.; Liu, X. H.; Norton, I.; Thompson, C. J.; Richardson, A. L.; Golshan, M.; Easterling, M. L.; Santagata, S.; Dillon, D. A.; Jolesz, F. A.; Agar, N. Y. R. Application of desorption electrospray ionization mass spectrometry imaging in breast cancer margin analysis. *Proc. Natl. Acad. Sci. U. S. A.* **2014**, *111*, 15184-15189.

14.   Calligaris, D.; Feldman, D. R.; Norton, I.; Brastianos, P. K.; Dunn, I. F.; Santagata, S.; Agar, N. Y. R. Molecular typing of meningiomas by desorption electrospray ionization mass spectrometry imaging for surgical decision-making. *Int. J. Mass Spectrom.* **2015**, *377*, 690-698.

15.   Jarmusch, A. K.; Pirro, V.; Baird, Z.; Hattab, E. M.; Cohen-Gadol, A. A.; Cooks, R. G. Lipid and metabolite profiles of human brain tumors by desorption electrospray ionization-MS. *Proc. Natl. Acad. Sci. U. S. A.* **2016**, *113*, 1486-1491.

16.   Jarmusch, A. K.; Alfaro, C. M.; Pirro, V.; Hattab, E. M.; Cohen-Gadol, A. A.; Cooks, R. G. Differential Lipid Profiles of Normal Human Brain Matter and Gliomas by Positive and Negative Mode Desorption Electrospray Ionization - Mass Spectrometry Imaging. *PLoS One* **2016**, *11*.

17.   Shariatgorji, M.; Strittmatter, N.; Nilsson, A.; Kallback, P.; Alvarsson, A.; Zhang, X. Q.; Vallianatou, T.; Svenningsson, P.; Goodwin, R. J. A.; Andren, P. E. Simultaneous imaging of multiple neurotransmitters and neuroactive substances in the brain by desorption electrospray ionization mass spectrometry. *Neuroimage* **2016**, *136*, 129-138.

18.   Louie, K. B.; Bowen, B. P.; McAlhany, S.; Huang, Y. R.; Price, J. C.; Mao, J. H.; Hellerstein, M.; Northen, T. R. Mass spectrometry imaging for in situ kinetic histochemistry. *Sci. Rep.* **2013**, *3*.

19.   Price, J. C.; Khambatta, C. F.; Li, K. W.; Bruss, M. D.; Shankaran, M.; Dalidd, M.; Floreani, N. A.; Roberts, L. S.; Turner, S. M.; Holmes, W. E.; Hellerstein, M. K. The Effect of Long Term Calorie Restriction on in Vivo Hepatic Proteostatis: A Novel Combination of Dynamic and Quantitative Proteomics. *Mol. Cell. Proteomics* **2012**, *11*, 1801-1814.

20.   Lee, W. N. P.; Bassilian, S.; Ajie, H. O.; Schoeller, D. A.; Edmond, J.; Bergner, E. A.; Byerley, L. O. In-Vivo Measurement of Fatty-acids and Cholesterol-synthesis Using D2O and Mass Isotopomer Analysis. *Am. J. Physiol.* **1994**, *266*, E699-E708.

21.   Guan, S. H.; Price, J. C.; Ghaemmaghami, S.; Prusiner, S. B.; Burlingame, A. L. Compartment Modeling for Mammalian Protein Turnover Studies by Stable Isotope Metabolic Labeling. *Anal. Chem.* **2012**, *84*, 4014-4021.

22.   Bodzon-Kulakowska, A.; Drabik, A.; Ner, J.; Kotlinska, J. H.; Suder, P. Desorption electrospray ionisation (DESI) for beginners - how to adjust settings for tissue imaging. *Rapid Commun. Mass Spectrom.* **2014**, *28*, 1-9.

23.   Wu, C. P.; Ifa, D. R.; Manicke, N. E.; Cooks, R. G. Molecular imaging of adrenal gland by desorption electrospray ionization mass spectrometry. *Analyst* **2010**, *135*, 28-32.

24.   Stryffler, R. B. New Analytical Approaches for Mass Spectrometry Imaging. Ph.D. Dissertation, Georgia Institute of Technology, Atlanta, GA, May 2015.

25.   Gao, L.; Li, G.; Cyriac, J.; Nie, Z.; Cooks, R. G. Imaging of Surface Charge and the Mechanism of Desorption Electrospray Ionization Mass Spectrometry. *J. Phys. Chem. C* **2010**, *114*, 5331-5337.

26.   Kessner, D.; Chambers, M.; Burke, R.; Agus, D.; Mallick, P. ProteoWizard: open source software for rapid proteomics tools development. *Bioinformatics* **2008**, *24*, 2534-2536.

27.   Race, A. M.; Styles, I. B.; Bunch, J. Inclusive sharing of mass spectrometry imaging data requires a converter for all. *J. Proteomics* **2012**, *75*, 5111-5112.

28.   Schramm, T.; Hester, A.; Klinkert, I.; Both, J.-P.; Heeren, R. M. A.; Brunelle, A.; Laprévote, O.; Desbenoit, N.; Robbe, M.-F.; Stoeckli, M.; Spengler, B.; Römpp, A. imzML — A

common data format for the flexible exchange and processing of mass spectrometry imaging data. *J. Proteomics* **2012**, *75*, 5106-5110.

29.   Parry, R. M.; Galhena, A. S.; Gamage, C. M.; Bennett, R. V.; Wang, M. D.; Fernández, F. M. OmniSpect: An Open MATLAB-Based Tool for Visualization and Analysis of Matrix-Assisted Laser Desorption/Ionization and Desorption Electrospray Ionization Mass Spectrometry Images. *J. Am. Soc. Mass Spectrom.* **2013**, *24*, 646-649.

30.   Dill, A. L.; Eberlin, L. S.; Costa, A. B.; Ifa, D. R.; Cooks, R. G. Data quality in tissue analysis using desorption electrospray ionization. *Anal. Bioanal. Chem.* **2011**, *401*, 1949-1961.

31.   Dong, Y. H.; Guella, G.; Franceschi, P. Impact of tissue surface properties on the desorption electrospray ionization imaging of organic acids in grapevine stem. *Rapid Commun. Mass Spectrom.* **2016**, *30*, 711-718.

32.   Price, J. C.; Holmes, W. E.; Li, K. W.; Floreani, N. A.; Neese, R. A.; Turner, S. M.; Hellerstein, M. K. Measurement of human plasma proteome dynamics with 2H2O and liquid chromatography tandem mass spectrometry. *Anal. Biochem.* **2012**, *420*, 73-83.

33.   Price, J. C.; Guan, S.; Burlingame, A.; Prusiner, S. B.; Ghaemmaghami, S. Analysis of proteome dynamics in the mouse brain. *Proc. Natl. Acad. Sci.* **2010**, *107*, 14508-14513.

34.   Kasumov, T.; Ilchenko, S.; Li, L.; Rachdaoui, N.; Sadygov, R. G.; Willard, B.; McCullough, A. J.; Previs, S. Measuring protein synthesis using metabolic (2)H labeling, high-resolution mass spectrometry, and an algorithm. *Anal. Biochem.* **2011**, *412*, 47-55.

35.   Lam, M. P. Y.; Wang, D.; Lau, E.; Liem, D. A.; Kim, A. K.; Ng, D. C. M.; Liang, X.; Bleakley, B. J.; Liu, C.; Tabaraki, J. D.; Cadeiras, M.; Wang, Y.; Deng, M. C.; Ping, P. Protein kinetic signatures of the remodeling heart following isoproterenol stimulation. *J. Clin. Invest.* **2014**, *124*, 1734-1744.

36.   Dill, A. L.; Ifa, D. R.; Manicke, N. E.; Zheng, O. Y.; Cooks, R. G. Mass spectrometric imaging of lipids using desorption electrospray ionization. *J. Chromatogr. B Analyt. Technol. Biomed. Life Sci.* **2009**, *877*, 2883-2889.

37.   Hsu, F.-F.; Turk, J. Characterization of phosphatidylinositol, phosphatidylinositol-4-phosphate, and phosphatidylinositol-4,5-bisphosphate by electrospray ionization tandem mass spectrometry: a mechanistic study. *J. Am. Soc. Mass Spectrom.* **2000**, *11*, 986-999.

38.   Angel, P. M.; Spraggins, J. M.; Baldwin, H. S.; Caprioli, R. Enhanced Sensitivity for High Spatial Resolution Lipid Analysis by Negative Ion Mode Matrix Assisted Laser Desorption Ionization Imaging Mass Spectrometry. *Anal. Chem.* **2012**, *84*, 1557-1564.

39.   O'Brien, J. S.; Sampson, E. L. Lipid composition of the normal human brain: gray matter, white matter, and myelin. *J. Lipid Res.* **1965**, *6*, 537-544.

40.   Mattson, M. P. Pathways towards and away from Alzheimer's disease. *Nature* **2004**, *430*, 631-639.

41.   Praticò, D.; Uryu, K.; Leight, S.; Trojanoswki, J. Q.; Lee, V. M.-Y. Increased lipid peroxidation precedes amyloid plaque formation in an animal model of Alzheimer amyloidosis. *J. Neurosci.* **2001**, *21*, 4183-4187.

42.   Calon, F.; Lim, G. P.; Yang, F.; Morihara, T.; Teter, B.; Ubeda, O.; Rostaing, P.; Triller, A.; Salem, N.; Ashe, K. H. Docosahexaenoic acid protects from dendritic pathology in an Alzheimer's disease mouse model. *Neuron* **2004**, *43*, 633-645.

43.   Puglielli, L.; Tanzi, R. E.; Kovacs, D. M. Alzheimer's disease: the cholesterol connection. *Nat. Neurosci.* **2003**, *6*, 345-351.

44.   Refolo, L. M.; Pappolla, M. A.; LaFrancois, J.; Malester, B.; Schmidt, S. D.; Thomas-Bryant, T.; Tint, G. S.; Wang, R.; Mercken, M.; Petanceska, S. S. A cholesterol-lowering drug reduces β-amyloid pathology in a transgenic mouse model of Alzheimer's disease. *Neurobiol. Dis.* **2001**, *8*, 890-899.

45.   Di Paolo, G.; Kim, T.-W. Linking lipids to Alzheimer's disease: cholesterol and beyond. *Nature Rev. Neurosci.* **2011**, *12*, 284-296.

46.   Wu, C. P.; Ifa, D. R.; Manicke, N. E.; Cooks, R. G. Rapid, Direct Analysis of Cholesterol by Charge Labeling in Reactive Desorption Electrospray Ionization. *Anal. Chem.* **2009**, *81*, 7618-7624.